A Study of Finite Gap Solutions to the Nonlinear Schrödinger Equation

Oliver H Warren

A thesis presented for the degree of Doctor of Philosophy of the University of London and the Diploma of Imperial College

29 March 2007

The work contained within this thesis is my own

Abstract

The vector nonlinear Schrödinger equation is an envelope equation which models the propagation of ultra-short light pulses and continuous-wave beams along optical fibres. Previous work has focused almost entirely on soliton solutions to the equation using a Lax representation originally developed by Manakov. We prove recursion formulae for the family of higher-order nonlinear Schrödinger equations, along with its associated Lax hierarchy, before investigating finite gap solutions using an algebrogeometric approach which introduces Baker-Akhiezer functions defined upon the Riemann surface of the relevant spectral curve. We extend this approach to account for solutions of arbitrary genus and compare it with an alternative method describing solutions of genus two. The scalar nonlinear Schrödinger and Heisenberg ferromagnet equations were shown to be equivalent following work by Lakshmanan; we generalise this idea by introducing the Heisenberg ferromagnet hierarchy and show it is entirely gauge equivalent to the scalar nonlinear Schrödinger hierarchy in the attractive case. We also investigate the polarisation state evolution of general solutions to the vector nonlinear Schrödinger equation and study possible degenerations to the Heisenberg ferromagnet equation.

Acknowledgements

Firstly, I owe a great debt of gratitude to my supervisor, Professor John Elgin, for his time, knowledge, inspiration and enthusiasm during my time at Imperial.

Mathematically I would also like to particularly thank Dr John Gibbons for his expert advice and Tom Woodcock for sharing his insight into the subject.

At Imperial there are many people who have helped me along the way and these include: Evangelia, whose support and coffee kept me on track; my other office mates Agneta, Filipe, Sandra and Roshani; Maria, my manchego dealer; Adam and Katie, without whom I wouldn't have stayed on; and all my lunch-mates in astrophysics, particularly Tom and Peter.

My friends from my time as an undergraduate also deserve mention: Patrick, who had a surreal influence throughout and banished the Ipswich stereotype; Sam and Chris, my flatmates for three years - thank you for putting up with me; and Xana, who always seemed to invite me out when I needed it most. I would like to give special mention to Steve and Rachel who provided my second homes in Elephant, Fulham and Chiswick and years of support, friendship and cordon bleu dinners.

Outside of university my friends have provided the perfect antidote to college life: Ian and Becky, who made evenings at Gaynesford Road something to look forward to; Gethin, my longest-serving friend, who encouraged me and extolled a positive outlook; Alex, Bo, Paul (Joycey) and Dilum, for some memorable evenings at home and in East Dulwich; all my friends from Norwich including Dan (Goodas), Jonny (JT) and Alister (Barker); and Sarah, who made me think positively and taught me to understand myself.

Lastly I would like to thank my family: Grandma Jean, for all her love and encouragement; Josh, for tolerating my teasing and sharing his perspective on life with me; and finally Mum and Dad, for being wonderful, loving parents.

In loving memory of Grandma Win, Grandpa Hugh and Grandpa Harry

Contents

Chapter 1

Introduction

The nonlinear Schrödinger equation is a universal nonlinear model applicable to many physical phenomena in areas of research ranging from hydrodynamics and quantum condensates to nonlinear acoustics. Of particular relevance to this thesis will be its applications to nonlinear optics as the governing equation of light propagation in monomode optical fibres. We begin by presenting the practical uses of optical fibres in telecommunications systems before introducing the equation, its variants and the methods used in finding their solutions.

1.1 Optical communications

Optical fibres currently provide the world with a fast, reliable and capacious telecommunications network. Dispersion-shifted fibres, designed to minimise dispersion and linearise light pulse propagation, connect North America, Europe and the Far East and provide data transferral at rates of 10^9 bits per second. Although this is sufficient for current demand, the burgeoning world population and growth of the massive technology-driven economies of the Far East and Indian subcontinent mean communications systems providing far greater capacity will soon be in demand.

A standard optical fibre consists of a cylindrical glass inner-core surrounded by an outer cladding also made of glass but of a refractive index slightly lower than that of the core. For telecommunications monomode fibres are used which usually have a core radius of 2 to 4μm and a cladding radius of between 50 and 60μm. At a fixed frequency, monomode fibres permit only one configuration of the electromagnetic field to propagate as opposed to multimode fibres where several are permitted. The governing principle of the light propagation in optical fibres is total internal reflection - the lower refractive index of the

cladding and the small radius of the core mean the angle of incidence at which the light hits the core-cladding interface is always less than the critical angle. To use optical fibres for communication, a message is encoded as a series of light pulses which propagate along the fibre and are decoded at the end of the fibre by a receiver. These series of optical pulses or bit streams are subject to the distorting and degrading effects of group velocity dispersion, Kerr nonlinearity, birefringence, and higher-order dispersion and nonlinearity. These will be discussed in the next section.

Advances in modern fibres have reduced signal degradation dramatically and meant no regeneration is required over tens of kilometres. These fibres carry solitons - light pulses which propagate nonlinearly but do not disperse and whose group velocities are directly linked to their spectral peaks. Wavelength division multiplexing involves transmitting light signals at many different wavelengths down a fibre. These may then be separated at the receiving end, creating several channels along which data may be sent and increasing enormously the capacity of the fibre. Indeed in 1998 a group led by Thierry Georges at France Télécom used this technique to demonstrate data transfer at 10^{12} bits per second. In addition to wavelength division multiplexing, a fibre's capacity may be increased by creating channels of different polarisation state, a process known as polarisation division multiplexing. Although experimental [MGH95] and theoretical [SE98] work suggests this is not in general compatible with wavelength division multiplexing, Silmon-Clyde [Sil99] has found results to indicate it might be possible to integrate the two processes for trains of orthogonal optical pulse pairs.

For long-range systems, repeaters or optical amplifiers are required to regenerate degraded signals. Repeaters, which are back-to-back receivers and transmitters, have long been replaced by optical amplifiers in modern fibres. These comprise sections of fibre, a few centimetres in length, doped with a rare-earth mineral like erbium where light of a shorter wavelength to that of the signal is pumped in to the fibre in order to produce the necessary population inversion in the doped ions to provide pulse amplification. Optical amplifiers are very reliable and have the advantage that multiplex channels do not need to be individually regenerated as was the case with repeaters. They do however provide a source of unwanted background radiation and birefringence.

1.2 Background to the equation

The vector nonlinear Schrödinger equation or VNLS is an idealised model of the propagation of ultrashort light pulses and continuous-wave beams along an optical fibre. Originally derived as the evolution equation of a light pulse envelope in an optical fibre, the derivation involved an asymptotic reduction of Maxwell's equations under sequentially slower

timescales. The form of the equation to which we shall refer throughout this thesis is

$$i\boldsymbol{q}_t + \boldsymbol{q}_{xx} \pm 2\boldsymbol{q}\boldsymbol{q}^\dagger\boldsymbol{q} = 0 \tag{1.1}$$

where suffices denote partial differentiation with respect to real variables t and x and $\boldsymbol{q}^\dagger = \overline{\boldsymbol{q}}^\mathsf{T}$ is the Hermitian conjugate of complex vector $\boldsymbol{q}(x,t) = (q_1, q_2)^\mathsf{T}$.

For an optical fibre with perfectly axisymmetric cylindrical core the propagating electromagnetic field of a light pulse envelope will have constant polarisation. In this case the vector $\boldsymbol{q}$ will take the form $\boldsymbol{q}(x,t) = q(x,t)\boldsymbol{c}$ for some constant complex unit vector $\boldsymbol{c}$ and complex scalar function $q(x,t)$. Equation (1.1) then reduces to the scalar nonlinear Schrödinger equation or SNLS:

$$iq_t + q_{xx} \pm 2q^2\overline{q} = 0. \tag{1.2}$$

Any solution to equation (1.2) multiplied by a constant unit vector forms a solution to the vector equation (1.1). This vector represents the polarisation state of the solution.

In reality the core will have some varying ellipticity along its length formed in the manufacturing process. In the monomode fibres upon which we shall concentrate, the ellipticity, along with the effects of impurities in the fibre material (particularly along the doped sections of fibre in optical amplifiers), higher order dispersion and perturbations caused by external strains, twists and bends, removes the degeneracy and distinct birefringence eigenmodes form along which the electromagnetic field components are directed. These determine the polarisation state of the light pulse. Light pulse propagation in a birefringent fibre is usefully and realistically modelled by a perturbed form of the VNLS which is presented in [BEG00]:

$$i\boldsymbol{q}_t + \boldsymbol{q}_{xx} \pm 2\boldsymbol{q}\boldsymbol{q}^\dagger\boldsymbol{q} + \beta\sigma_3\boldsymbol{q} - i\beta'\sigma_3\boldsymbol{q}_x + \gamma(t)\sigma_2\boldsymbol{q} + 2B\sigma_2\boldsymbol{q}\boldsymbol{q}^\dagger\sigma_2\boldsymbol{q} = 0. \tag{1.3}$$

$\boldsymbol{q}(x,t) = (q_1, q_2)^\mathsf{T}$ where q_1 and q_2 are the amplitudes of the fast and slow eigenmodes respectively. β is the frequency-dependent, weak birefringence parameter which measures the difference in phase velocity of the two eigenmodes and β', its derivative with respect to frequency, is the strong birefringence parameter, proportional to the difference in group velocity of the eigenmodes. These parameters are evaluated at the carrier frequency and are treated as constants. There is often a need to include a term $\gamma(t)$ which models the varying eccentricity and twisting of the fibre with propagation distance. These cause a variation in the polarisation state of a light pulse which is accompanied by a change in velocity. In reality $\gamma(t)$ will have a stochastic element accounting for the random nature of imperfections in the fibre produced in the manufacturing process. This, along with other related stochastic perturbations, are the main limiting factors in bandwidth capacity of

optical fibres. The final term corresponds to a four-wave interaction between the modes. Although (1.3) provides a realistic model of light pulse propagation, the integrable version (1.1) with which this thesis is concerned remains an equation of importance. Indeed, in analysis where the correlation length associated to $\gamma(t)$ is short enough, it is possible to average out the stochastic variation [WMC91].

The Pauli matrices σ_1, σ_2 and σ_3 are defined to be

$$\sigma_1 = \begin{pmatrix} 0 & 1 \\ 1 & 0 \end{pmatrix}, \quad \sigma_2 = \begin{pmatrix} 0 & -i \\ i & 0 \end{pmatrix}, \quad \sigma_3 = \begin{pmatrix} 1 & 0 \\ 0 & -1 \end{pmatrix}, \tag{1.4}$$

and will be referred to at various stages throughout this thesis.

In both equations (1.1) and (1.2), variable t represents the propagation distance along the fibre and variable x represents retarded time meaning the peak of a light pulse positioned at $x = x_0$ will remain at x_0 as the pulse propagates down the fibre. The use of a retarded time variable is analogous to the use of a travelling reference frame when modelling water wave propagation. However, in fibre optics research, a travelling frame is not experimentally practical as readings are taken only at the end of the fibre. The variables t and x are often defined the other way around in optical physics literature in order to reflect this but the definitions given here will be maintained throughout this thesis and we shall examine (1.1) in terms of a standard Cauchy problem for initial data $\boldsymbol{q}(x, 0)$.

The nonlinear term $2\boldsymbol{q}\boldsymbol{q}^\dagger\boldsymbol{q}$ models the Kerr effect, also known as the quadratic electro-optic effect, and is a consequence of the optical fibre glass possessing a refractive index dependent on the intensity of the electromagnetic field which is proportional to $\boldsymbol{q}^\dagger\boldsymbol{q}$.

The term $\boldsymbol{q}_{xx}$ in (1.1) models the chromatic or intramodal dispersion of the light pulse as it travels along the optical fibre. This is the effect of the differences in velocity of colours in the light spectrum and results in pulse broadening. The choice of plus and minus sign preceding the nonlinear term in equations (1.1) and (1.2) is dependent on the group velocity dispersion parameter. The plus sign case models propagation in an anomalously dispersive regime where higher frequency components of a pulse travel faster and so-called down-chirped pulses may occur whereas the minus sign case models propagation in a normally dispersive regime where lower frequency components travel faster and up-chirped pulses may be experienced. The two cases are often referred to as the attractive and repulsive forms of the nonlinear Schrödinger equation respectively and this terminology shall be used throughout this thesis.

Dispersive equations may be exemplified by applying trial harmonic wave solutions

$$u(x, t) \sim \exp(ikx - i\omega t).$$

As an example, applying to the simplest linear dispersive wave equation

$$u_t + u_x + u_{xxx} = 0$$

forces the dispersion relation $\omega = k - k^3$ for which the frequency ω is dependent on the wave number k. The phase velocity c_p is given by

$$c_p = \frac{\omega}{k} = 1 - k^2$$

and so waves of different number travel at different velocities. Fourier transforming to give

$$u(x,t) = \int_{-\infty}^{\infty} A(k) \exp(ikx - i\omega t) \mathrm{d}k$$

for some given $A(k)$ produces a wave profile which will spread out as it propagates as individual components travel at differing speeds. Another velocity, the group velocity, is defined by

$$c_g = \frac{\mathrm{d}\omega}{\mathrm{d}k} = 1 - 3k^2$$

and determines the velocity of a wave packet. An equation is dispersive if $\frac{\mathrm{d}^2\omega}{\mathrm{d}k^2} \neq 0$, anomalously for $\frac{\mathrm{d}^2\omega}{\mathrm{d}k^2} > 0$ and normally for $\frac{\mathrm{d}^2\omega}{\mathrm{d}k^2} < 0$. For most physical waves $c_g \leq c_p$ and c_g is the velocity at which the energy of the wave propagates. For nonlinear wave equations, the situation is more complicated - the wave profile may change with time. Solutions may only be valid for a finite time before becoming multi-valued, indicating that the wave has broken and subsequently needs to be modelled by a discontinuity. In general, solitons are an exception to this rule and do retain their profile as they propagate as we shall now examine.

In an anomalously dispersive regime, for certain light pulse profiles, the effect of the nonlinear term balances the pulse broadening caused by the dispersive term. In such circumstances a bright soliton may form.

A soliton is a nonlinear solitary wave of permanent form which decays to a constant as $x \to \pm\infty$. Most importantly, apart from a phase shift, a soliton will remain unaffected by nonlinear interaction with another soliton or more general localised disturbance, for example background radiation.

The first published example of a soliton is found in John Scott Russell's 'Report on Waves' presented to the British Association in 1844. In this work, Scott Russell describes a 'wave of translation', observed on the Union Canal in Edinburgh in 1834, which was set in motion

by the sudden arrest of a horse-drawn boat. The wave created travelled a considerable distance along the canal with its form and speed preserved before its height gradually began to diminish. After progress by Boussinesq and Rayleigh, it was eventually shown that the equation describing the motion of Scott Russell's shallow water wave was the Korteweg-de Vries equation (1.10) or KdV, named after the Dutch mathematicians who discovered it in 1895. The name soliton was coined in 1965 by Zabusky and Kruskal to compare particle-like solitary wave interaction with colliding photons or protons. Since then many equations have been shown to exhibit soliton solutions of which the nonlinear Schrödinger equations are but a few. Other well-studied examples include the modified KdV, sine-Gordon, Heisenberg ferromagnet and Benjamin-Ono equations.

Bright soliton solutions to the attractive case of the SNLS are pulses of positive light intensity on a dark background. A general bright single soliton solution is given by

$$q(x,t) = \frac{1}{2}\text{sech}\left(\frac{\eta_1 + \overline{\eta_1} + \phi_{1\bar{1}}}{2}\right)\exp\left(\frac{\eta_1 - \overline{\eta_1} - \phi_{1\bar{1}}}{2}\right) \tag{1.5}$$

with the various terms and parameters defined in Appendix B. For appropriate choices of these parameters this becomes the simplest bright single soliton solution:

$$q(x,t) = \text{sech}(x)\exp(it). \tag{1.6}$$

Conversely, in a normally dispersive regime, the nonlinear effect reinforces the dispersion and bright solitons are not supported. However so-called grey and dark solitons may form. Grey solitons are pulses of low intensity on a light background whose square intensity profiles take the form of 'holes' punched into a constant beam. In the case of zero intensity pulses these are termed dark solitons. A general grey soliton solution is given by

$$q(x,t) = \sqrt{\frac{\tau}{2}}\left\{\cos\psi + i\sin\psi\tanh\left(\frac{\eta(x,t)}{2}\right)\right\}\exp(i\theta(x,t) + i\psi) \tag{1.7}$$

where, again, the various parameters are defined in Appendix B. For appropriate choices of these parameters (1.7) becomes the simplest dark soliton solution:

$$q(x,t) = \tanh(x)\exp(-2it). \tag{1.8}$$

1.3 Pulse polarisation states

As has been mentioned, a single soliton solution to the VNLS in a perfectly axially symmetric fibre will take the form $\boldsymbol{q}(x,t) = q(x,t)\boldsymbol{c}$ for some constant complex unit vector $\boldsymbol{c}$ representing the soliton's polarisation state. Polarised light is light for which the vi-

brations of the electromagnetic field components transverse to the path of propagation have preferred direction. Current optical fibre communication systems will usually use completely polarised light although systems are being developed with adjacent pulses orthogonal. This would enable polarisation division multiplexing but, as Silmon-Clyde shows using Manakov's results [Sil99], the polarisation states of interacting solitons are altered by collisions. Along with the effects of perturbations caused by fibre irregularities this creates difficulties in building a reliable system of communication with pulse interaction.

A method of visualising the polarisation states is to map them bijectively onto unit Stokes vectors on the Poincaré sphere. The Stokes vector $\mathbf{S} = (S_1, S_2, S_3)^{\mathsf{T}}$ has components

$$S_j = \frac{\boldsymbol{q}^\dagger \sigma_j \boldsymbol{q}}{\boldsymbol{q}^\dagger \boldsymbol{q}} \qquad j = 1, 2, 3, \tag{1.9}$$

for which it is straightforward to check $\boldsymbol{S} \cdot \boldsymbol{S} = 1$.

The vector's position on the sphere uniquely characterises the polarisation state of the pulse. Diametrically opposed points on the sphere correspond to orthogonal polarisation states. This is a consequence of the link between the SU(2) representation of solutions to (1.1) and the O(3) representation of $\mathbf{S}$. A general point on the sphere represents an elliptically polarised light pulse, the two poles represent circularly polarised light and points on the equator represent linearly polarised light. Points on lines of constant latitude have the same eccentricity but differing orientation whilst points on lines of constant longitude have the same orientation but differing ellipticity.

By considering the evolution of polarisation states through Stokes' vectors, rather than eigenmode amplitudes directly, a great deal of analysis of the effects of birefringence on soliton interaction has been possible. For given deterministic forms of $\gamma(t)$, for example $\gamma(t)$ constant or $\gamma(t) = \cos(\Omega t)$ (corresponding to a periodic twisting or 'rocking' of the fibre), results have been obtained for the polarisation state's evolution. It has also been shown that the inclusion of stochastic terms leads to a chaotic system, see [GW86], [WMC91]. The mechanism of this chaos is similar to that found in other Hamiltonian systems - a breaking and transversal intersection of stable and unstable manifolds - and can be described using Melnikov's technique, see [BEG00].

The mapping of polarisation states to Stokes' vectors need not be confined to soliton solutions. Indeed any solution to the VNLS has an instantaneous polarisation state which evolves with x and t.

1.4 Inverse scattering transform method

This method of finding exact solutions to a large class of nonlinear partial differential equations (PDEs) was initially realised in the late 1960s by Gardner, Green, Kruskal and Miura [GGK67] as a technique by which solutions to the KdV equation

$$u_t + 6uu_x + u_{xxx} = 0 \tag{1.10}$$

might be found. Further developments, notably by Lax [Lax68] and Zakharov and Shabat [ZS72], culminated in a paper by Ablowitz, Kaup, Newell and Segur [AKN74] in which they presented a generalised eigenvalue problem or scattering problem to which the AKNS technique, taking its name from the authors' initials, could be applied. A detailed account of the method, its history and its applications may be found in [AS81]. The inverse scattering transform (IST) method is applicable to integrable nonlinear PDEs. The notion of integrability is a difficult one to describe and much work has been devoted to it. Indeed the title "What is Integrability?" of a book by leading authors in this field [Zak91] suggests its complexity. Integrable nonlinear PDEs do however share some important characteristics:

- they have soliton solutions;
- they have an infinite set of conserved densities - linked to discrete integrable systems having a constant of motion for each degree of freedom;
- they are soluble by the IST method;
- they are bi-Hamiltonian with the IST method representing a transformation to action-angle variables.

The Painlevé conjecture asserts that if every ordinary differential equation formed by an exact reduction - that is, for example, searching for travelling wave or similarity solutions - of the relevant PDE is, up to a re-scaling of variables, one of the 50 Painlevé equations, then that PDE is integrable and soluble by the IST method. This conjecture has yet to be proved or disproved but it has a great deal of evidence in its favour, see [DJ89].

To exemplify the IST method we briefly summarise its application to the SNLS (1.2) with infinite line and periodic boundary conditions before commenting on the difficulties in adapting it to the vector problem.

1.4.1 SNLS scattering problem

The SNLS equations (1.2) arise as consistency conditions of the Lax representations

$$L^{\pm}\boldsymbol{v} = z\boldsymbol{v}, \qquad \boldsymbol{v}_t = A^{\pm}\boldsymbol{v} \tag{1.11}$$

where, in the attractive (+) and repulsive (-) cases,

$$\begin{aligned} L^{\pm} &= 2i\sigma_3\partial_x + 2i\begin{pmatrix} 0 & -q \\ \mp\overline{q} & 0 \end{pmatrix}, \\ A^{\pm} &= 2i\sigma_3\partial_x^2 + 2i\begin{pmatrix} 0 & -q \\ \mp\overline{q} & 0 \end{pmatrix}\partial_x + \begin{pmatrix} \pm iq\overline{q} & -iq_x \\ \mp i\overline{q}_x & \mp iq\overline{q} \end{pmatrix}. \end{aligned}$$

For an isospectral flow $z_t = 0$ and the following consistency condition holds:

$$L_t^{\pm} = [A^{\pm}, L^{\pm}]. \tag{1.12}$$

This Lax pair was proposed originally, in a slightly differing form, by Zakharov and Shabat [ZS72]. If the sought function, $q(x,t)$, satisfies (1.12) then the spectra of the eigenvalue operators $L^{\pm}$ are time-independent and the asymptotic characteristics of its eigenfunctions may be calculated at any time t from the initial data. As an alternative to the Lax form (1.11), Ablowitz et al [AKN74] proposed the system be reformulated as two linear equations:

$$\boldsymbol{v}_x = \mathcal{L}_1^{\pm}(z)\boldsymbol{v}, \tag{1.13}$$

$$\boldsymbol{v}_t = \mathcal{L}_2^{\pm}(z)\boldsymbol{v} \tag{1.14}$$

where

$$\begin{aligned} \mathcal{L}_1^{\pm}(z) &= z\begin{pmatrix} -\frac{i}{2} & 0 \\ 0 & \frac{i}{2} \end{pmatrix} + \begin{pmatrix} 0 & q \\ \mp\overline{q} & 0 \end{pmatrix}, \\ \mathcal{L}_2^{\pm}(z) &= z^2\begin{pmatrix} -\frac{i}{2} & 0 \\ 0 & \frac{i}{2} \end{pmatrix} + z\begin{pmatrix} 0 & q \\ \mp\overline{q} & 0 \end{pmatrix} + \begin{pmatrix} \pm iq\overline{q} & iq_x \\ \pm i\overline{q}_x & \mp iq\overline{q} \end{pmatrix} \end{aligned}$$

and $\boldsymbol{v} = (v_1, v_2)^{\mathsf{T}}$ is a vector-valued function of x and t. Notice that, in contrast to $L^{\pm}$ and $A^{\pm}$, $\mathcal{L}_1^{\pm}$ and $\mathcal{L}_2^{\pm}$ are dependent upon q, $\overline{q}$ and their x derivatives as well as the additional complex spectral parameter z.

The consistency condition $\boldsymbol{v}_{xt} = \boldsymbol{v}_{tx}$ applied to (1.13) and (1.14) gives the zero-curvature

equation:

$$\frac{\partial \mathcal{L}_1^{\pm}(z)}{\partial t} - \frac{\partial \mathcal{L}_2^{\pm}(z)}{\partial x} = \left[\mathcal{L}_2^{\pm}(z), \mathcal{L}_1^{\pm}(z)\right] \tag{1.15}$$

from which equations (1.2) may be returned by expanding in powers of z. This equation holds for all z and is essentially the equivalent of equation (1.12). Faddeev and Takhtajan [FT87] point out the geometric interpretation of equations (1.13), (1.14) and the consistency condition (1.15). $\mathcal{L}_1^{\pm}$ and $\mathcal{L}_2^{\pm}$ are considered as the local connection coefficients in the vector bundle formed of a fibre space $\mathbb{C}^2$ in which the vector $\boldsymbol{v}$ takes values and the base space $\mathbb{R}^2$ in which x and t are the variables. The satisfaction of equation (1.15) implies the connection formed by $\mathcal{L}_1^{\pm}$ and $\mathcal{L}_2^{\pm}$ has zero-curvature, hence the terminology used. The zero-curvature relationship is ubiquitous in problems soluble by inverse scattering methods and is fundamental to their implementation.

By extending the Lax representation in a sensible way, we may consider a hierarchy of equations related to the SNLS but with higher-order dispersion and more complicated nonlinear terms. The main requirement we insist upon is that the symmetries present in the matrices $\mathcal{L}_1^{\pm}$ and $\mathcal{L}_2^{\pm}$ are present in all the hierarchy matrices $\mathcal{L}_n^{\pm}$, that is

$$(\mathcal{L}_n^{+})^{\dagger}(z) = -\mathcal{L}_n^{+}(z), \qquad (\mathcal{L}_n^{-})^{\dagger}(z) = -\sigma_3 \mathcal{L}_n^{-}(z)\sigma_3. \tag{1.16}$$

Developing this hierarchy allows a richer family of solutions to be found whose construction will be discussed in Chapter 3.

The IST method may be used to find solutions to the SNLS equations upon the infinite line or over a finite period. In the attractive case soliton solutions upon the infinite line are found studying rapidly decreasing potentials, $q(x,t) \to 0$ as $|x| \to \pm\infty$. In the repulsive case a finite density condition is needed to find dark solitons, this is normally given by $q(x,t) \to \rho$ as $x \to \infty^{+}$ and $q(x,t) \to \rho \exp(i\alpha)$ as $x \to \infty^{-}$ where α may be shown to be time-independent and ρ is a positive constant. The quasiperiodic case requires the smooth potential to satisfy the condition $q(x+2L,t) = \exp(i\theta)q(x,t)$ where $0 \leq \theta < 2\pi$ and is independent of time. In the following sections we will summarise the development of the IST method as applied to the SNLS - firstly on the infinite line in the attractive and repulsive cases and then for finite gap solutions. In each case we will examine the role of the scattering data and positions of the eigenvalues.

1.4.2 IST method on the infinite line - attractive case

For the purposes of comparison with the algebrogeometric technique which we will use later to construct finite gap potentials to the SNLS, we now outline the inverse scattering technique normally adopted for constructing potentials on the infinite line. For a full,

detailed discussion, the reader is referred to [AS81] and [APT04].

Consider the direct scattering problem, (1.13), in the attractive case. Define fundamental or Jost solutions $\boldsymbol{\phi}^{(1)}(x,z)$ and $\boldsymbol{\psi}^{(1)}(x,z)$ at fixed time $t = t_0$ with the asymptotic requirements that, for $z = \xi + i\eta$,

$$\boldsymbol{\phi}^{(1)} \sim \begin{pmatrix} 1 \\ 0 \end{pmatrix} \exp(-\frac{i\xi x}{2}) \qquad x \to -\infty,$$

$$\boldsymbol{\psi}^{(1)} \sim \begin{pmatrix} 1 \\ 0 \end{pmatrix} \exp(-\frac{i\xi x}{2}) \qquad x \to +\infty.$$

These solutions satisfy an anti-holomorphic involution so that complementary Jost solutions

$$\boldsymbol{\phi}^{(2)}(x,z) = \begin{pmatrix} -\overline{\phi_2^{(1)}}(x,z) \\ \overline{\phi_1^{(1)}}(x,z) \end{pmatrix}, \qquad \boldsymbol{\psi}^{(2)}(x,z) = \begin{pmatrix} -\overline{\psi_2^{(1)}}(x,z) \\ \overline{\psi_1^{(1)}}(x,z) \end{pmatrix}$$

may be defined with corresponding asymptotic behaviour.

Assuming the functions $q(x)$ and $\overline{q}(x)$ to be absolutely integrable over the infinite real line, the region of convergence of Neumann series associated to related functions reveals the regions of analyticity of the Jost solutions: $\boldsymbol{\phi}^{(1)}$ and $\boldsymbol{\psi}^{(2)}$ are analytic in the upper half z-plane whilst $\boldsymbol{\phi}^{(2)}$ and $\boldsymbol{\psi}^{(1)}$ are analytic in the lower half z-plane. The method may be followed in [AS81].

The pair $\boldsymbol{\psi}^{(1)}(x,z)$, $\boldsymbol{\psi}^{(2)}(x,z)$ forms a complete basis of solutions to (1.13) and therefore the solutions $\boldsymbol{\phi}^{(1)}(x,z)$ and $\boldsymbol{\phi}^{(2)}(x,z)$ may be expressed in terms of this basis via the equation

$$\boldsymbol{\phi}^{(i)}(x,z) = \sum_{j=1}^{2} S_{ij}(z)\boldsymbol{\psi}^{(j)}(x,z). \tag{1.17}$$

Here $S_{ij}(z)$ are elements of the scattering matrix S and are referred to as the scattering data. The relations $S_{11}(z) = \overline{S_{22}}(z)$ and $S_{12}(z) = -\overline{S_{21}}(z)$ may be derived by representing the scattering data as ratios of Wronskians of appropriate Jost solutions. S may also be shown unimodular on $\eta = 0$, that is $\det S(\xi) = 1$, from which it follows

$$S_{11}(\xi) = W\left(\boldsymbol{\phi}^{(1)}(\xi), \boldsymbol{\psi}^{(2)}(\xi)\right). \tag{1.18}$$

We deduce that, as $\boldsymbol{\phi}^{(1)}(x,z)$ and $\boldsymbol{\psi}^{(2)}(x,z)$ may be analytically continued to the upper-half z-plane, $S_{11}(z)$ is analytic for $\eta > 0$ and its zeros z_k represent the eigenvalues of the scattering problem for $k = 1, ..., n$. We assume these to be simple. Similarly $S_{22}(z)$

is analytic in the lower-half z-plane. The domains of analyticity of $S_{12}(z)$ and $S_{21}(z)$ are determined by the asymptotic decay of $q(x)$ as $|x| \to \infty$. If this is faster than any exponential, it transpires $S_{12}(z)$ and $S_{21}(z)$ are analytic in a band about the ξ-axis but for algebraically decaying potentials they need not be analytic anywhere.

The method proceeds by writing equations (1.17) as a pair of Riemann-Hilbert problems which may be solved using the calculus of residues and a suitable projection operator. The details may be followed in [APT04]. This leads to a reconstruction formula for $q(x)$ in terms of the scattering data, Jost solutions and eigenvalues z_k.

By considering time dependent Jost solutions which solve (1.14) in the limits $|x| \to \infty$, it may be shown that the scattering data has the simple time dependence:

$$\begin{aligned} S_{11}(x,t,z) &= S_{11}(x,t_0,z), \\ S_{12}(x,t,z) &= S_{12}(x,t_0,z)\exp\left(iz^2(t-t_0)\right). \end{aligned} \tag{1.19}$$

As $S_{11}(x,t,z)$ is constant in time its zeros z_k are fixed. The off-diagonal scattering data $S_{12}(z)$ and $S_{21}(z)$ give rise to radiation terms. The general solution consists of solitons and radiation with the solitons travelling in the midst of the radiation. Solutions with radiation terms have oscillatory behaviour which disperses and decays with time leaving soliton solutions in the asymptotic limit. However the exact phase shifts of soliton solutions upon interaction with the radiation are difficult to determine (see [AS81]) and the explicit solution is often intractable. Purely soliton solutions to the SNLS result from the reflectionless potential case, $S_{12}(z) \equiv 0$ and $S_{21}(z) \equiv 0$ on $\eta = 0$. The Jost solutions may then be solved for relatively easily to give the soliton solution if time dependence of scattering data and Jost solutions is also considered. For the one soliton case where $S_{11}(z)$ has a single simple zero $z_1 = \xi_1 + i\eta_1$ we find that

$$q(x,t) = \eta_1 \exp\left(-i\{\xi_1 x + (\xi_1^2 - \eta_1^2)(t-t_0) + \psi\}\right) \operatorname{sech}\left(\eta_1 x + 2\xi_1\eta_1(t-t_0) - \delta\right) \tag{1.20}$$

where

$$\exp(\delta) = \frac{1}{2\eta_1}\left|\frac{S_{12}(t_0,z_1)}{S_{11}'(t_0,z_1)}\right|, \qquad \exp(i\psi) = i\frac{S_{12}(t_0,z_1)}{S_{11}'(t_0,z_1)}\left|\frac{S_{12}(t_0,z_1)}{S_{11}'(t_0,z_1)}\right|^{-1}.$$

This is equivalent to (1.5) and we note that by setting $z_1 = i$ and $\delta = \psi = t_0$ we recover the soliton solution (1.6).

The procedure of this method is by no means the only one. Other approaches are explored in [FT87] and in Zakharov and Shabat's original paper [ZS72] the authors proceed using

linear algebra techniques to find the square intensity of a soliton solution in the form

$$|q(x,t)|^2 = 2\frac{\partial^2}{\partial x^2}\ln\left\{\det(\mathbb{I}_N + B\overline{B})\right\} \tag{1.21}$$

where the matrix $B = (B_{jk})$ for $j,k = 1,...,N$ has components

$$B_{jk} = \frac{\sqrt{c_j(t)\overline{c_k}(t)}}{z_j - \overline{z_k}}\exp\left(\frac{i}{2}(z_j - \overline{z_k})x\right)$$

with $c_j(t) = c_j(0)\exp(iz_j^2 t)$ and $\mathbb{I}_N$ the $N \times N$ identity matrix.

For the finite gap problem the single sheeted z-plane with simple zeros z_k is replaced by a two-sheeted Riemann surface linked by branch points with connecting branch cuts, as we will show later. A suitable asymptotic limit in which the branch cuts are closed will reproduce the soliton solutions presented in this section.

1.4.3 IST method on the infinite line - repulsive case

We now turn to the repulsive case of the SNLS for which rapidly decreasing boundary conditions are inappropriate - the self-adjoint nature means all eigenvalues must be real yet the condition $\det S(\xi) = 1$ reads

$$|S_{11}(\xi)|^2 - |S_{12}(\xi)|^2 = 1 \tag{1.22}$$

in the repulsive case. Thus $|S_{11}(\xi)| > 0$ and no eigenvalues exist on the real line $\eta = 0$. Instead, the finite density boundary conditions $q \to \rho\exp(i\alpha^{\pm})$ as $x \to \pm\infty$ are of physical interest. Up to a change of variables, α^+ may be set equal to zero and ρ unitised hence $q \to 1$ as $x \to +\infty$. Zakharov and Shabat [ZS73] allow α^- to be a function of t but prove during the course of their work that it is in fact independent of t. Jost solutions $\boldsymbol{\phi}^{(1)}(x,z)$ and $\boldsymbol{\phi}^{(1)}(x,z)$ to the scattering problem $\boldsymbol{v}_x = \mathcal{L}_1^-(z)\boldsymbol{v}$ have the asymptotic limits

$$\boldsymbol{\phi}^{(1)} \sim \begin{pmatrix} 1 \\ i(\frac{\xi}{2} - \zeta)\exp(-i\alpha^-) \end{pmatrix}\exp\{-i\zeta(\xi)x\} \qquad x \to -\infty,$$

$$\boldsymbol{\psi}^{(1)} \sim \begin{pmatrix} 1 \\ i(\frac{\xi}{2} - \zeta) \end{pmatrix}\exp\{-i\zeta(\xi)x\} \qquad x \to +\infty$$

where $z = \xi + i\eta$. $\zeta(z) = \sqrt{\left(\frac{z}{2}\right)^2 - 1}$ is a doubly-valued function of z defining a two-sheeted Riemann surface with branch cuts connecting $-\infty$ to -2 and 2 to ∞ along the real $\eta = 0$ axis. For the Jost solutions $\zeta(\xi)$ is considered real and so $|\xi| \geq 2$. These solutions possess

an anti-holomorphic involution allowing complementary Jost solutions

$$\boldsymbol{\phi}^{(2)}(x,z) = \begin{pmatrix} \overline{\phi_2^{(1)}}(x,z) \\ \overline{\phi_1^{(1)}}(x,z) \end{pmatrix}, \qquad \boldsymbol{\psi}^{(2)}(x,z) = \begin{pmatrix} \overline{\psi_2^{(1)}}(x,z) \\ \overline{\psi_1^{(1)}}(x,z) \end{pmatrix}$$

to be defined. As in the attractive case, soliton solutions to the repulsive SNLS are found by constructing a scattering matrix $S(z) = (S_{ij})$ which transforms the asymptotic forms as $x \to -\infty$ to those as $x \to +\infty$, that is

$$\boldsymbol{\phi}^{(i)} = \sum_{j=1}^{2} S_{ij}(z)\boldsymbol{\psi}^{(j)} \qquad i = 1, 2. \tag{1.23}$$

For real z the system $\boldsymbol{v}_x = \mathcal{L}_1^- \boldsymbol{v}$ is invariant under the involution $v_1 \to \overline{v_2}$ and $v_2 \to \overline{v_1}$. This means the scattering matrix has the conjugation properties

$$S_{11}(z) = \overline{S_{22}}(z), \qquad S_{12} = \overline{S_{21}}(z). \tag{1.24}$$

Given that the Wronskians $W\left(\boldsymbol{\psi}^{(1)}, \boldsymbol{\psi}^{(2)}\right)$ and $W\left(\boldsymbol{\phi}^{(1)}, \boldsymbol{\phi}^{(2)}\right)$ are constant with respect to x, we may evaluate them at $\pm\infty$ respectively to give

$$W\left(\boldsymbol{\psi}^{(1)}, \boldsymbol{\psi}^{(2)}\right) = W\left(\boldsymbol{\phi}^{(1)}, \boldsymbol{\phi}^{(2)}\right) = -2\zeta\left(\zeta - \frac{z}{2}\right) \tag{1.25}$$

and hence, as $W\left(\boldsymbol{\phi}^{(1)}, \boldsymbol{\phi}^{(2)}\right) = \det S(z) W\left(\boldsymbol{\psi}^{(1)}, \boldsymbol{\psi}^{(2)}\right)$,

$$\det S(z) = S_{11}(z)\overline{S_{11}}(z) - S_{12}(z)\overline{S_{12}}(z) = 1. \tag{1.26}$$

We may also notice that

$$S_{11}(z) = \frac{W\left(\boldsymbol{\phi}^{(1)}, \boldsymbol{\psi}^{(2)}\right)}{W\left(\boldsymbol{\psi}^{(1)}, \boldsymbol{\psi}^{(2)}\right)} = \frac{W\left(\boldsymbol{\psi}^{(2)}, \boldsymbol{\phi}^{(1)}\right)}{2\zeta\left(\zeta - \frac{z}{2}\right)}. \tag{1.27}$$

We now return to $\zeta(z) = \sqrt{\left(\frac{z}{2}\right)^2 - 1}$ but allow z to be imaginary and define $\mathrm{Im}(\zeta(z)) > 0$ on the upper sheet and $\mathrm{Im}(\zeta(z)) < 0$ on the lower sheet. Zakharov and Shabat [ZS73] prove that $\boldsymbol{\phi}^{(1)}$ and $\boldsymbol{\psi}^{(2)}$ may be analytically continued onto the upper sheet of the Riemann surface and hence $S_{11}(z, \zeta)$ is also analytic on the upper sheet. Eigenvalues of the system $L^-\boldsymbol{v} = z\boldsymbol{v}$ are possible for bounded Jost solutions and occur for linearly dependent $\boldsymbol{\phi}^{(1)}$ and $\boldsymbol{\psi}^{(2)}$, that is at the zeros of $S_{11}(z)$. As L^- is self-adjoint, any eigenvalues must be real and also, for real $\zeta(z)$, we have the relation (1.26) which rules out any zeros in the range $|z| > 2$. This means all eigenvalues must lie in the segment $(-2, 2)$ of the real z-axis. If a given eigenvalue is denoted Y_k, a useful variable to introduce is the angle ψ_k between

the lines OY_k and $O\sqrt{4-Y_k^2}$, see Figure 1.1. This will crop up in the Hirota dark soliton solutions described in Section 3.5.

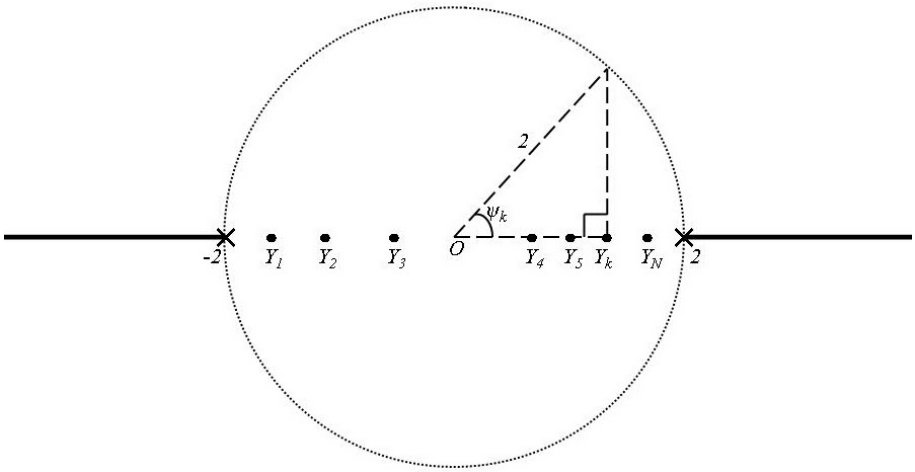

Figure 1.1: Dark soliton spectrum - *crosses represent branch points at* ± 2 *with branch cuts going to infinity. The scattering data are the points* Y_k *with the angle* ψ_k *forming an angle of the triangle with dashed sides.*

Having found the position of eigenvalues in the repulsive case we do not pursue the derivation of the solution any further. The eigenvalues' positions and the fact they lie on a two-sheeted Riemann surface will be of interest in later work investigating the soliton limits of finite gap solutions but forms of the dark soliton solutions themselves are well-known. The interested reader can follow the method through to solution in [ZS73].

1.4.4 Finite gap solutions

For periodic initial potentials $q(x)$ the scattering problem (1.13) becomes a Floquet problem with the condition that eigenfunctions remain bounded for all x imposed. Whilst in the attractive case the soliton solutions are determined by zeros of the scattering data $S_{11}(z)$ lying on a single complex sheet, in the periodic case two sets of scattering data are required to determine the solution and these lie on a Riemann surface, a complex manifold which shall be defined in the following chapter. There are various methods of finding reconstruction formulae for these sets of scattering data, the one followed here is presented in [Sil99] and involves the construction of a bilinear form.

Consider the scattering problem formed by (1.13) and (1.14) in the attractive case. $\mathcal{L}_1^+(z)$ and $\mathcal{L}_2^+(z)$ satisfy the conjugation property (1.16) and so, if $\boldsymbol{\phi}(z)$ is a solution, $\boldsymbol{\psi}(z) = \overline{\boldsymbol{\phi}}(z)$

satisfies the equations

$$\boldsymbol{\psi}_x^{\mathsf{T}}(z) = -\boldsymbol{\psi}^{\mathsf{T}}(z)\mathcal{L}_1^+(z), \qquad \boldsymbol{\psi}_t^{\mathsf{T}}(z) = -\boldsymbol{\psi}^{\mathsf{T}}(z)\mathcal{L}_2^+(z).$$

The matrix $\rho(z) = \boldsymbol{\phi}(z)\boldsymbol{\psi}^{\mathsf{T}}(z)$ may then be formed to give a bilinear version of the scattering problem:

$$\rho_x(z) = [\mathcal{L}_1^+(z), \rho(z)], \tag{1.28}$$
$$\rho_t(z) = [\mathcal{L}_2^+(z), \rho(z)]. \tag{1.29}$$

From these equations it is clear that $\mathrm{Tr}\rho$ is independent of x and t. Also $\det\rho = 0$ by construction. Defining

$$\rho(z) = \begin{pmatrix} \rho_{11}(z) & \rho_{12}(z) \\ \overline{\rho_{12}}(z) & \rho_{22}(z) \end{pmatrix},$$

these two results mean

$$\begin{aligned} \rho_{11}(z)\rho_{22}(z) - \rho_{12}(z)\overline{\rho_{12}}(z) = 0, \\ \rho_{11}(z) + \rho_{22}(z) = P(z) \end{aligned} \tag{1.30}$$

for $P(z)$ some real function of z, independent of x and t. Combination of equations (1.30) gives

$$\{\rho_{11}(z) - \rho_{22}(z)\}^2 = P^2(z) - 4\rho_{12}(z)\overline{\rho_{12}}(z). \tag{1.31}$$

If the assumption is made that each element of ρ is a polynomial in z of order $N+1$, then

$$P^2(z) = A\prod_{k=1}^{2N+2}(z - z_k) \tag{1.32}$$

where A is a constant multiplier. This defines a hyperelliptic curve of genus N. Hyperelliptic curves and Riemann surfaces in general shall be introduced in the next chapter. z_k, the zeros of $P(z)$, are also constant in x and t and are termed the main spectrum. As $P(z)$ has real coefficients, the z_k must occur in conjugate pairs. In contrast to the Riemann-Hilbert problem evaluation in the infinite line case, to reconstruct the potential $q(x,t)$ we must introduce a second set of spectral data called the improper or auxiliary data. This is composed of μ-variables satisfying

$$\rho_{12}(\mu_k) = 0 \qquad k = 1, ..., N, \tag{1.33}$$

where the improper data μ_k evolve with x and t. Given this and equation (1.28) we may

show that ρ_{12} takes the form

$$\rho_{12}(z) = iq(\rho_{11} - \rho_{22})^{(N+1)} \prod_{k=1}^{N} (z - \mu_k) \tag{1.34}$$

where $(\rho_{11} - \rho_{22})^{(k)}$ is the coefficient of z^k in the polynomial $(\rho_{11} - \rho_{22})(z)$. Hence, inspecting the coefficient of z^N in (1.28), we find the expression

$$\frac{q_x}{q} = i \sum_{k=1}^{N} \mu_k + i \frac{(\rho_{11} - \rho_{22})^{(N)}}{(\rho_{11} - \rho_{22})^{(N+1)}}$$

which may be simplified to

$$\frac{q_x}{q} = i \left(\sum_{k=1}^{N} \mu_k - \sum_{k=1}^{2N+2} z_k \right). \tag{1.35}$$

In a similar manner, the expression

$$\frac{q_t}{q} = i \left\{ \left(\sum_{k=1}^{N} \mu_k - \sum_{k=1}^{2N+2} z_k \right)^2 - \left(\sum_{k=1}^{N} \mu_k^2 - \sum_{k=1}^{2N+2} z_k^2 \right) \right\} \tag{1.36}$$

is found and using (1.34) we may calculate the evolution equations for the μ-variables:

$$\begin{aligned} \mu_{k,x} &= \pm i \frac{\prod_{i=1}^{2N+2} (\mu_k - z_i)^{\frac{1}{2}}}{\prod_{j \neq k} (\mu_k - \mu_j)}, \\ \mu_{k,t} &= \mu_{k,x} \left(\sum_{i=1}^{2N+2} z_i - \sum_{j \neq k} \mu_j \right). \end{aligned} \tag{1.37}$$

These both have square-root branch points at the values $\mu_k = z_i$ for $i = 1, ..., 2N + 2$, meaning the auxiliary spectra evolve on a two-sheeted hyperelliptic Riemann surface with the sign determining the choice of sheet.

An alternative way of deriving these equations is to consider a matrix solution $\Phi(x, t, z)$ to the scattering problem. Defining $\widetilde{\rho}(z) = \Phi(z)\Phi^\dagger(z)$, we find $\widetilde{\rho}(z)$ satisfies the same equations as $\rho(z)$. If $\widetilde{\rho}(z)$ is chosen to be traceless, the spectral curve is given by

$$w^2 = \det \widetilde{\rho}(z) = \widetilde{\rho}_{11}^2(z) + \widetilde{\rho}_{12}(z)\widetilde{\rho}_{21}(z) \tag{1.38}$$

and the auxiliary data is then defined to satisfy

$$\widetilde{\rho}(\widetilde{\mu}_k)\begin{pmatrix}1\\0\end{pmatrix} = w(\widetilde{\mu}_k)\begin{pmatrix}1\\0\end{pmatrix}. \tag{1.39}$$

The equations (1.37) are set in canonical form by transforming the dynamical variables μ_k to action variables η_k via an Abel mapping

$$\eta_k = \sum_{i=1}^{N}\int_{P_0}^{P_k} \mathrm{d}\omega_k.$$

$P_k = (\mu_k, \sigma_k)$, that is μ_k with a choice of sheet indicated by σ_k, P_0 is a base point and

$$\mathrm{d}\omega_k = \sum_{j=1}^{N} c_{kj}\frac{z^{g-j}\mathrm{d}z}{\prod_{i=1}^{2N+2}(z-z_i)^{\frac{1}{2}}} \qquad k = 1, ..., N$$

are normalised Abelian differentials. The evolution equations for the canonical variables are easily integrated and the potential $q(x,t)$ is then expressible as a ratio of theta functions - concepts which will be introduced in the next chapter. This identification of the action variables also provides a clear bridge to the algebrogeometric approach which we study later.

1.4.5 IST method and the VNLS

The extension of the IST method to finding soliton solutions to the attractive VNLS (1.1) goes through relatively straightforwardly. We do not pursue it here but direct the reader to and articles by Ablowitz, Prinari and Trubatch [APT04]. However, we do note that the one soliton solution to the VNLS is given simply by the one soliton solution to the SNLS (1.5) multiplied by a constant unit vector representing the polarisation state. This is not the case for interacting soliton solutions where differing polarisation states are altered by soliton collisions.

Work using the IST method to find grey-grey soliton and grey-bright soliton solutions to the repulsive VNLS has recently been published by Prinari, Ablowitz and Biondini [PAB06]. The terminology indicates either both solution components are grey solitons or one is grey and one bright. In principle, we should be able to derive these soliton solutions as the limits of finite gap solutions, found by appropriately 'pinching' branch cuts. We shall demonstrate this for the scalar problem but in the vector case the method is complicated by the three-sheeted structure of the Riemann surface.

Silmon-Clyde [Sil99] attempts to extend the bilinear method which we applied to the SNLS

in the previous section to the VNLS case. However, this approach runs into problems: As shall be shown in Chapter 4, the natural surface upon which the scattering data and μ-variables should lie is a three-sheeted surface but Silmon-Clyde's method forces these onto a two-sheeted hyperelliptic curve as in the scalar case. The solution is then, in general, intractable.

1.5 Algebrogeometric approach

Based upon an idea of Krichever this approach was developed in the late 1970s by various authors and applied to the SNLS by Its and Kotlyarov [IK76]. Solutions result from consideration of the spectral curve formed from the scattering problem, namely a compact Riemann surface and in the case of the SNLS a hyperelliptic curve. By defining Baker-Akhiezer functions with appropriate essential singularities at infinite points on the relevant Riemann surface, the finite gap potential may be constructed. This will, in general, be a quasiperiodic function and take the form of a ratio of generalised theta functions along with an exponential factor which acts to cancel any periodic growth or decay. A detailed analysis of this approach with particular attention to the SNLS and sine-Gordon equations may be found in [BBE94]. In the case of the VNLS, the spectral curve is in general three-sheeted and thus more complicated than in the scalar problem but quasiperiodic solutions have been found, in particular by Elgin et al. [EEI07] and Christiansen et al. [CEE00].

1.6 Hirota's method

Hirota's method is a standard method devised by Ryogo Hirota for obtaining single and multi-soliton solutions to a large class of nonlinear PDEs. Although its effectiveness is very clear, Hirota himself described the method as 'one based on intuition and experience' in his 1973 paper [Hir73]. However, in the 1980s, the theory came to be better understood, particulary as a result of work by Sato and the Kyoto school. Unlike the inverse scattering transform method, Hirota's method is applied directly to the PDE and generally produces results for any PDE that may be solved by the IST method and some equations where no IST is available. By a change of dependent variables, the PDEs may be transformed into bilinear differential equations involving the Hirota bilinear operator

$$D_x\left(a(x)\circ b(x)\right) = (\partial_x - \partial_{x'})a(x)b(x')\big|_{x=x'} \tag{1.40}$$

to which solutions may then be found by assuming a formal perturbation expansion for the new dependent variables.

Hirota's method may be used to construct arbitrary order soliton solutions to the SNLS and indeed the VNLS, as shown by Sheppard and Kivshar [SK97]. The form of these solutions is as ratios of sums of exponential phases which are clearly related to the ratios of theta functions found via the algebrogeometric approach. The procedure for developing soliton solutions to the SNLS is presented in Appendix B.

1.7 Thesis overview

The work of this thesis will largely focus on the algebrogeometric approach. This is the method most recently developed and is perhaps the most versatile. Use of the inverse scattering transform method to find finite gap solutions to the VNLS (1.1) has proved very difficult, whilst the algebrogeometric approach extends relatively easily from the scalar case [EEI07].

Chapter 2 will concentrate upon introducing the notions of Riemann surfaces, Abelian functions and differentials and Baker-Akhiezer functions which will be needed to apply the algebrogeometric method to the KdV and SNLS in Chapter 3. This provides an introduction to the theory and enables the VNLS case to be studied in a better context. Its [Its82] proved a link between the limits of finite gap solutions to the SNLS and soliton solutions given by Hirota [Hir73], [Hir76]. The results, in the attractive case particularly, are not entirely intuitive and in Section 3.5 we shall attempt to provide more robust reasons as well as elaborating on some of this work.

In Chapter 4 we introduce the VNLS hierarchy as a natural extension of the Manakov system. We also provide proofs of many of the results regarding the related spectral curves which were either postulated or obtained computationally by Elgin et al. [EEI07]. Conserved densities of the hierarchy are also derived. We then move on to calculate finite gap solutions to the VNLS using the method described in [EEI07].

Chapter 5 will be devoted to a method used by Christiansen et al. [CEE00] to find separable solutions to the VNLS with a trivial time dependence. We wish to compare these to those solutions found in [EEI07]. Interestingly the spectral curve of interest in [CEE00] is of genus two whereas those in [EEI07] are of only odd genus.

Finally, in Chapter 6, we shall map solutions to the VNLS of an entirely general form to a Stokes vector on the Poincaré sphere. By determining the evolution equation of this vector we will explore analogies to the gauge equivalence of the Heisenberg ferromagnet equation and SNLS as proven by Zakharov and Takhtadzhyan [ZT79] following earlier work by Lakshmanan [Lak77].

Chapter 2

Riemann surfaces

As we have already touched upon and shall show in Chapters 3 and 4, the spectral curves allied to the SNLS and VNLS hierarchies define hyperelliptic and trigonal Riemann surfaces respectively. The algebrogeometric method which we will use to find solutions to these hierarchies uses several valuable theorems involving Baker-Akhiezer functions defined upon Riemann surfaces. Before presenting these theorems at the end of this chapter, we shall first introduce Riemann surfaces, divisors, Abelian differentials and integrals and present several important results to be used in later work. Generalised theta functions shall then be discussed and used to define the Baker-Akhiezer functions of relevance to the method.

The interested reader will find many books on the theory of Riemann surfaces - a few of particular note are: [Spr57], [Sie71], [RF74] and [FK80]. We begin by defining a Riemann surface and giving some examples.

Definition 2.1 *A Riemann Surface is a complex analytic manifold X satisfying the following conditions:*

1. There exists a collection of open subsets U_i covering X with associated homeomorphisms $\phi_i : U_i \to V_i \subset \mathbb{C}$ where V_i are open subsets of $\mathbb{C}$. The homeomorphisms are called the local parameters of the Riemann surface.
2. If $U_i \cap U_j \neq \emptyset$, then $\phi_i \circ \phi_j^{-1} : \phi_j(U_i \cap U_j) \to \phi_i(U_i \cap U_j)$ is a holomorphic function of $\lambda \in \phi_j(U_i \cap U_j) \subset \mathbb{C}$.

Examples 2.1

1. *Any open subset of* $\mathbb{C}$

2. $\mathbb{C}$ *itself*

   In both these cases identity mappings may be used as local parameters.

3. *The sphere* $S^2 = \left\{ \mathbf{x} \in \mathbb{R}^3 \,\middle|\, |\mathbf{x}|^2 = 1 \right\}$

   This may be made into a Riemann surface by means of a stereographic projection. The open subsets covering S^2 are

   $$\begin{aligned} U_1 &= S^2 \backslash \{(0,0,1)\}, \\ U_2 &= S^2 \backslash \{(0,0,-1)\}, \end{aligned}$$

   and their respective local parameters are

   $$\begin{aligned} \phi_1(\boldsymbol{x}) &= \frac{x_1 + ix_2}{1 - x_3}, \\ \phi_2(\boldsymbol{x}) &= \frac{x_1 - ix_2}{1 + x_3}, \end{aligned}$$

   where $\boldsymbol{x} = (x_1, x_2, x_3)$.

4. $\mathbb{C} \cup \{\infty\}$ *the extended complex plane.*

   Mapping $\mathbb{C}$ to $S^2 \backslash \{(0,0,1)\}$ by an inverse stereographic projection with the point at infinity mapping to $(0,0,1)$, it may be shown $\mathbb{C} \cup \{\infty\}$ is topologically equivalent to S^2. In this context $\mathbb{C} \cup \{\infty\}$ is known as the Riemann sphere.

5. *Non-singular algebraic curves in* $\mathbb{C}^2$ *such as*

   $$X = \left\{ (\mu, z) \in \mathbb{C}^2 \,\middle|\, P(\mu, z) = 0, \left(\frac{\partial P}{\partial \mu}, \frac{\partial P}{\partial z} \right) \Big|_{P(\mu,z)=0} \neq (0,0) \right\}$$

   where P is a polynomial in its arguments. An important example from this class of Riemann surfaces is the hyperelliptic curve covered in the next section.

2.1 Hyperelliptic curves

Definition 2.2 *A compact Riemann surface X is defined to be hyperelliptic if there exists a meromorphic function on X with exactly two poles including multiplicities. X may be represented algebraically by the curve*

$$X = \left\{ (\mu, z) \,\middle|\, z \in \mathbb{C} \cup \{\infty\}, \mu^2 = \prod_{k=1}^{n} (z - e_k) \right\}, \tag{2.1}$$

where e_k are distinct branch points on the extended complex plane and $n > 2$.[1]

The hyperelliptic curve (2.1) is of the form given in Example 5 above. Technically there is a singularity as $z \to \infty$ (realised by homogenising the curve) but by having two points at infinity, one on each sheet, and choosing suitable local parameters the curve is desingularised. We shall bear this point in mind but for the curves studied in this thesis we will consider the desingularised version. X represents a multiply-valued function given by $f(z,\mu) = \mu^2 - \prod_{k=1}^{n}(z - e_k) = 0$. This function may also be represented as two extended complex planes with branch cuts. A continuous path crossing a branch cut will pass from one plane to the other. If n is even, the branch cuts connect the branch points e_k and there are two points at infinity, one on each extended plane, which shall be denoted $\infty^{\pm}$. This case is presented in Figure 2.1. If n is odd, there is only one point at infinity, denoted ∞, and it is a branch point. We can however send a finite branch point to infinity via an invertible rational mapping. In the case of (2.1), for n even, the mapping

$$z = e_n + \frac{1}{\widehat{z}}, \qquad e_k = e_n + \frac{1}{\widehat{e}_k}, \qquad \widehat{\mu}^2 = -\mu^2 \widehat{z}^n \prod_{k=1}^{n-1} \widehat{e}_k,$$

sends e_n to infinity:

$$\widehat{\mu}^2 = \prod_{k=1}^{n-1} (\widehat{z} - \widehat{e}_k).$$

The cycles a_j and b_j form a first homology group, introduced in Subsection 2.1.2. The surface is said to be of genus g and has $2g + 2$ branch points, see Theorem 2.5.

Local parameters enable a function holomorphic at a certain point $P = (z,\mu) \in X$ to be expressed as a convergent Taylor series in a neighbourhood of P. In the case of the hyperelliptic curve, at branch points $P = (e_k, 0)$ the local parameter $\xi = \sqrt{z - e_k}$ is used. For points at ∞ the relevant local parameter is $\xi = 1/z$ unless n is odd in which case $z \to \infty$ is a branch point and $\xi = 1/\sqrt{z}$. For all other points $(\widetilde{z}, \mu(\widetilde{z}))$, $\xi = z - \widetilde{z}$ suffices. Note that we will use z as the standard complex variable on the Riemann surfaces encountered in this thesis with appropriate local parameters used at any branch point or point at infinity.

[1] Some authors describe curves with $n = 3$ or 4 as elliptic and refer only to those with $n > 4$ as hyperelliptic.

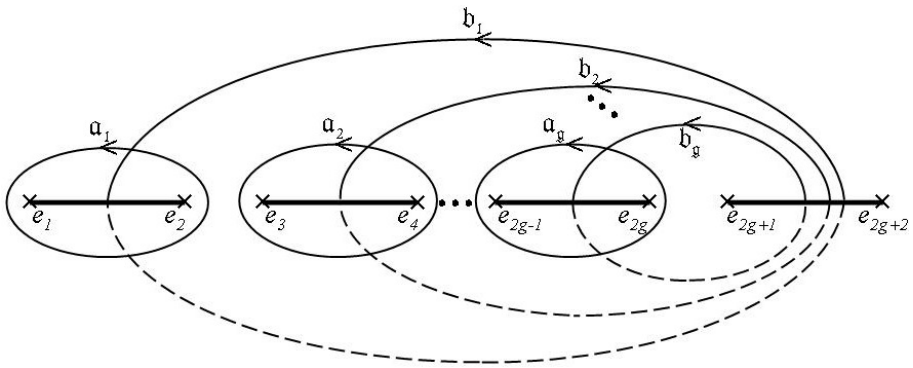

Figure 2.1: Real hyperelliptic surface of genus g - *real branch points* e_j *are denoted by crosses, branch cuts by bold lines and cycles in the first homology group by continuous lines on the top sheet and dashed lines on the bottom sheet*

2.1.1 The hyperelliptic curve as a Riemann sphere with handles

As well as being represented as two extended planes with branch cuts, X may be represented as a Riemann sphere with a given number of handles. The number of handles is termed the genus g of the Riemann surface. A Riemann sphere with g handles is topologically equivalent to a g-torus.

Consider the two extended planes forming X in (2.1) for $n = 6$ and map each to a sphere by stereographic projection. If the branch cuts are opened into tubes connecting the two spheres then the resulting surface is topologically equivalent to a Riemann sphere with g handles, where g is given by

$$g = \frac{n}{2} - \frac{\{3 + (-1)^n\}}{4}. \tag{2.2}$$

This, in turn, is topologically equivalent to a torus with g holes. Examples for $g = 1$ and $g = 2$ are given in Figures 2.2 and 2.3:

2.1.2 The first homology group

A cycle on a compact Riemann surface X is a closed contour with a prescribed direction of traverse. Cycles may be added to and subtracted from one another by suitable deformation and direction change. Any two cycles are equivalent or homotopic if their difference is zero, meaning the difference is a cycle that may be contracted to a point. Thus, if a, b and c are three cycles with $a + b = c$, then $a + b$ is equivalent to c as $a + b + (-c) = 0$ where $-c$ is c traversed in the opposite direction.

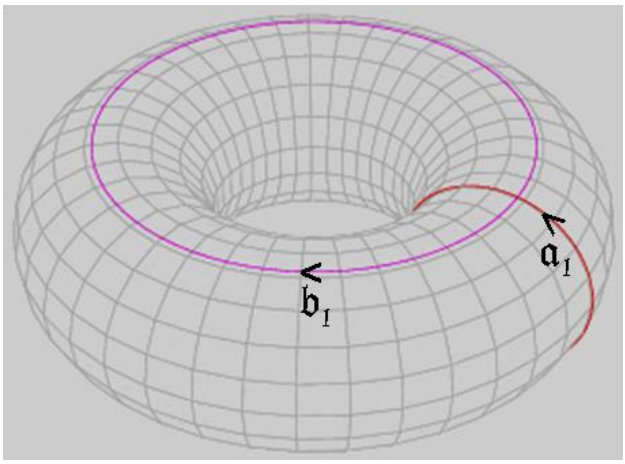

Figure 2.2: Torus of genus one with homology basis

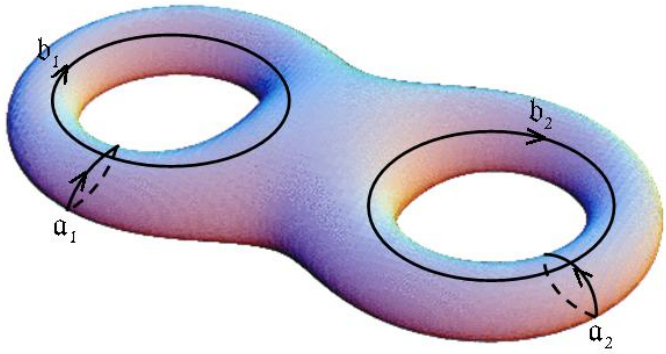

Figure 2.3: Torus of genus two with homology basis

Using the equivalence of cycles as a factorization of the set of all cycles, the first homology group $H_1(X, \mathbb{Z})$ of the Riemann surface X is formed. The group has dimension $2g$ and a basis

$$\{a_j, b_j \mid j = 1, ..., g\} \tag{2.3}$$

may be chosen such that there are g right-hand oriented cycle intersections between pairs a_j, b_j. By this it is meant $a_i \circ b_j = \delta_{ij}$ and $b_i \circ a_j = -\delta_{ij}$ where $\circ$ is the intersection operator. This basis is called the homology basis and is shown for the hyperelliptic curve in Figure 2.1. Notice that none of the $2g$ cycles may be contracted to points.

If we deform the basis such that the points of intersection all converge on a point. Then by cutting the Riemann surface along each cycle in turn and flattening the resulting surface a

$4g$-gon is formed. This process is known as the canonical dissection of a Riemann surface. The dodecagon formed in the genus 3 case is presented in Figure 2.4 where a_i^+ represents the left-hand side of the cut along a_i and a_i^- represents the right-hand side. Similarly for $b_i^{\pm}$. Thus the boundary of $\widetilde{X}$ is given by

$$\partial \widetilde{X} = \sum_{i=1}^{g} \left(a_i^+ + b_i^+ - a_i^- - b_i^- \right). \tag{2.4}$$

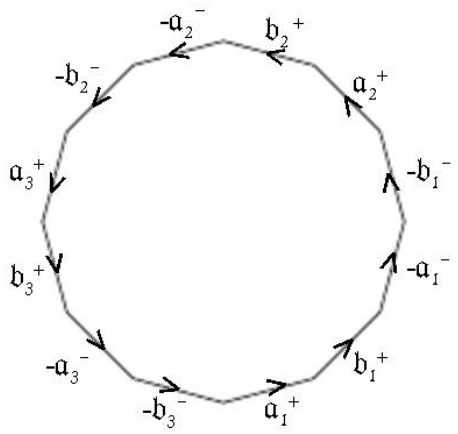

Figure 2.4: Canonical dissection of a Riemann Surface of genus 3

2.2 Divisors

A divisor $\mathcal{D}$ is a formal finite sum of points on a Riemann surface X with attached integral coefficients, written as

$$\mathcal{D} = \sum_{i=1}^{n} n_i P_i \qquad \text{for } P_i \in X,\ n_i \in \mathbb{Z}. \tag{2.5}$$

The degree of $\mathcal{D}$ is defined to be

$$\deg(\mathcal{D}) = \sum_{i=1}^{n} n_i. \tag{2.6}$$

In relation to functions and differentials defined upon X, divisors denote the zeros and poles of the relevant function or differential. $n_i > 0$ denotes a zero of order n_i at P_i and similarly $n_i < 0$ denotes a pole of order $-n_i$ at P_i.

A positive divisor is one for which $n_i \geq 0$ for all i and is written $\mathcal{D} \geq 0$. A negative divisor

similarly has $n_i \leq 0$ for all i. If the difference of two divisors is positive, that is $\mathcal{D}' - \mathcal{D} \geq 0$ then one may write $\mathcal{D}' \geq \mathcal{D}$ and say $\mathcal{D}'$ is divisible by $\mathcal{D}$.

The set of all divisors on a Riemann surface X is a group under the formal addition operation and is denoted $\mathrm{Div}(X)$.

2.3 Abelian differentials

Definition 2.3 *An Abelian differential is a holomorphic or meromorphic one-form* $\mathrm{d}\omega : X \to \mathbb{R}$ *on a Riemann surface* X.

Abelian differentials are given in local parameter z by

$$\mathrm{d}\omega = f(z)\mathrm{d}z \tag{2.7}$$

where $f(z)$ is a holomorphic or meromorphic function with a suitable Taylor or Laurent expansion in local parameters. The residue of a meromorphic Abelian differential at a pole $P \in X$ is then defined by

$$\mathrm{Res}(\mathrm{d}\omega, P \in X) = a_{-1} \tag{2.8}$$

where $f(z)$ has the Laurent expansion $f(z) = \sum_{i=-n}^{\infty} a_i \xi^i$ with ξ the local parameter in the neighbourhood of the point P. It may be proved that the residue at a point P is independent of the local parameter chosen.

It is common practice to divide Abelian differentials into three classes:

1. Holomorphic differentials
2. Meromorphic differentials with all poles having zero residue
3. Meromorphic differentials with the sum of all residues equal to zero.

Definition 2.4 *An Abelian differential of the second class,* $\mathrm{d}\Omega$*, is defined to be normalised if* $\int_{a_k} \mathrm{d}\Omega = 0$ *for* $k = 1, ..., g$.

Definition 2.5 *An Abelian differential of the third class,* $\mathrm{d}\Omega$*, is defined to be normalised if* $\int_{a_k} \mathrm{d}\Omega = 0$ *for* $k = 1, ..., g$ *and, in addition, it has two singularities at points* P *and* Q *with respective principal parts:* $\alpha \frac{\mathrm{d}z_P}{z_P}$ *and* $-\alpha \frac{\mathrm{d}z_Q}{z_Q}$ *where* z_P *and* z_Q *are the respective local parameters and* α *is a constant.*

Stokes's theorem may be applied to Abelian differentials on a Riemann surface and is stated as:

Theorem 2.1 *If R is a regular region of X, let ∂R be its boundary with a direction of traverse such that R is always on the left. Then any Abelian differential $\mathrm{d}\omega$ satisfies*

$$\int_{\partial R} \mathrm{d}\omega = \int\int_{R} \mathrm{d}\left(\mathrm{d}\omega\right). \tag{2.9}$$

Cauchy's residue theorem follows from this:

Theorem 2.2 *If R is a regular region of X with boundary ∂R described previously then, for any Abelian differential, $\mathrm{d}\omega$ meromorphic on R with poles at $z_k \in R$ for $k = 1, ..., n$,*

$$\int_{\partial R} \mathrm{d}\omega = 2\pi i \sum_{k=1}^{n} \mathrm{Res}\left(\mathrm{d}\omega, z_k\right). \tag{2.10}$$

2.3.1 Basis of holomorphic Abelian differentials

Theorem 2.3 (*Riemann*) *The space of holomorphic differentials on a Riemann surface of genus g has dimension g.*

For the hyperelliptic curve (2.1), a suitable basis $\{\mathrm{d}\widetilde{\omega}_1, ..., \mathrm{d}\widetilde{\omega}_g\}$ of the space of holomorphic differentials is given by

$$\mathrm{d}\widetilde{\omega}_j = \frac{z^{g-j}}{\mu}\mathrm{d}z. \tag{2.11}$$

Changing to local parameters at the branch points and the points at infinity $\infty^{\pm}$ verifies these differentials are holomorphic everywhere on X.

For more general Riemann surfaces finding a basis proves more difficult. Deconinck and van Hoeij [DH01] set out a method of calculation for singular and non-singular curves and include a Maple program which we have used in later work on trigonal curves.

Once a basis has been found, a normalised basis $\{\mathrm{d}\omega_1, ..., \mathrm{d}\omega_g\}$ may be defined with

$$\mathrm{d}\omega_j = \sum_{k=1}^{g} c_{jk}\mathrm{d}\widetilde{\omega}_k \tag{2.12}$$

and normalisation conditions

$$\int_{a_k} \mathrm{d}\omega_j = 2\pi i \delta_{jk} = \begin{cases} 2\pi i & j = k \\ 0 & j \neq k \end{cases} . \tag{2.13}$$

This is achieved by setting $C = 2\pi i A^{-1}$ where C is the matrix with components c_{jk} and A is the matrix with components $\int_{a_k} \mathrm{d}\omega_j$ for $j, k = 1, ..., g$. The $g \times g$ matrix B may then be defined with elements

$$B_{jk} = \int_{b_k} \mathrm{d}\omega_j. \tag{2.14}$$

2.4 Riemann-Roch and Riemann-Hurwitz theorems

Firstly, a function f or Abelian differential $\mathrm{d}\omega$ is said to be divisible by a divisor $\mathcal{D}$ if its divisor is divisible by $\mathcal{D}$. Then $F_{\mathcal{D}}$ is the linear space of functions meromorphic on a Riemann surface X with divisor divisible by $\mathcal{D}$ and similarly $\mathrm{d}\Omega_{\mathcal{D}}$ shall be the space of differentials divisible by $\mathcal{D}$. The Riemann-Roch theorem is then stated as:

Theorem 2.4 (*Riemann-Roch*) *If $\mathcal{D} \in \mathrm{Div}(X)$ where X is a Riemann surface of genus g, then*

$$\dim\left(F_{-\mathcal{D}}\right) - \dim\left(\mathrm{d}\Omega_{\mathcal{D}}\right) = 1 - g + \deg(\mathcal{D}). \tag{2.15}$$

In conjunction with the Riemann-Roch theorem, the idea of speciality and non-speciality for positive definite divisors of degree $\leq g$ may be introduced:

Definition 2.6 *Any positive definite divisor $\mathcal{D}$ is special if* $\dim\left(F_{-\mathcal{D}}\right) > 1$ *and non-special if* $\dim\left(F_{-\mathcal{D}}\right) = 1$.

Therefore for a non-special divisor $\mathcal{D}$ the only function with divisor divisible by $-\mathcal{D}$ is a constant. A divisor of degree $\leq g$ will be non-special if it has a general position meaning a holomorphic covering of the surface projects the points of the divisor to distinct points. In the case of the hyperelliptic curve (2.1), the holomorphic covering maps the curve to the extended complex plane via

$$\begin{aligned} &\pi : X \to \mathbb{C} \cup \{\infty\} \\ &\pi(P) = z, \qquad\qquad \text{where} \quad P = (z, \mu). \end{aligned}$$

So a non-special divisor $\mathcal{D} = \sum_{i=1}^{k} P_i$ satisfies $\pi(P_i) \neq \pi(P_j)$ if $P_i \neq P_j$.

We now present the Riemann-Hurwitz formula which is used to establish the genera of Riemann surfaces.

Theorem 2.5 *If X is a compact Riemann surface, realised as a p-sheeted cover of the Riemann sphere with branch cuts connecting sheets, then the genus of X, denoted g, is related to the total branch number N via the formula*

$$g = \frac{N}{2} - p + 1. \tag{2.16}$$

N is defined to be the sum of all branch point orders where a branch point connecting k sheets has order $k - 1$. Applied to a hyperelliptic curve with n branch points each connecting two sheets, $n = N$ and $p = 2$, which means

$$g = \frac{n}{2} - 1. \tag{2.17}$$

The hyperelliptic curve (2.1) may thus be written

$$\mu^2 = \prod_{k=1}^{2g+2} (z - e_k). \tag{2.18}$$

2.5 Abelian integrals and the Riemann bilinear relations

Definition 2.7 *If $\mathrm{d}\Omega$ is an Abelian differential on a Riemann surface X and P_0 is a base point on X, an Abelian integral is defined by*

$$\Omega(P) = \int_{P_0}^{P} \mathrm{d}\Omega. \tag{2.19}$$

$\Omega(P)$ is, in general, multiply-valued, taking different values according to the path taken between P_0 and P on X. Corresponding to the three classes of Abelian differential, Abelian integrals are divided into three classes:

1. Holomorphic integrals
2. Meromorphic integrals
3. Integrals with essential logarithmic singularities.

Let $\int_{P_0}^{P} \mathrm{d}\Omega_1$ and $\int_{P_0}^{P} \mathrm{d}\Omega_2$ be Abelian integrals of classes 1 and 2 respectively. If γ and δ are two continuous paths on X from P_0 to P then, for $i = 1, 2$

$$\int_{\gamma} \mathrm{d}\Omega_i - \int_{\delta} \mathrm{d}\Omega_i = \int_{\gamma-\delta} \mathrm{d}\Omega_i = \sum_{j=1}^{g} \left(m_j \int_{a_j} \mathrm{d}\Omega_i + n_j \int_{b_j} \mathrm{d}\Omega_i \right) \tag{2.20}$$

where $\{a_j, b_j | j = 1, ..., g\}$ is the chosen basis of the first homology group and $m_j, n_j \in \mathbb{Z}$.

This follows from the fact that the difference between γ and δ must be expressible as integer multiples of a_j and b_j plus a cycle homotopic to zero. But the integral of $\mathrm{d}\Omega_i$ around a cycle homotopic to zero must be zero as all residues are zero. Thus an Abelian integral of class 1 or class 2 is single-valued on the canonically dissected Riemann surface $\widetilde{X}$ as long as the path of integration does not intersect the boundary, $\partial\widetilde{X}$.

Theorem 2.6 ([BBE94],p27) *Given any pair of Abelian integrals, $\widetilde{\Omega}(P)$, $\hat{\Omega}(P)$, on a Riemann surface X, the following equality holds*

$$\int_{\partial\widetilde{X}} \hat{\Omega} \mathrm{d}\widetilde{\Omega} = \sum_{k=1}^{g} \left(\int_{a_k} \mathrm{d}\hat{\Omega} \int_{b_k} \mathrm{d}\widetilde{\Omega} - \int_{a_k} \mathrm{d}\widetilde{\Omega} \int_{b_k} \mathrm{d}\hat{\Omega} \right) \tag{2.21}$$

From Theorem 2.6 several corollaries may be deduced for different choices of Abelian integrals, $\widetilde{\Omega}(P)$ and $\hat{\Omega}(P)$.

Corollary 2.1 *For $\widetilde{\Omega}(P)$ and $\hat{\Omega}(P)$ both Abelian integrals of class* 1

$$\sum_{k=1}^{g} \left(\int_{a_k} \mathrm{d}\hat{\Omega} \int_{b_k} \mathrm{d}\widetilde{\Omega} - \int_{a_k} \mathrm{d}\widetilde{\Omega} \int_{b_k} \mathrm{d}\hat{\Omega} \right) = 0 \tag{2.22}$$

Corollary 2.2 *Setting $\mathrm{d}\widetilde{\Omega} = \mathrm{d}\omega_i$ and $\mathrm{d}\hat{\Omega} = \mathrm{d}\omega_j$ and applying* Corollary 2.1 *it follows*

$$B^{\mathsf{T}} = B \tag{2.23}$$

Corollary 2.3 *Setting $\mathrm{d}\widetilde{\Omega} = \mathrm{d}\Omega$ and $\mathrm{d}\hat{\Omega} = \mathrm{d}\overline{\Omega}$ it may be shown*

$$i \sum_{k=1}^{g} \left(\int_{a_k} \mathrm{d}\Omega \int_{b_k} \mathrm{d}\overline{\Omega} - \int_{a_k} \mathrm{d}\overline{\Omega} \int_{b_k} \mathrm{d}\Omega \right) \geq 0 \tag{2.24}$$

Proof: Let $\Omega(P) = u(P) + iv(P)$ where u and v are real functions. Then

$$\begin{aligned}\int_{\partial\widetilde{X}} \overline{\Omega}\mathrm{d}\Omega &= \int_{\partial\widetilde{X}} (u\,\mathrm{d}u + v\,\mathrm{d}v) + i\int_{\partial\widetilde{X}} (u\,\mathrm{d}v - v\,\mathrm{d}u) \\ &= 0 + 2i\int_{\partial\widetilde{X}} \mathrm{d}u\mathrm{d}v\end{aligned}$$

using Green's theorem. The final integral is the expression for the area of $\widetilde{X}$ under the conformal mapping $\Omega(P)$ and must be positive definite unless $\mathrm{d}\Omega = 0$ in which case the integral is zero. Applying the Riemann bilinear relation to the left-hand side and multiplying by $-i$ gives the required inequality. An immediate consequence of Corollary 2.3 is the following important property of the matrix B:

Corollary 2.4 *The matrix B has negative definite real part, meaning*

$$\boldsymbol{x}^{\mathsf{T}}\mathbb{R}\mathrm{e}(B)\boldsymbol{x} < 0 \tag{2.25}$$

for all $\boldsymbol{x} \in \mathbb{R}^g\backslash\{\mathbf{0}\}$ where $\mathbb{R}\mathrm{e}(B) = (B + \overline{B})/2$.

Proof: Set $\mathrm{d}\Omega = \boldsymbol{x}^{\mathsf{T}}\mathrm{d}\boldsymbol{\omega}$ where $\mathrm{d}\boldsymbol{\omega} = (\mathrm{d}\omega_1, ..., \mathrm{d}\omega_g)^{\mathsf{T}}$ and $\boldsymbol{x} \in \mathbb{R}^g\backslash\{\mathbf{0}\}$ and the condition follows from Corollary 2.3. This fact proves important when defining a convergent Riemann theta function in the following section.

2.6 Theta functions

Theta functions were first studied in detail by Jacobi and the genus one theta functions upon which he worked accordingly bear his name. Jacobi's theta functions $\theta_1(z,\tau)$, $\theta_2(z,\tau)$, $\theta_3(z,\tau)$ and $\theta_4(z,\tau)$ are functions of a complex variable z and may additionally be considered a function of τ, a constant complex number with positive imaginary part. $\theta_i(z,\tau)$ are defined by their series expansions but it suffices to write

$$\theta_4(z,\tau) = \sum_{n=-\infty}^{\infty} (-1)^n q^{n^2} \exp(2niz),$$

where $q = \exp(i\pi\tau)$, and then define

$$\begin{aligned}\theta_1(z,\tau) &= -i\exp\left(iz + \frac{\pi i\tau}{4}\right)\theta_4\left(z + \frac{\pi\tau}{2}, \tau\right), \\ \theta_2(z,\tau) &= \exp\left(iz + \frac{\pi i\tau}{4}\right)\theta_4\left(z + \frac{\pi}{2} + \frac{\pi\tau}{2}, \tau\right), \\ \theta_3(z,\tau) &= \theta_4\left(z + \frac{\pi}{2}, \tau\right).\end{aligned}$$

The notation used here is taken from Whittaker and Watson [WW27] who confirm its faithfulness to the original work. Jacobi produced extensive results for genus one theta functions [WW27] and although the definition of a theta function has been extended to higher genus, many of the corresponding results have not been found or proven. It is the general genus theta function developed by Riemann which we shall utilise in this thesis.

Theta functions are quasiperiodic with two 'periods', for example Jacobi's have periods π and $\pi\tau$ and satisfy

$$\theta_4(z+\pi,\tau) = \theta_4(z,\tau), \qquad \theta_4(z+\pi\tau,\tau) = -q^{-1}\exp(-2iz)\theta_4(z,\tau).$$

This quasiperiodicity means that ratios of appropriate theta functions, that is ones where multiplying period factors cancel, are doubly periodic and can be used to define elliptic functions. The Jacobi elliptic functions sn, cn and dn may be expressed as the theta function ratios

$$\begin{aligned}
\mathrm{sn}(z,k) &= \frac{\theta_3}{\theta_2}\frac{\theta_1\left(z/\theta_3^2,\tau\right)}{\theta_4\left(z/\theta_3^2,\tau\right)} \\
\mathrm{cn}(z,k) &= \frac{\theta_4}{\theta_2}\frac{\theta_2\left(z/\theta_3^2,\tau\right)}{\theta_4\left(z/\theta_3^2,\tau\right)} \\
\mathrm{sn}(z,k) &= \frac{\theta_4}{\theta_3}\frac{\theta_3\left(z/\theta_3^2,\tau\right)}{\theta_4\left(z/\theta_3^2,\tau\right)}
\end{aligned}$$

where $\theta_i = \theta_i(0,\tau)$ for $i = 1,2,3,4$. The variable k is given by $k^{\frac{1}{2}} = \frac{\theta_2}{\theta_3}$.

2.6.1 Characteristics

The four theta functions $\theta_1(z,\tau)$, $\theta_2(z,\tau)$, $\theta_3(z,\tau)$ and $\theta_4(z,\tau)$ each have one unique zero within the fundamental period parallelogram $0, \pi, \pi+\pi\tau, \pi\tau$ at the respective half-period points 0, $\frac{\pi}{2}$, $\frac{\pi}{2}+\frac{\pi\tau}{2}$ and $\frac{\pi\tau}{2}$. Each theta function corresponds to a different characteristic related to each half-period in the genus one case. We now introduce the notion of a characteristic in the general genus case although as later results will show, a theta function may have a zero at its characteristic point but will also have $g-1$ other zeros within its fundamental period parallelpiped.

Definition 2.8 *A g-characteristic* $[\varepsilon]$ *is defined as a* $2 \times g$ *matrix of integers:*

$$[\varepsilon] = \begin{bmatrix} \boldsymbol{\varepsilon}'^{\mathsf{T}} \\ \boldsymbol{\varepsilon}''^{\mathsf{T}} \end{bmatrix} = \begin{bmatrix} \varepsilon'_1 & \dots & \varepsilon'_g \\ \varepsilon''_1 & \dots & \varepsilon''_g \end{bmatrix} \tag{2.26}$$

Definition 2.9 *The character* $|\varepsilon|$ *of such a characteristic is defined by*

$$|\varepsilon| = (-1)^{\boldsymbol{\varepsilon}'^{\mathsf{T}}\boldsymbol{\varepsilon}''} \tag{2.27}$$

A characteristic is termed even or odd if its character is 1 *or* -1 *respectively.*

Definition 2.10 *The reduced characteristic of characteristic* $[\varepsilon]$ *is formed by reducing all its components modulo* 2 *such that all* ε_i' *and* ε_i'' *are* 0 *or* 1*.*

Theorem 2.7 *(i) The character of a reduced characteristic is the same as that of the original characteristic. (ii) For a g-characteristic there are* $2^{g-1}(2^g+1)$ *even and* $2^{g-1}(2^g-1)$ *odd reduced characteristics.*

Proof: See Appendix A.

Definition 2.11 *Let* $\boldsymbol{z} \in \mathbb{C}^g$ *and* B *be a* $g \times g$ *complex, symmetric matrix with negative definite real part. A theta function with characteristic* $[\varepsilon]$ *is defined by*

$$\theta[\varepsilon](\boldsymbol{z}, B) = \sum_{\boldsymbol{m}\in\mathbb{Z}^g} \exp\left\{(\boldsymbol{m}+\boldsymbol{\varepsilon}'/2)^{\mathsf{T}}\left\{\frac{1}{2}B(\boldsymbol{m}+\boldsymbol{\varepsilon}'/2) + (\boldsymbol{z}+\pi i\boldsymbol{\varepsilon}'')\right\}\right\} \tag{2.28}$$

The conditions on B provide convergence for all $z \in \mathbb{C} \cup \{\infty\}$. The series then converges absolutely for all z and B and can be thought of as a holomorphic function of both these variables. This definition, which is that used by Belokolos et al. [BBE94], is by no means unique but any variations may generally be reconciled by a complex scaling of the arguments. For example, compared with the Jacobi theta functions,

$$\theta\begin{bmatrix} 0 \\ 0 \end{bmatrix}(z, B) = \theta_3\left(\frac{z}{2i}, \frac{\tau}{2\pi i}\right).$$

2.6.2 Properties of theta functions

The following are important properties of theta functions which shall be used in later work. They are all readily proved using the theta function definition.

Property 2.1 (Quasiperiodicity)

$$\theta[\varepsilon](\boldsymbol{z}+2\pi i\boldsymbol{k}'+B\boldsymbol{k}'', B) = \exp\left\{-\boldsymbol{k}''^{\mathsf{T}}(B\boldsymbol{k}''/2+\boldsymbol{z}+\boldsymbol{\varepsilon}'')+\pi i\boldsymbol{k}'^{\mathsf{T}}\boldsymbol{\varepsilon}'\right\}\theta[\varepsilon](\boldsymbol{z}, B) \tag{2.29}$$

for any $\boldsymbol{k}'$,$\boldsymbol{k}'' \in \mathbb{Z}^g$.

Property 2.2 (Symmetry)

$$\theta[\varepsilon](-\boldsymbol{z}, B) = |\varepsilon|\theta[\varepsilon](\boldsymbol{z}, B) \tag{2.30}$$

Property 2.3 (Behaviour at zero)

$$\theta[\varepsilon](0, B) = 0 \tag{2.31}$$

if $[\varepsilon]$ is an odd g-characteristic.

Property 2.4 (Characteristic addition)

$$\theta[\varepsilon + \mu](\boldsymbol{z}, B) = \exp\left\{\frac{\boldsymbol{\mu}'^{\mathsf{T}}}{2}\left(\frac{B\boldsymbol{\mu}'}{4} + \pi i(\boldsymbol{\varepsilon}'' + \boldsymbol{\mu}'')\right)\right\}\theta[\varepsilon](\boldsymbol{z} + \pi i\boldsymbol{\mu}' + B\boldsymbol{\mu}''/2, B) \tag{2.32}$$

Definition 2.12 *The canonical theta function is defined to be the theta function with all elements of its characteristic equal to zero. It will be represented as* $\theta(\boldsymbol{z}, B)$.

Theorem 2.8

$$\theta(\pi i\boldsymbol{\mu}' + B\boldsymbol{\mu}''/2, B) = 0 \tag{2.33}$$

if $[\mu]$ *is any odd g-characteristic.*

Proof: Using Properties 2.4 and 2.3 applied to the canonical theta function.

2.7 Theta functions on Riemann surfaces

Theta functions play an important role in the construction of meromorphic functions with prescribed poles and zeros on Riemann surfaces. This leads to the development of Baker-Akhiezer functions, meromorphic functions which have in addition an arbitrary but finite number of essential singularities.

Before proceeding to the main results for theta functions on a Riemann surface we introduce the lattice

$$\Lambda = \{2\pi i\boldsymbol{m} + B\boldsymbol{n} \mid \boldsymbol{m}, \boldsymbol{n} \in \mathbb{Z}^g\} \tag{2.34}$$

and use it to define the Jacobian variety of a Riemann surface X,

$$J(X) = \mathbb{C}^g/\Lambda,$$

so that two points in $\mathbb{C}^g$ are equivalent modulo Λ if their difference is a lattice point. The Abelian map may then be introduced, defined by

$$\boldsymbol{\omega}(P) = \int_{P_0}^{P} \mathrm{d}\boldsymbol{\omega}, \tag{2.35}$$

which is the Abelian integral of the vector of normalised holomorphic differentials, $\mathrm{d}\boldsymbol{\omega} = (\mathrm{d}\omega_1, ..., \mathrm{d}\omega_g)$, with base point P_0. This maps from points $P \in X$ to the Jacobian $J(X)$ and allows us to consider correctly defined global Abelian integrals of the first kind where integrals with differing paths of integration will map to the same point modulo Λ. Equally the Abelian map may be defined for a divisor $\mathcal{D} = \sum_{i=1}^{n} k_i P_i$ by

$$\boldsymbol{\omega}(\mathcal{D}) = \sum_{i=1}^{n} k_i \int_{P_0}^{P_i} \mathrm{d}\boldsymbol{\omega} \tag{2.36}$$

where $k_i \in \mathbb{Z}$.

The Jacobi inversion problem asks the question of how we invert the Abelian map. The following theorem, known as Riemann's Vanishing Theorem, is concerned with this and shows where the zeros of a theta function lie upon the Jacobian variety.

Theorem 2.9 ([RF74],p160) *Consider a Riemann Surface, X, with base point $P_0 \in X$. Taking any path of integration on X from P_0 to a general point $P \in X$ define the function*

$$F(P) = \theta[\varepsilon]\left(\int_{P_0}^{P} \mathrm{d}\boldsymbol{\omega} - \boldsymbol{e}, B\right)$$

where $\mathrm{d}\boldsymbol{\omega} = (\mathrm{d}\omega_1, ..., \mathrm{d}\omega_g)^{\mathsf{T}}$ is the vector of normalised holomorphic differentials and $\boldsymbol{e} \in \mathbb{C}^g$. If P_0 and $\boldsymbol{e}$ are chosen such that $F(P) \not\equiv 0$, then F has exactly g (possibly multiple) zeros at positions $P = P_1, ..., P_g$ satisfying

$$\sum_{k=1}^{g} \int_{P_0}^{P_k} \mathrm{d}\boldsymbol{\omega} \equiv \boldsymbol{e} - \boldsymbol{K}(P_0) - \pi i \boldsymbol{\varepsilon}' - B\boldsymbol{\varepsilon}'' \mod \Lambda$$

where $\Lambda = \{2\pi i \boldsymbol{m} + B\boldsymbol{n} \mid \boldsymbol{m}, \boldsymbol{n} \in \mathbb{Z}^g\}$ and the Riemann vector $\boldsymbol{K}(P_0)$ has components

$$K_j(P_0) = \left(B_{jj}/2 + \int_{P_0}^{P^{(I)}} \mathrm{d}\omega_j - \int_{a_i} \omega_j^{+} \mathrm{d}\omega_i\right).$$

Proof: See Appendix A.

Lemma 2.1 ([CL02],p4691) *Consider a hyperelliptic curve $\mu^2 = \prod_{j=1}^{2g+2}(z - z_j)$ with branch cuts and homology basis presented in* Figure 2.1. *If the base point P_0 is set equal*

to the branch point z_1, the vector of Riemann constants is given by the half-period

$$\boldsymbol{K}(z_1) \equiv \pi i\,(1,1,...,1)^{\mathsf{T}} + \frac{1}{2}B\,(1,0,1,0,...)^{\mathsf{T}} \mod \Lambda. \tag{2.37}$$

Proof: According to a theorem presented by Rauch and Farkas ([RF74],p181), the vector of Riemann constants for a hyperelliptic curve is given by $\sum_{j=0}^{g}\int_{P_0}^{z_{2j+1}} \mathrm{d}\boldsymbol{\omega}$ and consequently, when $P_0 = z_1$, this becomes $\sum_{j=1}^{g}\int_{z_1}^{z_{2j+1}} \mathrm{d}\boldsymbol{\omega}$ which may be shown equal to the given half-period modulo the period lattice, Λ.

2.8 Baker-Akhiezer functions

The simplest example of a Baker-Akhiezer function is the exponential function on the zero-genus Riemann surface $\mathbb{C}$. This function is analytic in $\mathbb{C}\backslash\{\infty\}$ with a singularity at ∞ of the form $\exp(\xi^{-1})$ where $\xi = z^{-1}$ is the local parameter at ∞.

In the context of this thesis, the Baker-Akhiezer functions encountered will be functions satisfying the relevant scattering problems. The singularities will all be at infinite points. For example, in the case of the scalar nonlinear Schrödinger equation, the relevant Baker-Akhiezer function has singularities at the two points at infinity, $\infty^{\pm}$, one on each sheet of the hyperelliptic curve. By inspecting suitable asymptotic expansions at these singularities, expressions for the potential may be formed and expressed as ratios of theta functions, see Chapter 3.

The following theorem defines a general Baker-Akhiezer function and its properties:

Theorem 2.10 ([BBE94]) *Consider a non-special divisor $\mathcal{D} = \sum_{k=1}^{g} P_k \in \mathrm{Div}(X)$, where X is a Riemann surface of genus g. Consider also an arbitrary positive divisor $\widetilde{\mathcal{D}} \in \mathrm{Div}(X)$ of degree n. Then a meromorphic function on X with poles at the points $\mathcal{D} + \widetilde{\mathcal{D}}$ may be defined by*

$$\psi(P) = \frac{\theta\left(\int_{P_0}^{P} \mathrm{d}\boldsymbol{\omega} + \int_{\boldsymbol{b}} \mathrm{d}\Omega - \boldsymbol{e}, B\right)}{\theta\left(\int_{P_0}^{P} \mathrm{d}\boldsymbol{\omega} - \boldsymbol{e}, B\right)} \exp\{\Omega(P)\}. \tag{2.38}$$

Here, $\mathrm{d}\Omega$ is a Abelian differential of the third class satisfying the normalisation conditions $\int_{a_j} \mathrm{d}\Omega = 0$ and having simple poles with residue -1 at the points of $\widetilde{\mathcal{D}}$. $\Omega(P) = \int_{P_0}^{P} \mathrm{d}\Omega$ and $\int_{P_0}^{P} \mathrm{d}\boldsymbol{\omega}$ take the same paths of integration and $\int_{\boldsymbol{b}} \mathrm{d}\Omega = (\int_{b_1} \mathrm{d}\Omega, ..., \int_{b_g} \mathrm{d}\Omega)^{\mathsf{T}}$.

Proof: It is clear from Theorem 2.9 that $\psi(P)$ has simple poles at the points P_k. By the construction of $\mathrm{d}\Omega$, $\psi(P)$ also has simple poles at the points of $\widetilde{\mathcal{D}}$. It remains to show that

the function's value does not change upon adding any integer number of cycles a_j or b_j to the paths of integration. This is demonstrated by applying the quasiperiodicity (Property 2.1) of the theta functions.

Definition 2.13 *Fix n points $Q_k \in X$ with local parameters $z_k(P)$ for $k = 1, ..., n$ such that $z_k \to \infty$ as $P \to Q_k$. To every point Q_k associate an arbitrary polynomial $q_k(z_k)$ in local parameter z_k and, lastly, define an arbitrary positive divisor $\mathcal{D} = \sum_{k=1}^{g} P_k$ upon $X \backslash \{Q_k | k = 1, ..., n\}$. Then the space denoted $L(\mathcal{D}; Q_1, ..., Q_n; q_1, ..., q_n)$ is the linear space of functions $\psi(P)$, defined upon X, which satisfy the two conditions:*

1. $\psi(P)$ is meromorphic on $X \backslash \{Q_k | k = 1, ..., n\}$ and has divisor of poles $\mathcal{D}$,
2. In the neighbourhood of any Q_k, the following asymptotic expansion holds:

$$\psi(z_k) \exp\{-q_k(z_k)\} = O(1). \tag{2.39}$$

Theorem 2.11 ([BBE94]) *The space $L(\mathcal{D}; Q_1, ..., Q_n; q_1, ..., q_n)$ defined above is one-dimensional for a non-special divisor $\mathcal{D}$ and polynomials q_k of a suitably general form. Its basis is given explicitly, up to a multiplicative factor independent of P, by*

$$\psi_0(P) = \frac{\theta\left(\int_{P_0}^{P} \mathrm{d}\boldsymbol{\omega} + \int_{\boldsymbol{b}} \mathrm{d}\Omega - \boldsymbol{e}, B\right)}{\theta\left(\int_{P_0}^{P} \mathrm{d}\boldsymbol{\omega} - \boldsymbol{e}, B\right)} \exp\{\Omega(P)\}. \tag{2.40}$$

Here, $\Omega(P)$ is an Abelian integral of the second kind with the normalisation conditions $\int_{a_j} \mathrm{d}\Omega = 0$ and with poles at the points $Q_1, ..., Q_n$ whose principal parts are given by the polynomials $q_1(z_1), ..., q_n(z_n)$.

Proof: Theorem 2.9 proves the divisor of poles is $\mathcal{D}$ and the function's construction means it has essential singularities at $Q_1, ..., Q_n$. The function may be proved single-valued by adding on an arbitrary number of a and b cycles to the paths of integration. To demonstrate the space is one-dimensional, we imagine $\psi(P)$ to be another arbitrary function of $L(\mathcal{D}; Q_1, ..., Q_n; q_1, ..., q_n)$. The rational function $\psi/\psi_0(P)$ must have a divisor of poles given by the zeros of ψ_0. This divisor, which we shall denote $\mathcal{D}' = \sum_{k=1}^{g} P'_k$, is formed of the zeros of $\theta\left(\int_{P_0}^{P} \mathrm{d}\boldsymbol{\omega} + \int_{\boldsymbol{b}} \mathrm{d}\Omega - \boldsymbol{e}, B\right)$. So long as this theta function does not vanish identically, $\mathcal{D}'$ is non-special which in turn means $\dim(F_{-\mathcal{D}'}) = 1$ and the function $\psi/\psi_0(P)$ is a constant. Hence $\psi(P)$ is unique up to a multiplicative factor independent of P.

Corollary 2.5 ([BBE94]) *If, for a non-special divisor $\mathcal{D}$ and polynomials of suitably general form q_k, one or more of the conditions (2.39) read*

$$\psi(z_k)\exp\{-q_k(z_k)\} = o(1) \tag{2.41}$$

then equation (2.40) becomes $\psi_0(P) = 0$.

Proof: Following the proof of the previous theorem, we came to the conclusion that $\psi(P) = c\psi_0(P)$ for some constant c. But, by inspecting the asymptotic behaviour at a singularity where (2.41) occurs, we see that $c = 0$.

Corollary 2.5 is essential in proving that the Baker-Akhiezer functions developed in later chapters solve the Zakharov-Shabat and Manakov scattering problems.

In the following chapters we will be seeking to utilise Baker-Akhiezer functions to find expressions for matrices Ψ solving scattering problems like the Zakharov-Shabat system:

$$\Psi_x = \mathcal{L}_1(z)\Psi,$$
$$\Psi_t = \mathcal{L}_2(z)\Psi$$

and with asymptotic expansion

$$\Psi(x,t,z) = \left(\mathbb{I}_2 + \sum_{k=1}^{\infty}\Psi_k(x,t)z^{-k}\right)\exp\left(-\frac{i}{2}\sigma_3(zx+z^2t)\right)C(z).$$

All quantities will be defined in the following chapter. Importantly the components of Ψ will be formed of Baker-Akhiezer functions and taking asymptotic limits we will be able to derive expressions for finite gap solutions to the SNLS.

Chapter 3

Algebrogeometric solution of the KdV and SNLS

In this chapter we will introduce the algebrogeometric approach to solving nonlinear PDEs, developed by, among others, Krichever, Its, Kotlyarov and Matveev. As an instructive example we first consider the Korteweg-de Vries equation (1.10) to which the method may be applied relatively easily given the scalar nature of the scattering problem. In contrast, the Zakharov-Shabat system relevant to the scalar nonlinear Schrödinger equation requires a vector solution and hence a vector-valued Baker-Akhiezer function must be introduced.

3.1 Finite gap solutions to the Korteweg-de Vries equation

The KdV (1.10) arises as the consistency condition $L_t = [M, L]$ of the Lax pair equations

$$Lv = zv, \qquad v_t = Mv, \tag{3.1}$$

where

$$\begin{aligned} L &= \partial_x^2 + u(x,t), \\ M &= -\left(4\partial_x^3 + 6u(x,t)\partial_x + 3u_x(x,t)\right). \end{aligned}$$

The spectral curve of relevance to the KdV is the hyperelliptic curve,

$$\mu^2 = \prod_{i=1}^{2g+1}(z - E_i), \qquad E_i \in \mathbb{R}, \quad E_1 < E_2 < ... < E_{2g+1}, \tag{3.2}$$

see, for example, [AS81]. The idea of the method is to construct a Baker-Akhiezer function solving the scattering problem (3.1) with an appropriate asymptotic expansion at the single point at infinity P_∞.

To define the space $L(\mathcal{D}; P_\infty; q_1)$, we choose a local parameter $z_1(P_\infty) = \sqrt{z}$ which certainly tends to infinity as $z \to \infty$. We then select a polynomial in z_1,

$$q_1(z_1) = z_1 x - 4z_1^3 t \tag{3.3}$$

which is linear in x and t and whose use will become clear. If we now define a non-special divisor $\mathcal{D} = \sum_{k=1}^{g} P_k \in \mathrm{Div}(X)$, we are in a position to construct a Baker-Akhiezer function using Theorem 2.11. The space $L(\mathcal{D}; P_\infty; q_1)$ consists of functions $\psi(P)$ satisfying the two conditions

- $\psi(P)$ is meromorphic on $X \backslash \{P_\infty\}$,
- $\psi(z_1) = \{1 + O(z_1)\} \exp\left(q_1(z_1)\right) \qquad$ as $P \to P_\infty$.

Given that $\mathcal{D}$ is non-special, we may apply Theorem 2.11 and construct the unique function in this space:

$$\psi(P) = A \frac{\theta\left(\int_{P_\infty}^{P} \mathrm{d}\boldsymbol{\omega} + \int_{\boldsymbol{b}} \mathrm{d}\Omega - \boldsymbol{e}, B\right)}{\theta\left(\int_{P_\infty}^{P} \mathrm{d}\boldsymbol{\omega} - \boldsymbol{e}, B\right)} \exp\{\Omega(P)\}. \tag{3.4}$$

$\Omega(P) = \Omega_1(P)x + \Omega_2(P)t$ with $\mathrm{d}\Omega_1(P)$ and $\mathrm{d}\Omega_2(P)$ normalised Abelian differentials of the second class and with the asymptotic behaviour

$$\Omega_1(z_1) = z_1 + o(1), \qquad \Omega_2(z_1) = -4z_1^3 + o(1). \tag{3.5}$$

We have let the base point of integration be P_∞ which simplifies the formulae although the choice of base point is unimportant. A is a multiplicative constant which we specify as

$$A = \frac{\theta\left(\boldsymbol{e}, B\right)}{\theta\left(\int_{\boldsymbol{b}} \mathrm{d}\Omega - \boldsymbol{e}, B\right)} \tag{3.6}$$

in order that the asymptotic behaviour agrees with the conditions on $\psi(P)$. We now wish to prove $\psi(P)$ satisfies the Lax pair equations (3.1) for certain $u(x,t)$. Consider the functions

$$\psi_1(P) = (z - L)\psi(P),$$
$$\psi_2(P) = (\partial_t - M)\psi(P)$$

and require that, as $P \to P_\infty$,

$$\begin{aligned} \psi_1(P) &= O(z_1^{-1}) \exp\left(q_1(z_1)\right), \\ \psi_2(P) &= O(z_1^{-1}) \exp\left(q_1(z_1)\right). \end{aligned} \tag{3.7}$$

It is clear that both $\psi_1(P)$ and $\psi_2(P)$ are meromorphic on $X\backslash\{P_\infty\}$ with divisor of poles $\mathcal{D}$. Through our choice of $\Omega(P)$ they also have the appropriate behaviour at P_∞. We may therefore apply Corollary 2.5 and deduce $\psi_1(P) = \psi_2(P) = 0$. Thus $\psi(P)$ satisfies the Lax pair equations and it remains to find the $u(x,t)$ such that these conditions hold. To achieve this we give $\psi(P)$ the asymptotic form

$$\psi(P) = \left[1 + \sum_{k=1}^{\infty} \eta_k(x,t) z_1^{-k}\right] \exp(z_1 x - 4z_1^3 t) \tag{3.8}$$

as $P \to P_\infty$. Then, in order for conditions (3.7) to hold, $u(x,t) = -2\eta_{1,x}(x,t)$. Comparing (3.4) as $P \to P_\infty$ with the series just given, we see

$$\eta_1(x,t) = \frac{\partial}{\partial \xi}\left[\ln\left\{A\frac{\theta\left(\int_{P_\infty}^{P} \mathrm{d}\boldsymbol{\omega} + \int_{\boldsymbol{b}} \mathrm{d}\Omega - \boldsymbol{e}, B\right)}{\theta\left(\int_{P_\infty}^{P} \mathrm{d}\boldsymbol{\omega} - \boldsymbol{e}, B\right)}\right\} - (\Omega(P) - q_\infty(\xi))\right]\Bigg|_{\xi=0} \tag{3.9}$$

where $\xi = z_1^{-1}$ is the local parameter at $P = P_\infty$, and conclude

$$u(x,t) = -2\,\frac{\partial^2}{\partial \xi \partial x} \ln\left\{\theta\left(\int_{P_\infty}^{P} \mathrm{d}\boldsymbol{\omega} + \int_{\boldsymbol{b}} \mathrm{d}\Omega - \boldsymbol{e}, B\right)\right\}\Bigg|_{\xi=0} + c \tag{3.10}$$

where $\Omega_1(P) = \xi^{-1} + \frac{c}{2}\xi + O(\xi^2)$ as $P \to P_\infty$. This formula can be greatly neatened by noticing that the asymptotic expansion

$$\int_{P_\infty}^{P} \mathrm{d}\boldsymbol{\omega} = -\xi \int_{\boldsymbol{b}} \mathrm{d}\Omega_1 + O(\xi^2) \tag{3.11}$$

holds near P_∞ (this may be shown via the Riemann bilinear relations) and hence that ∂_ξ acts like $-\partial_x$ so

$$u(x,t) = \frac{\partial^2}{\partial x^2} \ln\left\{\theta\left(\int_{\boldsymbol{b}} \mathrm{d}\Omega - \boldsymbol{e}, B\right)\right\}^2 + c. \tag{3.12}$$

This is the general quasiperiodic solution to the KdV equation which agrees with that found using inverse scattering theory, see [AS81].

3.2 SNLS hierarchy

This section is concerned with developing a hierarchy of scalar nonlinear Schrödinger equations by generating higher-order version of the Lax pair found by Zakharov and Shabat. The algebrogeometric approach appeals to this hierarchy to find solutions of general genus.

The Zakharov-Shabat system, (1.13) and (1.14), may be extended to a hierarchy of linear evolution equations defined by

$$\boldsymbol{v}_{t_n} = \mathcal{L}_n^{\pm}(z)\boldsymbol{v} \qquad n = 1, 2, ... \tag{3.13}$$

with $\mathcal{L}_n^{\pm}(z)$ taking the polynomial structure

$$\mathcal{L}_n^{\pm}(z) = \sum_{k=0}^{n} z^{n-k} L_k^{\pm} \qquad \text{where } L_k^{\pm} = \begin{pmatrix} \alpha_k^{\pm} & \beta_k^{\pm} \\ \mp\beta_k^{\pm} & -\alpha_k^{\pm} \end{pmatrix}. \tag{3.14}$$

It should be noted that the 2×2 matrices $\mathcal{L}_n^{\pm}(z)$ obey the conjugation formulae

$$(\mathcal{L}_n^{+})^{\dagger}(z) = -\mathcal{L}_n^{+}(z), \qquad (\mathcal{L}_n^{-})^{\dagger}(z) = -\sigma_3 \mathcal{L}_n^{-}(z)\sigma_3, \tag{3.15}$$

or, alternatively,

$$\overline{\mathcal{L}_n^{+}}(z) = \sigma_2 \mathcal{L}_n^{+}(z)\sigma_2, \qquad \overline{\mathcal{L}_n^{-}}(z) = \sigma_1 \mathcal{L}_n^{-}(z)\sigma_1 \tag{3.16}$$

where σ_1, σ_2 and σ_3 are the Pauli matrices defined by (1.4).

Henceforth, in order to develop a tidy notation, we shall drop the $\pm$ signs attached to the matrices $\mathcal{L}_n$ and distinguish between attractive and repulsive cases where necessary. In future equations the upper sign will represent the attractive case.

From the commuting flows $\boldsymbol{v}_{xt_n} = \boldsymbol{v}_{t_n x}$ (where we have set $t_1 = x$), the zero-curvature equation

$$\frac{\partial \mathcal{L}_n(z)}{\partial x} - \frac{\partial \mathcal{L}_1(z)}{\partial t_n} = [\mathcal{L}_1(z), \mathcal{L}_n(z)] \tag{3.17}$$

may be derived. Expanding in powers of z gives the matrix equations

$$L_{k,x} = [L_0, L_{k+1}] + [L_1, L_k], \qquad 0 \le k \le n-1 \tag{3.18}$$

$$L_{n,x} - L_{1,t_n} = [L_1, L_n] \tag{3.19}$$

and, if the matrices $L_0^{\pm}$ and $L_1^{\pm}$ assume the forms

$$L_0^{\pm} = -\frac{i}{2}\sigma_3, \qquad L_1^{\pm} = \begin{pmatrix} 0 & q \\ \mp\overline{q} & 0 \end{pmatrix}, \tag{3.20}$$

the following evolution equations hold:

$$\begin{aligned} \alpha_{k,x} &= \mp(q\overline{\beta_k} - \beta_k\overline{q}), \\ \beta_{k,x} &= -i\beta_{k+1} - 2q\alpha_k. \end{aligned}$$

From these, the recurrence relation

$$\beta_{k+1} = i\beta_{k,x} \mp 4q\int^x \mathrm{Im}(\overline{q}\beta_k)\mathrm{d}x' \tag{3.21}$$

may be formed, which we will write as

$$\beta_{k+1} = \mathcal{D}^{\pm}\beta_k \qquad k = 0, ..., n-1 \tag{3.22}$$

in attractive and repulsive cases respectively. The recursion operators $\mathcal{D}^{\pm}$ act on a complex function $f(x)$ according to

$$\mathcal{D}^{\pm}f = if_x \pm 2iq\int^x (\overline{q}f - q\overline{f})\mathrm{d}x'. \tag{3.23}$$

If all integration constants are taken equal to zero, then $\mathcal{D}^{\pm}$ may be applied recursively and, making use of (3.19), this gives the n^{th} order flows

$$q_{t_n} = -i(\mathcal{D}^{\pm})^n q, \tag{3.24}$$

the first few of which are

$$q_{t_1} = q_x, \tag{3.25}$$

$$q_{t_2} = iq_{xx} \pm 2iq^2\overline{q}, \tag{3.26}$$

$$q_{t_3} = -q_{xxx} \mp 6q_x q\overline{q}. \tag{3.27}$$

It is interesting to note that for a real function $q(x,t)$, (3.27) is the modified Korteweg-de Vries equation, a completely integrable equation obtained from the KdV equation via a Miura map. The recurrence formula

$$\alpha_k = -i\sum_{j=1}^{k-1}(\alpha_j\alpha_{k-j} \mp \overline{\beta_j}\beta_{k-j}) \tag{3.28}$$

may also be derived by considering elements of $\mathcal{L}_n^2(z)$. Indeed we can form the following closed form recurrence relation for the matrices L_k:

Theorem 3.1

$$L_{k+1} = [L_{k,x}, L_0] + [L_0, [L_1, L_k]] + \sum_{j=1}^{k} \{L_j, L_{k+1-j}\} L_0, \tag{3.29}$$

where curly brackets denote the matrix anti-commutator.

Proof: This is demonstrated by applying the commutator of L_0 with equation (3.18) and then applying equation (3.28).

Thus we have formed a family of equations, often referred to as higher-order nonlinear Schrödinger equations. These are consistency conditions of a Lax pair hierarchy for which we have closed form solutions, see (3.22) and (3.28). The equations are therefore all completely integrable. The development of these techniques with reference to the vector nonlinear Schrödinger hierarchy will be considered in Chapter 4. We define a fixed spectral curve by considering the n^{th} stationary flow to be dependent only upon times $t_1, t_2, ..., t_{n-1}$. The zero-curvature equation (3.17) then becomes

$$\frac{\partial \mathcal{L}_n(z)}{\partial x} = [\mathcal{L}_1(z), \mathcal{L}_n(z)] \tag{3.30}$$

and the spectral curve is given by the characteristic equation of $\mathcal{L}_n(z)$ with the eigenvalue parameter $i\mu/2$ chosen for convenience:

$$\mu^2 + 2i\mathrm{Tr}\mathcal{L}_n\mu - 4\det \mathcal{L}_n = 0. \tag{3.31}$$

The form chosen for $\mathcal{L}_n$ ensures

$$\mathrm{Tr}\mathcal{L}_n(z) = 0 \tag{3.32}$$

and hence

$$4\det \mathcal{L}_n(z) = 2(\mathrm{Tr}\mathcal{L}_n)^2 - \mathrm{Tr}\mathcal{L}_n^2 = -2\mathrm{Tr}\mathcal{L}_n^2. \tag{3.33}$$

$\mathrm{Tr}\mathcal{L}_n^2$ is a polynomial in z of order $2n$ which, in the general case, will have distinct roots and may be written as

$$\mathrm{Tr}\mathcal{L}_n^2 = -\frac{1}{2}\prod_{k=1}^{2n}(z - z_k^{\pm}) \tag{3.34}$$

with $z_k^{\pm}$ distinguishing the attractive and repulsive cases. The spectral curve is therefore the hyperelliptic curve

$$\mu^2 = \prod_{k=1}^{2g+2} (z - z_k^{\pm}), \tag{3.35}$$

where the Riemann-Hurwitz formula (2.16) has been used to deduce $n = g+1$. $\mathrm{Tr}\mathcal{L}_n^2(z)$ is a real polynomial in z and so all roots occur in complex conjugate pairs or are real. In the repulsive case the scattering problem is self-adjoint implying $z_k^- \in \mathbb{R}$ for $k = 1, ..., 2g+2$. In the attractive case we assume all roots are distinct conjugate pairs.

3.3 Finite gap solutions to the SNLS

We now want to construct a Baker-Akhiezer function solving the Zakharov-Shabat scattering problem. These Baker-Akhiezer functions must be vector-valued given the vector nature of the scattering problem. To begin with we state two theorems which will allow us to express the finite gap potential explicitly once the Baker-Akhiezer function has been found.

Theorem 3.2 *Consider a 2×2 matrix function $\Psi(x,t,z)$ which is holomorphic in a neighbourhood of infinity on the Riemann sphere, $\mathbb{C} \cup \{\infty\}$, and smoothly dependent on real variables x and t. Suppose Ψ has the following asymptotic expansion as $z \to \infty$:*

$$\Psi(x,t,z) = \left(\mathbb{I}_2 + \sum_{k=1}^{\infty} \Psi_k(x,t) z^{-k}\right) \exp\left(-\frac{i}{2}\sigma_3(zx + z^2 t)\right) C(z); \tag{3.36}$$

where $C(z)$ is a 2×2 invertible matrix, independent of x and t. Then, assuming (3.36) to be differentiable in x and t, as $z \to \infty$,

$$\begin{aligned} \Psi_x \Psi^{-1} &= \mathcal{K}_1^{\pm}(z) + O(z^{-1}), \\ \Psi_t \Psi^{-1} &= \mathcal{K}_2^{\pm}(z) + O(z^{-1}). \end{aligned} \tag{3.37}$$

Here,

$$\begin{aligned} \mathcal{K}_1^{\pm}(z) &= -\frac{i}{2}\sigma_3 z - \frac{i}{2}\left[\Psi_1, \sigma_3\right], \\ \mathcal{K}_2^{\pm}(z) &= -\frac{i}{2}\sigma_3 z^2 - \frac{i}{2} z \left[\Psi_1, \sigma_3\right] - \frac{i}{2}\left[\Psi_2, \sigma_3\right] + \frac{i}{2}\left[\Psi_1, \sigma_3\right]\Psi_1. \end{aligned}$$

Proof: Finding the first few terms of the asymptotic expansion

$$\Psi^{-1}(x,t,z) = C^{-1}(z)\exp\left(\frac{i}{2}\sigma_3(zx+z^2t)\right)\left(\mathbb{I}_2+\sum_{k=1}^{\infty}\Upsilon_k(x,t)z^{-k}\right),$$

by applying $\Psi\Psi^{-1}=\mathbb{I}_2$, it may be shown equations (3.37) hold.

Theorem 3.3 *If $\Psi(x,t,z)$ satisfies the conditions and asymptotic expansions of* Theorem 3.2 *and, in addition, Ψ is an exact solution to*

$$\Psi_x = \mathcal{K}_1^{\pm}(z)\Psi, \qquad \Psi_t = \mathcal{K}_2^{\pm}(z)\Psi \tag{3.38}$$

then, if

$$q(x,t) = i\Psi_{1,12}, \qquad \overline{q} = \pm i\Psi_{1,21}, \tag{3.39}$$

it may be shown Ψ is an exact solution to the Zakharov-Shabat system.

Proof: To prove the theorem, it is only required to show that

$$-\frac{i}{2}\left[\Psi_2,\sigma_3\right]+\frac{i}{2}\left[\Psi_1,\sigma_3\right]\Psi_1 \quad = \quad L_2^{\pm}.$$

This may be checked by splitting all matrices into diagonal and off-diagonal elements.

We now turn to the construction of the Baker-Akhiezer function. We select a first homology group basis $\{a_j,b_j|j=1,...,g\}$ and a set of g holomorphic differentials $\mathrm{d}\omega_j$, normalised according to (2.13). These differentials have an associated period matrix B. To define a unique Baker-Akhiezer function we need to know its divisor of poles, which we denote $\mathcal{D}=\sum_{k=1}^{g}P_k$, and its asymptotic behaviour at the two essential singularities ∞^+ and ∞^-. At these points we choose local parameter $\xi=z^{-1}$ and define three Abelian integrals, two of the second class and one of the third class, with asymptotic behaviour

$$\begin{aligned}
\Omega_1(z) &= \pm\left\{\frac{i}{2}z+\frac{E}{2}+\frac{R}{z}+O(z^{-2})\right\},\\
\Omega_2(z) &= \pm\left\{\frac{i}{2}z^2+\frac{N}{2}+O(z^{-1})\right\},\\
H(z) &= \pm\left\{\log\frac{z}{\delta}+O(z^{-1})\right\}
\end{aligned} \tag{3.40}$$

at $P \to \infty^{\pm}$ respectively. The constant terms E, N and δ are specified for later results and may be determined by the formulae

$$\int_{P^-}^{P^+} \mathrm{d}\Omega_1 = iz + E + O(z^{-1}), \tag{3.41}$$

$$\int_{P^-}^{P^+} \mathrm{d}\Omega_2 = iz^2 + N + O(z^{-1}), \tag{3.42}$$

$$\int_{P^-}^{P^+} \mathrm{d}H = 2\log z - 2\log\delta + O(z^{-1}) \tag{3.43}$$

where z is assumed real and positive as $P^{\pm} \to \infty^{\pm}$. The contours of integration pass through one branch cut and do not intersect the homology basis. Finding the anti-holomorphic involutions of these paths it is possible to deduce that E and N are pure imaginary constants.

Before defining the Baker-Akhiezer function we present two results of use in later work.

Proposition 3.1

$$\int_{b_k} \mathrm{d}H(P) = \omega_k(\infty^-) - \omega_k(\infty^+) \qquad \text{for } k = 1, ..., g. \tag{3.44}$$

Proof: Using Theorem 2.6

$$\begin{aligned} \int_{\partial\widetilde{X}} \omega_k \mathrm{d}H &= 2\pi i \int_{b_k} \mathrm{d}H \\ 2\pi i \left\{ \mathrm{Res}\left(\omega_k \mathrm{d}H, \infty^-\right) + \mathrm{Res}\left(\omega_k \mathrm{d}H, \infty^+\right) \right\} &= 2\pi i \int_{b_k} \mathrm{d}H \\ \omega_k(\infty^-) - \omega_k(\infty^+) &= \int_{b_k} \mathrm{d}H \end{aligned}$$

remembering to change to a suitable local parameter z^{-1} at $\infty^{\pm}$.

Proposition 3.2

$$\begin{aligned} &\int_{b_k} \mathrm{d}\Omega_1(P) = \mathrm{Res}\left(\omega_k \mathrm{d}\Omega_1, \infty^-\right) + \mathrm{Res}\left(\omega_k \mathrm{d}\Omega_1, \infty^+\right) = ic_{k1}, \\ &\int_{b_k} \mathrm{d}\Omega_2(P) = \mathrm{Res}\left(\omega_k \mathrm{d}\Omega_2, \infty^-\right) + \mathrm{Res}\left(\omega_k \mathrm{d}\Omega_2, \infty^+\right) = i\left(\frac{c_{k1}}{2}\sum_{j=1}^{2g+2} z_j^{\pm} + c_{k2}\right). \end{aligned} \tag{3.45}$$

Proof: As for Proposition 3.1 but with $\mathrm{d}\Omega_1$ and $\mathrm{d}\Omega_2$ replacing $\mathrm{d}H$ respectively. c_{k1} and c_{k2} are coefficients defining the normalised basis of holomorphic differentials, given in

equation (2.12).

Proposition 3.3

$$\begin{aligned} E &= \frac{1}{2\pi}\sum_{k=1}^{g}\int_{a_k} z\mathrm{d}\omega_k - \frac{i}{2}\sum_{j=1}^{2g+2} z_j^{\pm}, \\ N &= \frac{1}{2\pi}\sum_{k=1}^{g}\int_{a_k} z^2\mathrm{d}\omega_k - \frac{i}{2}\sum_{j=1}^{2g+2} \left(z_j^{\pm}\right)^2 - 2R. \end{aligned} \tag{3.46}$$

Proof: See Appendix A.

The vector-valued Baker-Akhiezer function $\boldsymbol{\psi}(P) = (\psi_1, \psi_2)^{\mathsf{T}}$ from which the finite gap potential $q(x,t)$ shall be derived, is defined on the hyperelliptic curve (3.35) and is fixed by two conditions:

1. $\boldsymbol{\psi}$ is meromorphic on $X\backslash\{\infty^{\pm}\}$ with divisor of poles $\mathcal{D}$
2. $\boldsymbol{\psi}$ has the following asymptotic expansions in z at $\infty^{\pm}$:

$$\begin{aligned} \boldsymbol{\psi}(P) &= \left[\begin{pmatrix} 1 \\ 0 \end{pmatrix} + O(z^{-1})\right] \exp\{-\frac{i}{2}(zx + z^2 t)\} \qquad P \to \infty^{-}, \\ \boldsymbol{\psi}(P) &= \left[\begin{pmatrix} 0 \\ 1 \end{pmatrix} + O(z^{-1})\right] z\exp\{\frac{i}{2}(zx + z^2 t)\} \qquad P \to \infty^{+}. \end{aligned} \tag{3.47}$$

Forms for ψ_1 and ψ_2 are uniquely specified by these two conditions and may be constructed explicitly using Theorem 2.11. They are given by

$$\begin{aligned} \psi_1(P) &= A_1(x,t)\frac{\theta(\boldsymbol{\omega}(P) + \boldsymbol{g}(x,t) - \boldsymbol{e})}{\theta(\boldsymbol{\omega}(P) - \boldsymbol{e})}\exp\{\Phi_1(x,t,P)\}, \\ \psi_2(P) &= A_2(x,t)\frac{\theta(\boldsymbol{\omega}(P) + \widehat{\boldsymbol{g}}(x,t) - \boldsymbol{e})}{\theta(\boldsymbol{\omega}(P) - \boldsymbol{e})}\exp\{\Phi_2(x,t,P) + H(P)\} \end{aligned} \tag{3.48}$$

where

$$\begin{aligned} g_k(x,t) &= x\int_{b_k}\mathrm{d}\Omega_1(P) + t\int_{b_k}\mathrm{d}\Omega_2(P), \\ \widehat{g}_k(x,t) &= g_k(x,t) + \int_{b_k}\mathrm{d}H(P) = g_k(x,t) + \omega_k(\infty^{-}) - \omega_k(\infty^{+}), \\ \Phi_1(x,t,P) &= x\left(\Omega_1(P) + \frac{E}{2}\right) + t\left(\Omega_2(P) + \frac{N}{2}\right), \\ \Phi_2(x,t,P) &= x\left(\Omega_1(P) - \frac{E}{2}\right) + t\left(\Omega_2(P) - \frac{N}{2}\right) \end{aligned}$$

and $\boldsymbol{\omega}(P) = \int_{P_0}^{P} \mathrm{d}\boldsymbol{\omega}$ takes the same path of integration as $\Omega_i(P)$ and $H(P)$. $A_1(x,t)$ and $A_2(x,t)$ are specified by inspecting behaviour as $P \to \infty^{\pm}$ and are found to be

$$A_1(x,t) = \frac{\theta(\boldsymbol{\omega}(\infty^-) - \boldsymbol{e})}{\theta(\boldsymbol{\omega}(\infty^-) + \boldsymbol{g}(x,t) - \boldsymbol{e})}, \tag{3.49}$$

$$A_2(x,t) = \frac{\theta(\boldsymbol{\omega}(\infty^+) - \boldsymbol{e})}{\theta(\boldsymbol{\omega}(\infty^-) + \boldsymbol{g}(x,t) - \boldsymbol{e})}\delta. \tag{3.50}$$

To show that these functions satisfy the SNLS scattering problem, we consider the matrix

$$\Psi(x,t,z) = \big(\boldsymbol{\psi}(P^-), \boldsymbol{\psi}(P^+)\big) \qquad\qquad P^{\pm} \to \infty^{\pm} \tag{3.51}$$

which satisfies the conditions of Theorem 3.2 if

$$C(z) = \begin{pmatrix} 1 & 0 \\ 0 & z \end{pmatrix}.$$

To show $\Psi(x,t,z)$ satisfies the conditions of Theorem 3.3 we consider the function

$$\boldsymbol{\phi}^{(1)}(P) = \{\partial_x - \mathcal{L}_1(z)\}\boldsymbol{\psi}(P) \tag{3.52}$$

which at $P^- \to \infty^-$ reads

$$\boldsymbol{\phi}^{(1)}(P^-) = o(1)\exp\{-\frac{i}{2}\sigma_3(zx + z^2 t\}.$$

This allows us to apply Corollary 2.5 and prove $\boldsymbol{\phi}^{(1)}(P) = 0$. Similarly we may prove $\phi^{(2)}(P) = (\partial_t - \mathcal{L}_2(z))\,\boldsymbol{\psi}(P) = 0$ thereby showing $\Psi(x,t,z)$ satisfies the scattering problem. Comparing (1,2) elements of the two representations for $\Psi(x,t,z)$, (3.51) and (3.36), in the limit $P^+ \to \infty^+$, we find the finite gap solution to be

$$\begin{aligned} q(x,t) &= i\psi_1(\infty^+)\exp\{-\frac{i}{2}(zx + z^2 t)\} \\ &= Q\frac{\theta(\boldsymbol{\omega}(\infty^+) + \boldsymbol{g}(x,t) - \boldsymbol{e})}{\theta(\boldsymbol{\omega}(\infty^-) + \boldsymbol{g}(x,t) - \boldsymbol{e})}\exp(Ex + Nt) \end{aligned} \tag{3.53}$$

where $Q = i\frac{\theta(\boldsymbol{\omega}(\infty^-) - \boldsymbol{e})}{\theta(\boldsymbol{\omega}(\infty^+) - \boldsymbol{e})}$. $\overline{q}(x,t)$ is similarly given by

$$\overline{q}(x,t) = \pm iz\psi_2(\infty^-)\exp\{\frac{i}{2}(zx + z^2 t)\}$$

in attractive and repulsive cases respectively.

Proposition 3.4 *In attractive and repulsive cases respectively*

$$|q(x,t)|^2 = \mp\partial_x^2 \log\left\{\theta(\boldsymbol{\omega}(\infty^+) + \boldsymbol{g} - \boldsymbol{e})\right\} \pm iR. \tag{3.54}$$

Proof: This is a simplification of Proposition 4.2 which will state an analogous result for the vector problem.

3.4 Separable quasiperiodic solutions to the SNLS

Although in the previous section we found general quasiperiodic solutions to the SNLS, it is interesting to see that the simplest such solutions are easily obtained via a simple separable ansatz. These solutions are defined in terms of the Jacobi elliptic functions $\mathrm{cn}(u|k)$, $\mathrm{dn}(u|k)$ and $\mathrm{sn}(u|k)$ whose definitions in terms of Jacobi theta function were given previously. Further information on their properties may be found in Whittaker and Watson, [WW27].

Consider the simple separable ansatz $q(x,t) = Q(x)\exp(i\lambda t)$, where λ is a real constant and $Q(x)$ is a real function of x, as a solution to the SNLS (1.2). Substitution gives

$$-\lambda Q + Q_{xx} \pm 2Q^3 = 0 \tag{3.55}$$

and, if we then multiply by Q_x and integrate, this forms an 'energy' equation

$$Q_x^2 - \lambda Q^2 \pm Q^4 = C \tag{3.56}$$

where C is a real constant of integration. From the forms of the potentials $U^{\pm}(Q) = \pm Q^4 - \lambda Q^2$, the appropriateness of the terms attractive and repulsive becomes evident and different solutions are possible according to the sign of λ.

In the attractive case, for $\lambda < 0$ and $C \leq 0$, the solution for $Q(x)$ may be expressed in terms of the Jacobi elliptic cnoidal function as

$$Q(x) = a\,\mathrm{cn}\left(\frac{a}{k}x\middle|\, k\right) \tag{3.57}$$

with $C = \frac{a^4(k^2-1)}{k^2}$, $\lambda = \frac{a^2(2k^2-1)}{k^2}$ and $0 < k^2 < \frac{1}{2}$.

For $\lambda > 0$ and $C < 0$ the form is the same but with $\frac{1}{2} < k^2 < 1$. For both these cases, the solution

$$q(x,t) = a\,\mathrm{cn}\left(\frac{a}{k}x|k\right)e^{i\lambda t}$$

is doubly quasiperiodic with periodicity defined by

$$\mathrm{cn}\left(\frac{a}{k}x + 2mK + 2niK' \middle| k\right) = (-1)^{m+n}\mathrm{cn}\left(\frac{a}{k}x \middle| k\right)$$

where m and n are integers and

$$\begin{aligned} K &= \int_0^{\frac{\pi}{2}} (1 - k^2\sin^2\phi)^{-\frac{1}{2}}\mathrm{d}\phi, \\ K' &= \int_0^1 (1-t^2)^{-\frac{1}{2}}(1 - t^2 + k^2t^2)^{-\frac{1}{2}}\mathrm{d}t. \end{aligned}$$

For $\lambda > 0$, $0 < C < \frac{\lambda^2}{4}$ the solution is

$$Q(x) = a\mathrm{dn}(ax|k) \tag{3.58}$$

with $C = a^4(1-k^2)$ and $\lambda = a^2(2-k^2)$. Here the solution is trapped in one of two potential wells and the quasiperiodicity is given by

$$\mathrm{dn}\left(ax + 2mK + 2niK'|k\right) = (-1)^n\mathrm{dn}(ax|k). \tag{3.59}$$

For both cases, $C > 0$ and $C < 0$, as $k^2 \to 1$ we approach the soliton solution

$$q(x,t) = \sqrt{\lambda}e^{i\lambda t}\mathrm{sech}(\sqrt{\lambda}x)$$

which for $\lambda = 1$ is the simple 1-soliton (1.6).

In the repulsive case, stable quasiperiodic solutions exist for $\lambda < 0$ and $0 < C < \frac{\lambda^2}{4}$ and are written

$$Q(x) = a\mathrm{sn}\left(\frac{a}{k}x \middle| k\right) \tag{3.60}$$

with $C = \frac{a^4}{k^2}$ and $\lambda = -\frac{a^2}{k^2}(1+k^2)$ for $0 < k^2 < 1$. The periodicity is given by

$$\mathrm{sn}\left(\frac{a}{k}x + 2mK + 2niK' \middle| k\right) = (-1)^n\mathrm{sn}\left(\frac{a}{k}x \middle| k\right)$$

and in the limit $k^2 \to 1$, the solution $q(x,t) = a\mathrm{sn}\left(\frac{a}{k}x|k\right)e^{i\lambda t}$ approaches the soliton solution

$$q(x,t) = \sqrt{-\frac{\lambda}{2}}\tanh\left(\sqrt{-\frac{\lambda}{2}}x\right)\exp(i\lambda t)$$

which for $\lambda = -2$ is the dark soliton (1.8). In the next section we will expand the idea of finding soliton solutions as limits to finite gap solutions.

3.5 Soliton limit to finite gap solutions

Hirota's method of finding soliton solutions to a range of nonlinear PDEs was developed in the 1970s and applied to the attractive and repulsive scalar nonlinear Schrödinger equations in two articles, [Hir73] and [Hir76]. Unlike the IST method, Hirota's method is applied directly to the PDE and generally produces results for any PDE that may be solved by the IST method and some equations where no IST is available. By a change of dependent variables, the PDEs may be transformed into bilinear differential equations involving the Hirota bilinear operator

$$D_x\left(a(x)\circ b(x)\right) = (\partial_x - \partial_{x'})a(x)b(x')\big|_{x=x'} \tag{3.61}$$

which may then be solved by assuming a formal perturbation expansion for the new dependent variables.

Hirota's method may be used to construct arbitrary order soliton solutions to the SNLS and indeed the VNLS, as shown by Sheppard and Kivshar [SK97] and Prinari, Ablowitz and Biondini [PAB06]. The constructions of 1- and 2-soliton solutions to the SNLS are presented in Appendix B. The form of these solutions is as ratios of sums of exponential phases which are clearly related to the ratio of theta functions solutions found via the algebrogeometric approach. This connection was studied by Its [Its82] for the SNLS with soliton solutions found as the limiting case of quasiperiodic solutions if branch points are 'pinched' together appropriately. The dark soliton limit to the repulsive quasiperiodic solutions is readily demonstrated and shall be presented in this chapter. Its finds bright soliton solutions by taking a further limit to the formulae calculated in the repulsive case, although, as he himself states, 'it is not at all a priori clear that a similar limiting process can be organized'. Indeed the nice relations between terms cropping up in the finite gap case and Hirota's dark soliton formulae are not as obvious in the bright soliton limit.

The general Hirota soliton solutions to the SNLS (1.2) are given by

$$q(x,t) = \frac{G(x,t)}{F(x,t)}. \tag{3.62}$$

$G(x,t)$ and $F(x,t)$ take differing forms for attractive and repulsive cases. The development of these solutions may be followed in Appendix B and the proofs found in Hirota's papers [Hir73] and [Hir76]. The results

$$|q(x,t)|^2 = \partial_x^2 \log F(x,t), \tag{3.63}$$

$$|q(x,t)|^2 = \frac{\tau}{2} - \partial_x^2 \log F(x,t) \tag{3.64}$$

in attractive and repulsive cases also follow where τ is a positive constant appearing in the dark soliton solution.

In the attractive case $F(x,t)$ and $G(x,t)$ are defined by

$$\begin{aligned} F(x,t) &= \sum_{\mu_i\in\{0,1\}}^{(A)} \exp\left(\sum_{j<k}\phi(j,k)\mu_j\mu_k + \sum_{j=1}^{2N}\mu_j\eta_j\right), \\ G(x,t) &= \sum_{\mu_i\in\{0,1\}}^{(B)} \exp\left(\sum_{j<k}\phi(j,k)\mu_j\mu_k + \sum_{j=1}^{2N}\mu_j\eta_j\right) \end{aligned} \tag{3.65}$$

for $i,j,k \in \{1,...,2N\}$ and

$$\phi(j,k) = \begin{cases} \ln(P_j - P_k)^2 & j<k\leq N \text{ or } N<j<k \\ \ln(P_j+P_k)^{-2} & j\leq N<k, \end{cases} \tag{3.66}$$

where P_j are distinct complex constants and $P_k = \overline{P_{k-N}}$ for $k > N$. The terms η_j are defined by

$$\left.\begin{array}{ll} \eta_j & = P_j x + iP_j^2 t + \eta_j^{(0)} \\ \eta_{j+N} & = \overline{\eta_j} \end{array}\right\} \; j = 1,...,N \tag{3.67}$$

where $\eta_j^{(0)}$ are complex constants.

$\sum_{\mu_i\in\{0,1\}}^{(A)}$ means the sum over all combinations of $\mu_i = 0$ or 1 for $i \in \{1,...,2N\}$ satisfying $\sum_{i=1}^{N}\mu_i = \sum_{i=N+1}^{2N}\mu_i$

$\sum_{\mu_i\in\{0,1\}}^{(B)}$ means the sum over all combinations of $\mu_i = 0$ or 1 for $i \in \{1,...,2N\}$ satisfying $\sum_{i=1}^{N}\mu_i = 1 + \sum_{i=N+1}^{2N}\mu_i$.

In the repulsive case

$$\begin{aligned} F(x,t) &= \sum_{\mu_j\in\{0,1\}} \exp\left(\frac{1}{2}\boldsymbol{\mu}^T\Psi\boldsymbol{\mu} + \boldsymbol{\mu}^T\boldsymbol{\eta}\right), \\ G(x,t) &= \sum_{\mu_j\in\{0,1\}} \exp\left(\frac{1}{2}\boldsymbol{\mu}^T\Psi\boldsymbol{\mu} + \boldsymbol{\mu}^T(\boldsymbol{\eta}+2i\boldsymbol{\psi})\right)\sqrt{\frac{\tau}{2}}\exp(i\theta). \end{aligned} \tag{3.68}$$

τ is a real, positive constant whilst

$$\theta = kx - (k^2+\tau)t + \theta^{(0)} \tag{3.69}$$

with k and $\theta^{(0)}$ real constants. $\boldsymbol{\eta}$ is an N-tuple with components

$$\eta_i = p_i x - \omega_i t + \eta_i^{(0)} \tag{3.70}$$

where p_i are real distinct constants satisfying $p_i^2 \leq 2\tau$ and

$$\omega_i = p_i \left(2k \pm \sqrt{2\tau - p_i^2} \right). \tag{3.71}$$

$\boldsymbol{\psi}$ is also an N-tuple with components satisfying

$$\exp(2i\psi_i) = -\frac{p_i \pm i\sqrt{2\tau - p_i^2}}{p_i \mp i\sqrt{2\tau - p_i^2}} \tag{3.72}$$

Ψ is the $N \times N$ matrix with components

$$\Psi_{mn} = \begin{cases} \ln\left[\dfrac{\sin(\frac{\psi_m - \psi_n}{2})}{\sin(\frac{\psi_m + \psi_n}{2})}\right]^2 & m \neq n \\ \\ 0 & m = n \end{cases} \tag{3.73}$$

for $m, n = 1, ..., N$.

$\sum_{\mu_j \in \{0,1\}}$ means the sum over all vectors $\boldsymbol{\mu}$ with components μ_j taking the values 0 or 1 for $j = 1, .., N$. Note the summations in this case are much simpler than those in the attractive case.

3.5.1 Dark soliton limit

As calculated in Chapter 3, the repulsive SNLS has finite gap solution

$$q(x,t) = Q\frac{\theta(\boldsymbol{\omega}(\infty^+) + \boldsymbol{g}(x,t) - \boldsymbol{e})}{\theta(\boldsymbol{\omega}(\infty^-) + \boldsymbol{g}(x,t) - \boldsymbol{e})} \exp(Ex + Nt).$$

For the purposes of finding the dark soliton solutions in Hirota's form, it is convenient to set the base point P_0 at ∞^-. The solution then becomes

$$q(x,t) = Q(\infty^-)\frac{\theta(\boldsymbol{g}(x,t) - \boldsymbol{e}(\infty^-) + \boldsymbol{r})}{\theta(\boldsymbol{g}(x,t) - \boldsymbol{e}(\infty^-))} \exp(Ex + Nt) \tag{3.74}$$

where $\boldsymbol{r} = \int_{\infty^-}^{\infty^+} \mathrm{d}\boldsymbol{\omega}$ and $Q(\infty^-)$, $\boldsymbol{e}(\infty^-)$ mean Q and $\boldsymbol{e}$ evaluated with base point ∞^-. The associated hyperelliptic curve is:

$$\mu^2(z) = \prod_{k=1}^{2g+2} (z - z_k^-)$$

with branch points z_k^- all real and ordered such that $z_1^- < z_2^- < ... < z_{2g+2}^-$. To aid computation the Riemann sheets are translated by setting

$$\begin{aligned} \beta &= \frac{z_{2g+2}^- + z_1^-}{2}, \\ \alpha &= \frac{z_{2g+2}^- - z_1^-}{2} \end{aligned} \tag{3.75}$$

and using translated coordinates

$$\begin{aligned} y &= z - \beta, \\ y_k^- &= z_k^- - \beta \qquad k = 1, ..., 2g+2. \end{aligned} \tag{3.76}$$

The hyperelliptic curve is then written as

$$\mu^2(y) = \prod_{k=1}^{2g+2} (y - y_k^-) = (y^2 - \alpha^2) \prod_{k=2}^{2g+1} (y - y_k^-). \tag{3.77}$$

Dark soliton solutions are found by examining the limiting behaviour of the system as

$$y_{2k}^-, y_{2k+1}^- \to Y_k \qquad k = 1, ..., g. \tag{3.78}$$

In this case the Riemann surface of genus g degenerates to one of genus 0, given by

$$\mu(y) \to \mu^{(0)}(y) = \sqrt{y^2 - \alpha^2} \prod_{k=1}^{g} (y - Y_k) \tag{3.79}$$

where it shall be assumed that $\sqrt{y^2 - \alpha^2}$ takes a positive sign on the top sheet of the Riemann surface above the branch emerging from α along the real axis. The basis of normalised holomorphic differentials on (3.77) is given in general form by

$$\mathrm{d}\omega_k = \frac{c_k^{(1)} y^{g-1} + c_k^{(2)} y^{g-2} + ... + c_k^{(g)}}{\mu(y)} \mathrm{d}y \qquad k = 1, ..., g. \tag{3.80}$$

In order to retain the normalisation conditions (2.13), these must become, in the limit (3.78),

$$\mathrm{d}\omega_k \to \mathrm{d}\omega_k^{(0)}(y) = \frac{\sqrt{Y_k^2 - \alpha^2}}{\sqrt{y^2 - \alpha^2}(y - Y_k)}\mathrm{d}y \qquad k = 1, ..., g. \tag{3.81}$$

The limit of elements forming the period matrix B are then given by

$$B_{jk} = \int_{b_k} \mathrm{d}\omega_j \to B_{jk}^{(0)} = 2\int_{-\alpha}^{Y_k} \mathrm{d}\omega_j^{(0)}(y). \tag{3.82}$$

If the path of integration is taken along the real y axis, it may be seen that elements of B are real and, after closer inspection, non-diagonal elements may be expressed as

$$B_{jk}^{(0)} = 2\int_{-\alpha}^{Y_k} \frac{\sqrt{\alpha^2 - Y_j^2}}{\sqrt{\alpha^2 - y^2}(y - Y_j)}\mathrm{d}y \qquad j > k \tag{3.83}$$

which ensures $\mathbb{R}\mathrm{e}(B_{jk}^{(0)}) < 0$, as required by Corollary 2.4. The substitution

$$u = \sqrt{\frac{\alpha + Y_j}{\alpha - Y_j}}\sqrt{\frac{\alpha - y}{\alpha + y}}$$

enables the integral to be calculated as

$$B_{jk}^{(0)} = \ln\left\{\frac{\sqrt{\frac{\alpha+Y_j}{\alpha-Y_j}} - \sqrt{\frac{\alpha+Y_k}{\alpha-Y_k}}}{\sqrt{\frac{\alpha+Y_j}{\alpha-Y_j}} + \sqrt{\frac{\alpha+Y_k}{\alpha-Y_k}}}\right\}^2. \tag{3.84}$$

Notice $B_{kj}^{(0)} = B_{jk}^{(0)}$ so the symmetry of B is preserved. In contrast the terms along the leading diagonal of B diverge logarithmically:

$$B_{jj}^{(0)} \sim \ln\left\{\frac{\sqrt{\frac{\alpha+Y_j}{\alpha-Y_j}} - \sqrt{\frac{\alpha+y}{\alpha-y}}}{\sqrt{\frac{\alpha+Y_j}{\alpha-Y_j}} + \sqrt{\frac{\alpha+y}{\alpha-y}}}\right\}^2 \to -\infty \qquad \text{as} \quad y \to Y_j. \tag{3.85}$$

The Abelian integrals $\Omega_1(y)$, $\Omega_2(y)$ and $H(y)$ satisfy the asymptotic expansions (3.40) and are normalised to have zero a-cycles. The general forms for the corresponding Abelian

differentials are

$$\begin{aligned}
\mathrm{d}\Omega_1(y) &= \frac{d_{g+1}^{(1)}y^{g+1} + d_g^{(1)}y^g + ... + d_0^{(1)}}{\mu(y)}\mathrm{d}y, \\
\mathrm{d}\Omega_2(y) &= \frac{d_{g+2}^{(2)}y^{g+2} + d_{g+1}^{(2)}y^{g+1} + ... + d_0^{(2)}}{\mu(y)}\mathrm{d}y, \\
\mathrm{d}H(y) &= \frac{d_g^{(3)}y^g + d_{g-1}^{(3)}y^{g-1} + ... + d_0^{(3)}}{\mu(y)}\mathrm{d}y
\end{aligned}$$

for constants $d_j^{(k)}$. Taking limits (3.78) whilst retaining the normalisation and asymptotic conditions implies

$$\begin{aligned}
\mathrm{d}\Omega_1 \to \mathrm{d}\Omega_1^{(0)} &= \frac{i}{2}\frac{y}{\sqrt{y^2-\alpha^2}}\mathrm{d}y = \frac{i}{2}\mathrm{d}\left\{\sqrt{y^2-\alpha^2}\right\}, \\
\mathrm{d}\Omega_2 \to \mathrm{d}\Omega_2^{(0)} &= \frac{i}{2}\frac{2y^2+2\beta y-\alpha^2}{\sqrt{y^2-\alpha^2}}\mathrm{d}y = \frac{i}{2}\mathrm{d}\left\{(y+2\beta)\sqrt{y^2-\alpha^2}\right\}, \\
\mathrm{d}H \to \mathrm{d}H^{(0)} &= \frac{\mathrm{d}y}{\sqrt{y^2-\alpha^2}} = \mathrm{d}\left\{\operatorname{arcosh}\left(\frac{y}{\alpha}\right)\right\}.
\end{aligned}$$

From these equations, expressions for $E \to E^{(0)}, N \to N^{(0)}$ and $g_k(x,t) \to g_k^{(0)}(x,t)$ in the limits (3.78) may be calculated and found to be:

$$\begin{aligned}
E^{(0)} &= -i\beta \\
N^{(0)} &= -i\left(\beta^2 + \frac{\alpha^2}{2}\right)
\end{aligned} \tag{3.86}$$

$$\begin{aligned}
g_k^{(0)}(x,t) &= x\int_{b_k}\mathrm{d}\Omega_1^{(0)}(P) + t\int_{b_k}\mathrm{d}\Omega_2^{(0)}(P) \\
&= i\sqrt{Y_k^2-\alpha^2}\left\{x + (Y_k+2\beta)t\right\}
\end{aligned} \tag{3.87}$$

$\boldsymbol{r} \to \boldsymbol{r}^{(0)}$ may also be found when Proposition 3.1 is applied:

$$\begin{aligned}
r_k \to r_k^{(0)} &= -\int_{b_k}\mathrm{d}H^{(0)} \\
&= -2\operatorname{arcosh}\left(\frac{y}{\alpha}\right)\Big|_{\alpha}^{Y_k} \\
&= \log\left\{\frac{\alpha^2}{2Y_k^2-\alpha^2 \pm 2iY_k\sqrt{\alpha^2-Y_k^2}}\right\}.
\end{aligned} \tag{3.88}$$

Set $k = -\beta$, $\tau = \frac{\alpha^2}{2}$, $p_k = i\sqrt{Y_k^2 - \alpha^2}$ and substitute into (3.88). This yields

$$r_k^{(0)} = \log\left\{ -\frac{p_k \pm i\sqrt{2\tau - p_k^2}}{p_k \mp i\sqrt{2\tau - p_k^2}} \right\} = 2i\psi_k \tag{3.89}$$

with reference to equation (3.72). Also substituting into off-diagonal elements $B_{jk}^{(0)}$ gives

$$B_{jk}^{(0)} = \ln\left\{ \frac{\sin\left(\frac{\psi_j - \psi_k}{2}\right)}{\sin\left(\frac{\psi_j + \psi_k}{2}\right)} \right\}^2 = \Psi_{jk} \tag{3.90}$$

in reference to equation (3.73). The vector $\boldsymbol{e}(\infty^-)$ is defined in Theorem 2.9 and its components may be written in the form

$$e_k(\infty^-) = \frac{1}{2}B_{kk} - \eta_k^{(0)}$$

for some finite term $\eta_k^{(0)}$. We also set

$$Q(\infty^-) = \sqrt{\frac{\tau}{2}}\exp(i\theta^{(0)}).$$

Finally, inspecting the behaviour of the theta functions present in the finite gap solution (3.74), it becomes clear that, as all diagonal elements of the period matrix B diverge to $-\infty$ in the limits (3.78), the only terms remaining in the expansions of the theta functions will be those with $m_k = 0, 1$. This means the finite gap solution in the limit (3.78) is indeed the dark g-soliton solution given by equation (3.62).

3.5.2 Bright soliton limit

Its [Its82] proceeds towards the bright soliton solution by considering the previous calculations but with the poles Y_k occurring in conjugate pairs rather than along the real axis and then taking appropriate limits as $\alpha \to 0$. This effectively separates the complex plane into upper and lower halves analogous to the formation of regions of analyticity of the scattering data in the IST method. We now give a brief summary of Its' method.

Take the choices $m_k = 0, 1$ found using the dark soliton derivation but consider the points Y_k to be positioned off the real axis such that $Y_{k+N} = \overline{Y_k}$ for $k = 1, ..., N$. It is also helpful to legitimately set $\mathrm{d}\Omega_2 \to -\mathrm{d}\Omega_2$ the effect of which is to change the sign of any t

dependence in the solution. We also set $\beta = 0$. As $\alpha \to 0$ we then find

$$\begin{aligned} g_k^{(0)}(x,t) &= iY_k x - iY_k^2 t \\ &= P_k x + iP_k^2 t, \qquad \text{where } iY_k = P_k \text{ for } k = 1, ..., N \\ g_{k+N}^{(0)}(x,t) &= \overline{P_k} x - i\overline{P_k}^2 t \end{aligned} \tag{3.91}$$

and

$$B_{jk}^{(0)} = \begin{cases} \ln \alpha^2 + \ln \frac{(P_j - P_k)^2}{P_j^2 P_k^2} + \text{ finite terms} & j < k \leq N \\ -\ln \alpha^2 - \ln \frac{(P_j + P_k)^2}{P_j^2 P_k^2} + \text{ finite terms} & j \leq N < k \\ \ln \alpha^2 + \ln \frac{(P_j - P_k)^2}{P_j^2 P_k^2} + \text{ finite terms} & N < j < k \end{cases} \tag{3.92}$$

Its also assumes $e_k^{(0)} = \ln \alpha - \eta_k^{(0)}$ and considering the argument of the theta function $\theta(\boldsymbol{g}^{(0)} - \boldsymbol{e}^{(0)})$ finds the divergence as $\alpha \to 0$ is:

$$\begin{aligned} &\ln \alpha^2 \left\{ \sum_{j<k\leq N} m_j m_k - \sum_{j\leq N<k} m_j m_k + \sum_{N<j<k} m_j m_k - \frac{1}{2} \sum_{j=1}^{2N} m_j \right\} \\ &= \ln \alpha \Big(\sum_{k\leq N} m_k - \sum_{k>N} m_k \Big)^2. \end{aligned}$$

This is zero only for $\sum_{k\leq N} m_k = \sum_{k>N} m_k$ which is the Hirota sum (A) occurring in equation (3.65). Substituting the possible values for m_k into $\frac{1}{2}\boldsymbol{m}^\mathsf{T} B^{(0)} \boldsymbol{m} + \boldsymbol{m}^\mathsf{T}(\boldsymbol{g}^{(0)} - \boldsymbol{e}^{(0)})$ with $B_{jj}^{(0)} = \ln Y_j^{-4}$, we find $\theta(\boldsymbol{g} - \boldsymbol{e}) \to F(x,t)$ given by (3.65). Similarly Its demonstrates $Q\theta(\boldsymbol{g}(x,t) - \boldsymbol{e}(\infty^-) + \boldsymbol{r}) \exp(Ex + Nt) \to G(x,t)$, thereby reformulating the Hirota bright soliton solution.

Although this procedure does indeed produce Hirota's bright soliton solutions, the reasons behind it are not intuitive - firstly, the spectrum associated with attractive quasiperiodic solutions comprises all conjugate pairs but in this method α is considered real. This is best explained by comparing with the IST method where $S_{11}(z)$ is analytic only in the upper-half z-plane and its zeros represent the eigenvalues of the scattering problem. This is the reason for taking the limit $\alpha \to 0$ such that the branch cut extends across the entire real axis. Furthermore Its' method requires the limits as the branch point conjugate pairs coalesce and as $\alpha \to 0$ to be considered independently. This certainly works but it may also be possible for a scheme to be constructed in which these limits are taken in conjunction with one and other. With this in mind we now present multinomial equations with solutions that are shown to be linked to the functions $F(x,t)$ and $G(x,t)$.

Definition 3.1 *The multinomial equations, $\mathcal{P}_1(\boldsymbol{n})$ and $\mathcal{P}_2(\boldsymbol{n})$, are defined by*

$$\begin{aligned}\mathcal{P}_1(\boldsymbol{n}) &= \left(\sum_{i=1}^{g} n_i\right)^2 + n^2 - g - \left(\frac{1-(-1)^g}{2}\right),\\ \mathcal{P}_2(\boldsymbol{n}) &= \left(\sum_{i=1}^{g} n_i - 2(-1)^g\right)^2 + n^2 - g - \left(\frac{1-(-1)^g}{2}\right).\end{aligned} \tag{3.93}$$

$\boldsymbol{n} = (n_1, ..., n_g)^{\mathsf{T}}$ has non-zero integer components with $n^2 = \sum_{i=1}^{g} n_i^2$ and g a positive integer.

Theorem 3.4 *$\mathcal{P}_1(\boldsymbol{n})$ has roots $n_i = \pm 1$ with $\frac{g \pm \phi(g)}{2}$ choices of n_i equal to 1 and the remaining terms equal to -1, where*

$$\phi(g) = \frac{1-(-1)^g}{2}.$$

This represents

$$\begin{pmatrix} g + \phi(g) \\ \frac{g+\phi(g)}{2} \end{pmatrix}$$

different solutions.

Proof: n_i all non-zero implies $n^2 \geq g$, however the form of $\mathcal{P}_1$ means $n^2 \leq g$. Therefore $n^2 = g$ which in turn means $n_i = \pm 1$ for $i = 1, ..., g$. Substituting this last result into $\mathcal{P}_1$ gives

$$\begin{aligned}\left(\sum_{i=1}^{g} n_i\right)^2 &= \phi(g)\\ \sum_{i=1}^{g} n_i &= \pm\phi(g)\end{aligned}$$

which have the required solutions.

Theorem 3.5 *$\mathcal{P}_2(\boldsymbol{n})$ has roots $n_i = \pm 1$ with, if g is even, $\frac{g+2}{2}$ choices equal to 1 and the remaining terms equal to -1 and, if g is odd, either $\frac{g-1}{2}$ choices equal to 1 and the remaining choices equal to -1, or $\frac{g-3}{2}$ equal to 1 and the other terms equal to -1. This leads to*

$$\begin{pmatrix} g + \phi(g) \\ \frac{g+2+\phi(g)}{2} \end{pmatrix}$$

different solutions.

Proof: As in Theorem 3.4, the fact that n_i are all non-zero integers implies $n^2 \geq g$ whilst the form of $\mathcal{P}_2(\boldsymbol{n})$ implies $n^2 \leq g$. Thus $n^2 = g$ and $n_i = \pm 1$. Substituting this into $\mathcal{P}_2(\boldsymbol{n})$ gives

$$\sum_{i=1}^{g} n_i = \begin{cases} 2 & g \text{ even} \\ -1 \text{ or } -3 & g \text{ odd} \end{cases}$$

which imply the required results.

3.5.3 Even genus case

Take the solutions to $\mathcal{P}_1(\boldsymbol{n})$ and $\mathcal{P}_2(\boldsymbol{n})$ for g even and translate them according to

$$\mu_i = \begin{cases} \left.\begin{array}{ll} 1 & \text{if } n_i = 1 \\ 0 & \text{if } n_i = -1 \end{array}\right\} & \text{for } i = 1, ..., \frac{g}{2} \\ \\ \left.\begin{array}{ll} 1 & \text{if } n_i = -1 \\ 0 & \text{if } n_i = 1 \end{array}\right\} & \text{for } i = \frac{g}{2}+1, ..., g. \end{cases} \tag{3.94}$$

Some simple calculations then reveal $\sum_{i=1}^{g/2} \mu_i$ must equal $\sum_{i=g/2+1}^{g} \mu_i$ in the case of $\mathcal{P}_1(\boldsymbol{n})$ and $\sum_{i=1}^{g/2} \mu_i$ must equal $1 + \sum_{i=g/2+1}^{g} \mu_i$ in the case of $\mathcal{P}_2(\boldsymbol{n})$. These are respectively the conditions over which the sums $\sum_{\mu_i \in \{0,1\}}^{(A)}$ and $\sum_{\mu_i \in \{0,1\}}^{(B)}$ are taken in equations (3.65).

3.5.4 Odd genus case

Consider the following injective mapping between solutions $\boldsymbol{n}$ to $\mathcal{P}_1(\boldsymbol{n})$:

$$\mu_1 = \begin{cases} 1 & \text{if } \sum_{i=1}^{g} n_i = 1 \\ 0 & \text{if } \sum_{i=1}^{g} n_i = -1 \end{cases} \tag{3.95}$$

and

$$\mu_{i+1} = \begin{cases} \left.\begin{array}{ll} 1 & \text{if } n_i = -1 \\ 0 & \text{if } n_i = 1 \end{array}\right\} & \text{for } i = 1, ..., \frac{g-1}{2} \\ \\ \left.\begin{array}{ll} 1 & \text{if } n_i = 1 \\ 0 & \text{if } n_i = -1 \end{array}\right\} & \text{for } i = \frac{g+1}{2}, ..., g. \end{cases} \tag{3.96}$$

Then, after some consideration, we may show $\sum_{i=1}^{(g+1)/2} \mu_i$ must equal $\sum_{i=(g+3)/2}^{g+1} \mu_i$ the relevant condition over which $\sum_{\mu_i \in \{0,1\}}^{(A)}$ is performed to give $F(x,t)$ with $N = g+1$.

For $\mathcal{P}_2(\boldsymbol{n})$ the appropriate mapping is the same but with equation (3.95) replaced by

$$\mu_1 = \begin{cases} 1 & \text{if } \sum_{i=1}^{g} n_i = -1 \\ 0 & \text{if } \sum_{i=1}^{g} n_i = -3. \end{cases} \tag{3.97}$$

From this we may show $\sum_{i=1}^{g/2} \mu_i$ must equal $1 + \sum_{i=g/2+1}^{g} \mu_i$, the condition over which $\sum_{\mu_i \in \{0,1\}}^{(B)}$ is taken.

Thus we have shown that $\mathcal{P}_1(\boldsymbol{n})$ and $\mathcal{P}_1(\boldsymbol{n})$ are directly linked to the choices for μ_i over which sums $\sum_{\mu_i \in \{0,1\}}^{(A)}$ and $\sum_{\mu_i \in \{0,1\}}^{(B)}$ are taken respectively. So there is a clear indication that, if appropriate limits are taken, the quasiperiodic solutions may form soliton solutions of Hirota's form in both even and odd genera case.

Chapter 4

VNLS hierarchy

The original Manakov system [Man74] is a natural extension of Zakharov and Shabat's [ZS72] in the scalar case and is given in Lax pair form. The scattering problem considered in this thesis is a related Lax form, slightly generalised from that presented in [EEI07], which, up to a re-scaling of variables, may be written in Manakov's original form. In this chapter we will consider a hierarchy of vector nonlinear Schrödinger equations by invoking a natural extension of the Manakov system. We prove closed form solutions for the zero-curvature representations of these higher-order equations and examine the associated spectral curves. We also find conserved densities of the hierarchy which allow the Hamiltonian structure of the hierarchy to be expressed.

Results of parts of this chapter form an article [WE07] which has been published in Physica D.

4.1 VNLS scattering problem

The Lax representations relevant to equations (1.1) are given by:

$$\begin{aligned} \boldsymbol{v}_x &= \mathcal{L}_1^{\pm}(z)\boldsymbol{v} = \left(zL_0^{\pm} + L_1^{\pm}\right)\boldsymbol{v}, \\ \boldsymbol{v}_t &= \mathcal{L}_2^{\pm}(z)\boldsymbol{v} = \left(z^2L_0^{\pm} + zL_1^{\pm} + L_2^{\pm}\right)\boldsymbol{v} \end{aligned} \tag{4.1}$$

where

$$L_0^{\pm} = \begin{pmatrix} \alpha_0^{\pm} & \mathbf{0}^{\mathsf{T}} \\ \mathbf{0} & (i+\alpha_0^{\pm})\mathbb{I}_2 \end{pmatrix}, \quad L_1^{\pm} = \begin{pmatrix} 0 & \boldsymbol{q}^{\mathsf{T}} \\ \mp\overline{\boldsymbol{q}} & \mathbb{O}_2 \end{pmatrix}, \quad L_2^{\pm} = \begin{pmatrix} \pm i\boldsymbol{q}^{\mathsf{T}}\overline{\boldsymbol{q}} & i\boldsymbol{q}_x^{\mathsf{T}} \\ \pm i\overline{\boldsymbol{q}}_x & \mp i\overline{\boldsymbol{q}}\boldsymbol{q}^{\mathsf{T}} \end{pmatrix} \tag{4.2}$$

are 3×3 matrices. $\mathbf{0}$ is the zero 2-vector, $\mathbb{I}_2$ is the 2×2 identity matrix and $\mathbb{O}_2$ is the 2×2 zero matrix. The VNLS (1.1) results from the consistency condition $\boldsymbol{v}_{xt} = \boldsymbol{v}_{tx}$ at order

z^0. A slight generalisation of the work of Elgin et al. [EEI07] is that $\alpha_0^{\pm}$ is allowed to be a free imaginary constant whereas in [EEI07] $\alpha_0^{\pm}$ is fixed at $-i/2$. This leads to some simplifications in later calculation but, importantly, the main results are independent of the choice of $\alpha_0^{\pm}$ and the genus of the resulting trigonal curve is the same.

The original Lax pair form may be found by rewriting the first of equations (4.1) as

$$\widehat{L}\boldsymbol{v} = z\boldsymbol{v}, \tag{4.3}$$

where $\widehat{L} = (L_0^{\pm})^{-1}(\mathbb{I}_3\partial_x - L_1^{\pm})$. Differentiating with respect to t and applying equations (4.1) and (4.3) repeatedly gives

$$\begin{aligned}\widehat{L}_t\boldsymbol{v} &= (z - \widehat{L})\boldsymbol{v}_t \\ &= \left[(L_0^{\pm}\widehat{L}^2 + L_1^{\pm}\widehat{L} + L_2^{\pm}), \widehat{L}\right]\boldsymbol{v} \\ &= [\widehat{A}, \widehat{L}]\boldsymbol{v}.\end{aligned}$$

The Lax form then comprises equation (4.3) and

$$\widehat{L}_t = [\widehat{A}, \widehat{L}]. \tag{4.4}$$

The evolution equations (4.1) are the first two of a general infinite VNLS hierarchy of commuting flows defined by

$$\boldsymbol{v}_{t_n} = \mathcal{L}_n^{\pm}(z)\boldsymbol{v} \tag{4.5}$$

for $n \in \mathbb{N}$. The 3×3 matrices $\mathcal{L}_n^{\pm}(z)$ are given polynomial expansions in z:

$$\mathcal{L}_n^{\pm}(z) = \begin{pmatrix} \boldsymbol{\alpha}^{\pm} & \boldsymbol{\beta}^{\pm\,\mathsf{T}} \\ \boldsymbol{\gamma}^{\pm} & A^{\pm} \end{pmatrix} = \sum_{k=0}^{n} z^{n-k} L_k^{\pm} \tag{4.6}$$

which satisfy the conjugation properties

$$\begin{aligned}\left(\mathcal{L}_n^{+}\right)^{\dagger}(z) &= -\mathcal{L}_n^{+}(z), \\ \left(\mathcal{L}_n^{-}\right)^{\dagger}(z) &= -\Gamma\mathcal{L}_n^{-}(z)\Gamma\end{aligned} \tag{4.7}$$

where $\Gamma = \begin{pmatrix} 1 & \mathbf{0}^{\mathsf{T}} \\ \mathbf{0} & -\mathbb{I}_2 \end{pmatrix}$.

The 3×3 matrices $L_k^{\pm}$ forming the polynomial coefficients are given the structure:

$$L_k^{\pm} = \begin{pmatrix} \alpha_k^{\pm} & \boldsymbol{\beta}_k^{\pm\,\mathsf{T}} \\ \boldsymbol{\gamma}_k^{\pm} & A_k^{\pm} \end{pmatrix} \tag{4.8}$$

with the first three matrices defined by (4.2). In order to agree with conditions (4.7) these must satisfy

$$\begin{aligned} &\mathbb{R}\mathrm{e}(\alpha_k^{\pm}), \mathbb{R}\mathrm{e}(A_{k,11}^{\pm}), \mathbb{R}\mathrm{e}(A_{k,22}^{\pm}) = 0, \\ &A_{k,21}^{\pm} = -\overline{A_{k,12}^{\pm}}, \\ &\boldsymbol{\gamma}_k^{\pm} = \mp\overline{\boldsymbol{\beta}_k^{\pm}} \end{aligned} \tag{4.9}$$

where $A_k^{\pm}$ is a 2×2 matrix with components $A_{k,ij}^{\pm}$ for $i, j = 1, 2$.

Through cross-differentiation, the general zero-curvature representations

$$\frac{\partial \mathcal{L}_k^{\pm}}{\partial t_j} - \frac{\partial \mathcal{L}_j^{\pm}}{\partial t_k} = \left[\mathcal{L}_j^{\pm}, \mathcal{L}_k^{\pm}\right] \tag{4.10}$$

are satisfied from which the Manakov system may be recovered by setting $t_1 = x$ and $t_2 = t$.

4.2 Closed form for the VNLS hierarchy

In this section we shall calculate closed form relations for the elements of the matrices $L_k^{\pm}$. We shall drop $\pm$ signs in order to improve clarity and distinguish attractive and repulsive case results as appropriate. Take the specific flow

$$\frac{\partial \mathcal{L}_n}{\partial x} - \frac{\partial \mathcal{L}_1}{\partial t_n} = [\mathcal{L}_1, \mathcal{L}_n] \tag{4.11}$$

where $t_1 = x$. Comparing powers of z we obtain:

$$\left.\begin{aligned} \alpha_{k,x} &= \boldsymbol{q}^{\mathsf{T}}\boldsymbol{\gamma}_k \pm \boldsymbol{\beta}_k^{\mathsf{T}}\overline{\boldsymbol{q}} \\ A_{k,x} &= -\left(\boldsymbol{\gamma}_k\boldsymbol{q}^{\mathsf{T}} \pm \overline{\boldsymbol{q}}\boldsymbol{\beta}_k^{\mathsf{T}}\right) \end{aligned}\right\} \qquad k = 0, ..., n,$$

$$\boldsymbol{\beta}_{k,x} = -i\boldsymbol{\beta}_{k+1} + \left(A_k^{\mathsf{T}} - \alpha_k\right)\boldsymbol{q} \qquad k = 0, ..., n-1, \tag{4.12}$$

$$\boldsymbol{\beta}_{n,x} = \boldsymbol{q}_{t_n} + \left(A_n^{\mathsf{T}} - \alpha_n\right)\boldsymbol{q}$$

and from these the recurrence relation

$$\boldsymbol{\beta}_{k+1} = \mathcal{D}^{\pm}\boldsymbol{\beta}_k \qquad k = 0, ..., n-1 \tag{4.13}$$

may be derived in attractive and repulsive cases respectively. The integro-differential operators $\mathcal{D}^{\pm}$ act on a complex vector $\boldsymbol{f}(x)$ according to the formulae

$$\mathcal{D}^{\pm}\boldsymbol{f}(x) = i\boldsymbol{f}_x \pm i\int^x \left\{\boldsymbol{q}^\dagger(x'), \boldsymbol{f}(x')\right\}_A \mathrm{d}x'\,\boldsymbol{q} \tag{4.14}$$

where

$$\left\{\boldsymbol{a}^\dagger, \boldsymbol{b}\right\}_A = (\boldsymbol{a}^\dagger\boldsymbol{b} - \boldsymbol{b}^\dagger\boldsymbol{a})\mathbb{I}_2 + (\boldsymbol{b}\boldsymbol{a}^\dagger - \boldsymbol{a}\boldsymbol{b}^\dagger)$$

is twice the anti-Hermitian part of the anti-commutator of complex vectors $\boldsymbol{a}^\dagger$ and $\boldsymbol{b}$. Interestingly the only difference between the attractive and repulsive cases is the sign choice in (4.14). For the time being we shall assume all elements α_k and A_k, for $k = 1, ..., n$, have constants of integration equal to zero and thus the formal integrals involved in the recurrence relation (4.13) also have zero constants of integration for $k = 1, ..., n$. Under this assumption, taking the trace of equation (4.11) and integrating with respect to x implies

$$\mathrm{Tr}\mathcal{L}_n(z) = z^n(3\alpha_0 + 2i), \tag{4.15}$$

so $\mathcal{L}_n(z)$ is traceless up to order z^n. From (4.12) the general n^{th} flows of the VNLS hierarchy in attractive and repulsive cases respectively may be derived:

$$\boldsymbol{q}_{t_n} = -i\mathcal{D}^{\pm}\boldsymbol{\beta}_n = -i(\mathcal{D}^{\pm})^n\boldsymbol{q}, \tag{4.16}$$

the first few of which are

$$\begin{aligned}
\boldsymbol{q}_{t_1} &= \boldsymbol{q}_x, \\
\boldsymbol{q}_{t_2} &= i\boldsymbol{q}_{xx} \pm 2i\boldsymbol{q}\boldsymbol{q}^\dagger\boldsymbol{q}, \\
\boldsymbol{q}_{t_3} &= -\boldsymbol{q}_{xxx} \mp 3\{\boldsymbol{q}^\dagger, \boldsymbol{q}_x\}\boldsymbol{q},
\end{aligned} \tag{4.17}$$

where the second of these is the VNLS (1.1) derived from the Manakov system. Recurrence formulae for the terms α_k and A_k are found through analysis of the matrix $\mathcal{Q}_n(z) = \mathcal{L}_n^2(z)$ which may be given the structure

$$\mathcal{Q}_n(z) = \begin{pmatrix} \widehat{\alpha} & \widehat{\boldsymbol{\beta}}^{\mathsf{T}} \\ \widehat{\boldsymbol{\gamma}} & \widehat{A} \end{pmatrix} = \sum_{k=0}^{2n} z^{2n-k} Q_k \tag{4.18}$$

with

$$Q_k = \begin{pmatrix} \widehat{\alpha}_k & \widehat{\boldsymbol{\beta}}_k^{\mathsf{T}} \\ \widehat{\boldsymbol{\gamma}}_k & \widehat{A}_k \end{pmatrix}.$$

Conjugation conditions (4.7) imply

$$\begin{aligned}\left(\mathcal{Q}_n^+\right)^\dagger(z) &= \mathcal{Q}_n^+(z),\\ \left(\mathcal{Q}_n^-\right)^\dagger(z) &= \Gamma\mathcal{Q}_n^-(z)\Gamma\end{aligned} \tag{4.19}$$

where $\pm$ signs indicate attractive and repulsive cases and it thus follows

$$\begin{aligned}&\mathbb{I}\mathrm{m}(\widehat{\alpha}_k), \mathbb{I}\mathrm{m}(\widehat{A}_{k,11}), \mathbb{I}\mathrm{m}(\widehat{A}_{k,22}) = 0,\\ &\widehat{A}_{k,21} = \overline{\widehat{A}_{k,12}},\\ &\widehat{\boldsymbol{\gamma}}_k = \pm\,\overline{\widehat{\boldsymbol{\beta}}_k}.\end{aligned} \tag{4.20}$$

From the zero-curvature equation (4.11) the PDE

$$\frac{\partial\mathcal{Q}_n}{\partial x} = \left\{\mathcal{L}_n, \frac{\partial\mathcal{L}_1}{\partial t_n}\right\} + [\mathcal{L}_1, \mathcal{Q}_n] \tag{4.21}$$

may be deduced. This in turn implies the recurrence relation

$$\widehat{\boldsymbol{\beta}}_{k+1} = \widehat{\mathcal{D}}^{\pm}\widehat{\boldsymbol{\beta}}_k \qquad k = 0, ..., n-1 \tag{4.22}$$

where the operators $\widehat{\mathcal{D}}^{\pm}$ act on vector $\boldsymbol{f}(x)$ according to the formulae

$$\widehat{\mathcal{D}}^{\pm}\boldsymbol{f}(x) = i\boldsymbol{f}_x \pm i\int^x \left\{\boldsymbol{q}^\dagger(x'), \boldsymbol{f}(x')\right\}_H \mathrm{d}x'\,\boldsymbol{q} \tag{4.23}$$

and

$$\left\{\boldsymbol{a}^\dagger, \boldsymbol{b}\right\}_H = (\boldsymbol{a}^\dagger\boldsymbol{b} + \boldsymbol{b}^\dagger\boldsymbol{a})\mathbb{I}_2 + (\boldsymbol{b}\boldsymbol{a}^\dagger + \boldsymbol{a}\boldsymbol{b}^\dagger)$$

is twice the Hermitian part of the anti-commutator of complex vectors $\boldsymbol{a}^\dagger$ and $\boldsymbol{b}$. Comparing this with (4.14) we see that the only difference is that the anti-Hermitian part has been replaced by the Hermitian part. As it has already been assumed that the elements of L_k have constants of integration equal to zero, it follows that so too do the elements of Q_k. This leads to the following theorem:

Theorem 4.1 *In both attractive and repulsive cases,*

$$\begin{aligned}\widehat{\boldsymbol{\beta}}_k &= (i + 2\alpha_0)\boldsymbol{\beta}_k \qquad k = 0, ..., n,\\ \widehat{\boldsymbol{\gamma}}_k &= (i + 2\alpha_0)\boldsymbol{\gamma}_k \qquad k = 0, ..., n.\end{aligned} \tag{4.24}$$

Proof: For $k = 0$ the result is trivial as $\boldsymbol{\beta}_0 = \mathbf{0}$ determines $\widehat{\boldsymbol{\beta}}_0 = \mathbf{0}$. For $k = 1$,

$$\begin{aligned}\widehat{\boldsymbol{\beta}}_1 &= (A_1^{\mathsf{T}} + \alpha_1)\boldsymbol{\beta}_0 + (A_0^{\mathsf{T}} + \alpha_0)\boldsymbol{\beta}_1 \\ &= (i + 2\alpha_0)\boldsymbol{\beta}_1,\end{aligned}$$

to which the operators $\widehat{\mathcal{D}}^{\pm}$ may be applied. This gives, using (4.22),

$$\begin{aligned}\widehat{\boldsymbol{\beta}}_2 &= \widehat{\mathcal{D}}^{\pm}\{(i + 2\alpha_0)\boldsymbol{\beta}_1\} \\ &= (i + 2\alpha_0)\mathcal{D}^{\pm}\boldsymbol{\beta}_1 \\ &= (i + 2\alpha_0)\boldsymbol{\beta}_2\end{aligned}$$

where the fact that, if κ is a purely imaginary constant,

$$\widehat{\mathcal{D}}^{\pm}\{\kappa \boldsymbol{f}(x)\} = \kappa \mathcal{D}^{\pm}\boldsymbol{f}(x)$$

has been used. Applying $\widehat{\mathcal{D}}^{\pm}$ repeatedly gives the first of equations (4.24) whose complex conjugate is the second. We notice that the choice of $\alpha_0 = -i/2$ in [EEI07] simplifies both equations (4.24) considerably. However, as we shall see when the spectral curve is formulated, the choice of α_0 has little effect on its properties.

Corollary 4.1

$$\sum_{j=1}^{k-1} \boldsymbol{\beta}_j^{\mathsf{T}}(A_{k-j} + \alpha_{k-j}) = 0 \qquad k = 2, ..., n. \tag{4.25}$$

Proof: Application of Theorem 4.1 to

$$\widehat{\boldsymbol{\beta}}_k^{\mathsf{T}} = \sum_{j=0}^{k} \boldsymbol{\beta}_j^{\mathsf{T}}(A_{k-j} + \alpha_{k-j}).$$

Corollary 4.2

$$\sum_{j=1}^{k-1} \begin{vmatrix} A_{j,11} & A_{j,12} \\ A_{k-j,21} & A_{k-j,22} \end{vmatrix} = 0 \qquad k = 2, ..., n. \tag{4.26}$$

Proof: Application of the Cayley-Hamilton theorem to $\widetilde{A} = \sum_{p=1}^{n} z^{n-p} A_p$ followed by Corollary 4.1 gives the required result.

Corollary 4.3

$$\sum_{j=1}^{k-1}(A_j+\alpha_j)A_{k-j}=0 \qquad k=2,...,n. \tag{4.27}$$

Proof: Application of the Cayley-Hamilton theorem to $A=\sum_{p=0}^{n} z^{n-p}A_p$ then Corollary 4.2 at order z^{2n-k}.

Recurrence formulae for α_k and A_k may now be constructed and are presented in the following two theorems:

Theorem 4.2

$$\alpha_k=-i\sum_{j=1}^{k-1}(\alpha_j\alpha_{k-j}+\boldsymbol{\beta}_j^{\mathsf{T}}\boldsymbol{\gamma}_{k-j}) \qquad k=2,...,n. \tag{4.28}$$

Proof: From (4.21)

$$\widehat{\alpha}_{k,x} = \boldsymbol{\beta}_1^{\mathsf{T}}\widehat{\boldsymbol{\gamma}}_k-\widehat{\boldsymbol{\beta}}_k^{\mathsf{T}}\boldsymbol{\gamma}_1$$

which means, using Theorem 4.1,

$$\begin{aligned}\widehat{\alpha}_{k,x} &= (i+2\alpha_0)(\boldsymbol{\beta}_1^{\mathsf{T}}\boldsymbol{\gamma}_k-\boldsymbol{\beta}_k^{\mathsf{T}}\boldsymbol{\gamma}_1)\\ &= (i+2\alpha_0)\alpha_{k,x}.\end{aligned}$$

Integrate to give

$$\begin{aligned}\widehat{\alpha}_k &= (i+2\alpha_0)\alpha_k\\ \sum_{j=0}^{k}(\alpha_j\alpha_{k-j}+\boldsymbol{\beta}_j^{\mathsf{T}}\boldsymbol{\gamma}_{k-j}) &= (i+2\alpha_0)\alpha_k,\end{aligned}$$

the required result.

Theorem 4.3

$$A_k=i\sum_{j=1}^{k-1}(\boldsymbol{\gamma}_j\boldsymbol{\beta}_{k-j}^{\mathsf{T}}-\alpha_jA_{k-j}) \qquad k=2,...,n \tag{4.29}$$

Proof: From (4.21)

$$\widehat{A}_{k,x} = \boldsymbol{\gamma}_1\widehat{\boldsymbol{\beta}}_k^{\mathsf{T}}-\widehat{\boldsymbol{\gamma}}_k\boldsymbol{\beta}_1^{\mathsf{T}}$$

which means, using Theorem 4.1,

$$\begin{aligned}\widehat{A}_{k,x} &= (i+2\alpha_0)(\boldsymbol{\gamma}_1\boldsymbol{\beta}_k^{\mathsf{T}} - \boldsymbol{\gamma}_k\boldsymbol{\beta}_1^{\mathsf{T}}) \\ &= (i+2\alpha_0)A_{k,x}.\end{aligned}$$

Integrate to give

$$\begin{aligned}\widehat{A}_k &= (i+2\alpha_0)A_k \\ \sum_{j=0}^{k}(A_jA_{k-j} + \boldsymbol{\gamma}_j\boldsymbol{\beta}_{k-j}^{\mathsf{T}}) &= (i+2\alpha_0)A_k \\ \Leftrightarrow \sum_{j=1}^{k-1}(A_jA_{k-j} + \boldsymbol{\gamma}_j\boldsymbol{\beta}_{k-j}^{\mathsf{T}}) &= -iA_k\end{aligned}$$

which is the required result when Corollary 4.3 is applied.

As a direct consequence of these theorems, $\mathcal{Q}_n(z)$ takes the form

$$\mathcal{Q}_n(z) = z^{2n}L_0^2 + (i+2\alpha_0)\sum_{k=1}^{n} z^{2n-k}L_k + \sum_{k=n+1}^{2n} z^{2n-k}Q_k. \tag{4.30}$$

We may also find the following closed form recurrence relation for the matrices L_k similar to that found in the scalar case:

Theorem 4.4 *If* $\alpha_0 = -i/2$,

$$L_{k+1} = [L_{k,x}, L_0] + [L_0, [L_1, L_k]] + \sum_{j=1}^{k}\{L_j, L_{k+1-j}\}L_0. \tag{4.31}$$

Proof: Apply the commutator of L_0 with the z^{n-k} coefficients of equation (4.11) and then Theorems 4.2 and 4.3.

4.3 Spectral curve of the Manakov hierarchy

We now investigate the form of the spectral curves associated with the VNLS hierarchy. In [EEI07] the form that these take was verified using the Maple computer package for low genus examples. We provide proofs that these forms are indeed correct for all genera using the results of the previous section and also identify the structure of the coefficients.

The spectral curve, $f(z,\mu)$, associated to $\mathcal{L}_n(z)$ is found from its characteristic polynomial:

$$f(z,\mu) = -\det\left(\mathcal{L}_n(z) - \mu\mathbb{I}_3\right) = \mu^3 + a_2(z)\mu^2 + a_1(z)\mu + a_0(z) \tag{4.32}$$

with

$$\begin{aligned} a_2(z) &= -\mathrm{Tr}\mathcal{L}_n \\ a_1(z) &= \left((\mathrm{Tr}\mathcal{L}_n)^2 - \mathrm{Tr}\mathcal{Q}_n\right)/2 \\ a_0(z) &= -\det\mathcal{L}_n = -\left((\mathrm{Tr}\mathcal{L}_n)^3 - 3\mathrm{Tr}\mathcal{L}_n\mathrm{Tr}\mathcal{Q}_n + 2\mathrm{Tr}\mathcal{R}_n\right)/6 \end{aligned}$$

where $\mathcal{R}_n(z) = \mathcal{L}_n^3(z)$. Notice that if we consider (4.11) for a stationary flow, independent of t_n, we have

$$\frac{\partial\mathcal{L}_n}{\partial x} = [\mathcal{L}_1, \mathcal{L}_n]\,. \tag{4.33}$$

From this it follows that $\mathrm{Tr}\mathcal{L}_n(z)$, $\mathrm{Tr}\mathcal{Q}_n$ and $\mathrm{Tr}\mathcal{R}_n$ are all constant in x and t_n and hence so are $a_1(z)$, $a_2(z)$ and $a_3(z)$. We now consider more specifically the form of the spectral curve in terms of elements of the matrices L_k which will allow us to determine its genus.

Theorem 4.5

$$\mathrm{Tr}\mathcal{Q}_n(z) = (3\alpha_0^2 + 4i\alpha_0 - 2)z^{2n} + P_{n-1}(z) \tag{4.34}$$

where $P_{n-1}(z) = \sum_{k=n+1}^{2n} z^{2n-k}\lambda_k$ *is a polynomial of order* $n-1$ *with real coefficients* λ_k *taking the form*

$$\lambda_k = \sum_{j=k-n}^{n}\left(\alpha_j\alpha_{k-j} + 2\boldsymbol{\beta}_j^{\mathsf{T}}\boldsymbol{\gamma}_{k-j} + \mathrm{Tr}(A_jA_{k-j})\right). \tag{4.35}$$

Proof: Referring to (4.6), $\mathrm{Tr}\mathcal{Q}_n$ takes the form

$$\begin{aligned} \mathrm{Tr}\mathcal{Q}_n &= \alpha^2 + 2\boldsymbol{\beta}^{\mathsf{T}}\boldsymbol{\gamma} + \mathrm{Tr}A^2 \\ &= \sum_{k=0}^{n} z^{2n-k}\sum_{j=0}^{k}\left(\alpha_j\alpha_{k-j} + 2\boldsymbol{\beta}_j^{\mathsf{T}}\boldsymbol{\gamma}_{k-j} + \mathrm{Tr}(A_jA_{k-j})\right) + P_{n-1}(z) \end{aligned}$$

which, upon applying (4.15), (4.27) and (4.28), can be shown equal to (4.34).

Theorem 4.6

$$\mathrm{Tr}\mathcal{R}_n(z) = (3\alpha_0^3 + 6i\alpha_0^2 - 6\alpha_0 - 2i)z^{3n} + \frac{3}{2}(i + 2\alpha_0)z^nP_{n-1}(z) + T_{n-2}(z). \tag{4.36}$$

Here $T_{n-2}(z)$ *is a polynomial of order* $n-2$ *with purely imaginary coefficients which will*

be defined.

Proof: The following PDE may be derived from (4.11):

$$\mathcal{R}_{n,x} = \{L_{1,t_n}, \mathcal{Q}_n\} + \mathcal{L}_n L_{1,t_n} \mathcal{L}_n + [\mathcal{L}_1, \mathcal{R}_n]\,.$$

Taking traces and applying Theorem 4.1 gives, in attractive and repulsive cases,

$$\begin{aligned}\mathrm{Tr}\mathcal{R}_{n,x} &= 3\left(\boldsymbol{q}_{t_n}^{\mathsf{T}}\widehat{\boldsymbol{\gamma}} \mp \widehat{\boldsymbol{\beta}}^{\mathsf{T}}\overline{\boldsymbol{q}}_{t_n}\right) \\ &= 3(i+2\alpha_0)z^n\left(\boldsymbol{q}_{t_n}^{\mathsf{T}}\boldsymbol{\gamma} \mp \boldsymbol{\beta}^{\mathsf{T}}\overline{\boldsymbol{q}}_{t_n}\right) + 3\sum_{k=n+1}^{2n} z^{2n-k}\left(\boldsymbol{q}_{t_n}^{\mathsf{T}}\widehat{\boldsymbol{\gamma}}_k \mp \widehat{\boldsymbol{\beta}}_k^{\mathsf{T}}\overline{\boldsymbol{q}}_{t_n}\right).\end{aligned}$$

Similarly, if traces of (4.21) are taken,

$$\mathrm{Tr}\mathcal{Q}_{n,x}(z) = 2\left(\boldsymbol{q}_{t_n}^{\mathsf{T}}\boldsymbol{\gamma} \mp \boldsymbol{\beta}^{\mathsf{T}}\overline{\boldsymbol{q}}_{t_n}\right)$$

and hence

$$\mathrm{Tr}\mathcal{R}_{n,x} = \frac{3}{2}(i+2\alpha_0)z^n\mathrm{Tr}\mathcal{Q}_{n,x} + 3\sum_{k=n+1}^{2n} z^{2n-k}\left(\boldsymbol{q}_{t_n}^{\mathsf{T}}\widehat{\boldsymbol{\gamma}}_k \mp \widehat{\boldsymbol{\beta}}_k^{\mathsf{T}}\overline{\boldsymbol{q}}_{t_n}\right).$$

Noticing that $\widehat{\boldsymbol{\beta}}_{n+1}^{\mathsf{T}} = \sum_{j=1}^{n}\boldsymbol{\beta}_{n+1-j}^{\mathsf{T}}(A_j + \alpha_j)$, Corollary 4.1 may be applied but with $n+1$ replacing n. Then $\widehat{\boldsymbol{\beta}}_{n+1} = 0$ and so too must $\widehat{\boldsymbol{\gamma}}_{n+1} = 0$. Thus

$$\mathrm{Tr}\mathcal{L}_{n,x}^3 = \frac{3}{2}(i+2\alpha_0)z^n\mathrm{Tr}\mathcal{L}_{n,x}^2 + T_{n-2,x}$$

and upon integrating this expression, as no integration constants were permitted for the terms forming $\mathcal{L}_n(z)$, it follows that

$$\begin{aligned}\mathrm{Tr}\mathcal{R}_n &= z^{3n}\mathrm{Tr}L_0^3 + \frac{3}{2}(i+2\alpha_0)z^nP_{n-1}(z) + T_{n-2}(z) \\ &= (3\alpha_0^3 + 6i\alpha_0^2 - 6\alpha_0 - 2)z^{3n} + \frac{3}{2}(i+2\alpha_0)z^nP_{n-1}(z) + T_{n-2}(z),\end{aligned}$$

as required. $T_{n-2}(z)$ is the polynomial of order $n-2$ given by

$$T_{n-2}(z) = \sum_{p=2n+2}^{3n} z^{3n-p}\eta_p$$

with

$$\eta_p = \sum_{\substack{i,j,k=2,\\ i+j+k=p}}^{n} \Big(\alpha_i\alpha_j\alpha_k + 3\boldsymbol{\beta}_i^{\mathsf{T}}(A_j+\alpha_j)\boldsymbol{\gamma}_k + \mathrm{Tr}(A_iA_jA_k)\Big). \tag{4.37}$$

We choose $\alpha_0 = -i$ in which case the general spectral curve takes the form

$$f(z,\mu) = \mu^2(\mu + iz^n) - \mu\frac{P_{n-1}(z)}{2} - \frac{T_{n-2}(z)}{3} = 0. \tag{4.38}$$

For purposes of comparison with [EEI07] we also inspect the case $\alpha_0 = -i/2$ for the genus 1 curve where $n = 2$. This is given explicitly by

$$f(z,\mu) = (\mu - \frac{i}{2}z^2)^2(\mu + \frac{i}{2}z^2) - (\mu - \frac{i}{2}z^2)\frac{P_1(z)}{2} - \frac{T_0(z)}{3} = 0 \tag{4.39}$$

with

$$\begin{aligned} P_1(z) &= \pm 2iz\left(\boldsymbol{q}_x^\dagger\boldsymbol{q} - \boldsymbol{q}^\dagger\boldsymbol{q}_x\right) - 2\left((\boldsymbol{q}^\dagger\boldsymbol{q})^2 \pm \boldsymbol{q}_x^\dagger\boldsymbol{q}_x\right), \\ T_0(z) &= 3i(\boldsymbol{q}^\dagger\boldsymbol{q}_x\boldsymbol{q}_x^\dagger\boldsymbol{q} - \boldsymbol{q}^\dagger\boldsymbol{q}\boldsymbol{q}_x^\dagger\boldsymbol{q}_x) = -3i|q_{1,x}q_2 - q_{2,x}q_1|^2 \end{aligned}$$

and agrees with [EEI07] up to the change of variables $z \mapsto 2z$, $\mu \mapsto w$ in the attractive case.

The curve

$$X = \{(z,\mu)|f(z,\mu) = 0\} \tag{4.40}$$

defines, in general, a three-sheeted or trigonal Riemann surfaces, with branch cuts connecting pairs of sheets. To date, studies on integrable systems with trigonal curves have largely concentrated on the degenerate case when $a_2, a_1 \equiv 0$. This leads to a cyclic curve with branch cuts connecting all three sheets, see for example [BG06]. The genus of X may be calculated using the Riemann-Hurwitz formula once the total number of branch points has been derived. The branch points are the roots of the discriminant of $f(z,\mu)$, considered as a cubic in μ:

$$\mathrm{Disc}f(z,\mu) = a_1^2a_2^2 - 4a_0a_2^3 - 4a_1^3 + 18a_0a_1a_2 - 27a_0^2. \tag{4.41}$$

If Theorems 4.5 and 4.6 are applied

$$\begin{aligned} \mathrm{Disc}f(z,\mu) = z^{2n}&\left(-\frac{(P_{n-1}(z))^2}{4} - z^n\frac{4i}{3}T_{n-2}(z)\right) \\ &+ \left(\frac{(P_{n-1}(z))^3}{2} + 3iz^nP_{n-1}(z)T_{n-2}(z)\right) - 3\left(T_{n-2}(z)\right)^2. \end{aligned} \tag{4.42}$$

Assuming the highest order term is non-zero, that is

$$\Delta = \lambda_{n+1}^2 + \frac{16i}{3}\eta_{2n+2} \neq 0, \tag{4.43}$$

Disc$f(z,w)$ is, in general, a polynomial in z with $4n-2$ simple, finite roots and thus, applying the Riemann-Hurwitz formula for a three-sheeted covering, the genus of X is given by

$$g = 2n-3. \tag{4.44}$$

It should be noted that this means only curves of odd genus result from this structure. The possibility of even genus curves results from the inclusion of constants of integration which we shall explore in the next section.

4.4 Introduction of constants of integration

All constants of integration were previously set equal to zero. In this section we relax this condition and permit the terms α_k and A_k to take the forms, in attractive and repulsive cases respectively,

$$\begin{aligned} \alpha_k &= \int^x (\boldsymbol{q}^\dagger \boldsymbol{\beta}_k \mp \boldsymbol{\beta}_k^\dagger \boldsymbol{q})\mathrm{d}x' + b_k \qquad k = 1, ..., n, \\ A_k &= -\int^x (\overline{\boldsymbol{q}}\boldsymbol{\beta}_k^\mathsf{T} \mp \overline{\boldsymbol{\beta}_k}\boldsymbol{q}^\mathsf{T})\mathrm{d}x' + B_k \qquad k = 1, ..., n. \end{aligned} \tag{4.45}$$

Here the 2×2 constant matrices B_k preserve the conjugation conditions (4.7) so that

$$\mathbb{R}\mathrm{e}(b_k) = 0, \qquad B_k^\dagger = -B_k \qquad k = 1, ..., n.$$

The relation (4.13) is now replaced by

$$\boldsymbol{\beta}_{k+1} = \mathcal{D}^\pm \boldsymbol{\beta}_k + i(B_1^\mathsf{T} - b_1)\boldsymbol{\beta}_k - i(B_k^\mathsf{T} - b_k)\boldsymbol{q}. \tag{4.46}$$

In order to find the general n^{th} flow it is necessary to apply this relation recursively. For general constant matrices B_k this is not possible without leaving non-local terms so we now consider two choices that preserve the local structure of the hierarchy. In the first instance we require B_k to be proportional to the identity matrix and set

$$c_k \mathbb{I}_2 = -i(B_k - \mathbb{I}_2 b_k) \qquad k = 0, ..., n \tag{4.47}$$

where $c_k \in \mathbb{R}$ and $c_0 = 1$ derived from (4.2). The n^{th} flow is then given by

$$\boldsymbol{q}_{t_n} = -i \sum_{k=0}^{n} d_k (\mathcal{D}^{\pm})^{n-k} \boldsymbol{q} \tag{4.48}$$

where

$$d_k = \sum_{j=0}^{k} c_j \begin{pmatrix} n-j \\ k-j \end{pmatrix} (-c_1)^{k-j}.$$

Equation (4.48) is a sum over the first n flows generated by equation (4.16) for which no integration constants were included. Apart from $d_0 = 1$, the real coefficients d_k are arbitrary if it is assumed that the constants of integration c_k may be chosen at will for $k = 1, ..., n$. From (4.48) it is possible to consider various integrable equations derived from the VNLS hierarchy. For example, the VNLS (1.1) with an additional term incorporating third order dispersion might be given by

$$i\boldsymbol{q}_\tau + \boldsymbol{q}_{xx} \pm 2\boldsymbol{q}\boldsymbol{q}^\dagger\boldsymbol{q} + i\epsilon \left(\boldsymbol{q}_{xxx} \pm 3\{\boldsymbol{q}^\dagger, \boldsymbol{q}_x\}\boldsymbol{q} \right) = 0. \tag{4.49}$$

This may be derived from (4.48) using a time scaling $t_3 = \epsilon\tau$ and the choice of constants $d_1 = \epsilon^{-1}$ and $d_2 = d_3 = 0$. (4.49) is referred to as the coupled Hirota equation by Nakkeeran [Nak00] and was first investigated by Tasgal and Potasek [TP92] who obtained soliton solutions using inverse scattering transform techniques. Although we do not pursue it here, the geometric technique described in [EEI07] could well be applied to such equations to give finite gap solutions, of which the soliton solutions given in [TP92] are a degenerate case.

Notice also that setting $d_k = 0$ (or equivalently $c_k = 0$) for $k = 1, ..., n$ gives the same flow equations (4.16) as setting all integration constants equal to zero. In this case it is clear from (4.45) that the recursion relations (4.28) and (4.29) become

$$\alpha_k = -i \sum_{j=1}^{k-1} \left((\alpha_j - b_j)(\alpha_{k-j} - b_{k-j}) + \boldsymbol{\beta}_j^{\mathsf{T}} \boldsymbol{\gamma}_{k-j} \right) + b_k,$$
$$A_k = i \sum_{j=1}^{k-1} \left(\boldsymbol{\gamma}_j \boldsymbol{\beta}_{k-j}^{\mathsf{T}} - (\alpha_j - b_j)(A_{k-j} - \mathbb{I}_2 b_{k-j}) \right) + \mathbb{I}_2 b_k.$$

We find that as long as $d_k = 0$ for $k = 1, ..., n$ the discriminant of the curve is still given by (4.42) and hence the genus of the curve is unaltered. That is, if the flow equations $\boldsymbol{q}_{t_k}$ for $k = 1, ..., n$ are given by the recurrence relation (4.16), the genus of the curve will remain as $g = 2n - 3$ whether integration constants have been included or not.

In the second instance we introduce constants of integration appended only to the matrix L_n. We still require B_n to be diagonal but allow a free choice of the two purely imaginary

entries. Setting

$$\begin{pmatrix} a_1 & 0 \\ 0 & a_2 \end{pmatrix} = -i(B_n - \mathbb{I}_2 b_n) \tag{4.50}$$

we find the n^{th} flow is now given by

$$\boldsymbol{q}_{t_n} = -i(\mathcal{D}^{\pm})^n \boldsymbol{q} - i \begin{pmatrix} a_1 q_1 \\ a_2 q_2 \end{pmatrix}. \tag{4.51}$$

The polynomials corresponding to P_{n-1} and T_{n-2} are now both of order n. This means the discriminant of the resulting curve is of order $4n$ and the genus equals $2n-2$ thereby introducing even genus curves to the hierarchy. The algebrogeometric approach pursued in [EEI07] and presented later in this chapter is equally applicable to these curves and so the full family of general finite gap solutions to the VNLS is accessible. In Chapter 5 we will explore the curve of genus two.

4.5 Conserved densities of the hierarchy

In [DE00], explicit conserved densities associated with the VNLS (1.1) in the attractive case are derived by analysing asymptotic limits of Jost solutions to the associated eigenvalue problem on the infinite line. These are given recursively by

$$C_n = \int_{-\infty}^{+\infty} \left(\boldsymbol{q}^{\mathsf{T}} \boldsymbol{\rho}_n \right) \mathrm{d}x \tag{4.52}$$

where

$$\boldsymbol{\rho}_{n+2} = \boldsymbol{\rho}_{n+1,x} + \sum_{i=0}^{n} \boldsymbol{\rho}_i \boldsymbol{q}^{\mathsf{T}} \boldsymbol{\rho}_{n-i} \qquad n = 0, 1, ...$$

with $\boldsymbol{\rho}_0 = \overline{\boldsymbol{q}}$ and $\boldsymbol{\rho}_1 = \overline{\boldsymbol{q}}_x$.

An alternative but related set of conserved densities for (1.1) in both attractive and repulsive cases is given by

$$\mathcal{C}_k = -\frac{1}{k+1} \int_p \alpha_{k+2} \mathrm{d}x \qquad k = 1, 2, ... \tag{4.53}$$

Integration along the path p may be over the infinite line as above or over a period in x, dependent on whether soliton or quasiperiodic solutions are considered. The factor of $-1/(k+1)$ is to neaten the Hamiltonian forms found later. These conserved densities are derived from the following continuity equation:

Theorem 4.7 *In attractive and repulsive cases respectively,*

$$\alpha_{k,t} = \left(2\alpha_{k+1} + i\boldsymbol{q}^{\mathsf{T}}\boldsymbol{\gamma}_k \mp i\boldsymbol{\beta}_k^{\mathsf{T}}\overline{\boldsymbol{q}}\right)_x \qquad k = 0, 1, ... \tag{4.54}$$

where $x = t_1$ *and* $t = t_2$.

Proof: Comparing (1,1) elements of the zero-curvature equations

$$\begin{aligned} \frac{\partial \mathcal{L}_n}{\partial t} - \frac{\partial \mathcal{L}_2}{\partial t_n} &= [\mathcal{L}_2, \mathcal{L}_n], \\ \frac{\partial \mathcal{L}_n}{\partial x} - \frac{\partial \mathcal{L}_1}{\partial t_n} &= [\mathcal{L}_1, \mathcal{L}_n] \end{aligned} \tag{4.55}$$

at orders z^{n-k} and $z^{n-(k+1)}$ respectively gives

$$\alpha_{k,t} = \left(\alpha_{k+1} + i\boldsymbol{q}^{\mathsf{T}}\boldsymbol{\gamma}_k \mp i\boldsymbol{\beta}_k^{\mathsf{T}}\overline{\boldsymbol{q}}\right)_x - i\left(\boldsymbol{q}^{\mathsf{T}}\boldsymbol{\gamma}_{k,x} \mp \boldsymbol{\beta}_{k,x}^{\mathsf{T}}\overline{\boldsymbol{q}}\right). \tag{4.56}$$

Forming the anti-commutator $\{L_1, L_{k,x}\}$ by making use of the second of equations (4.55) at order z^{n-k} shows that the final term in (4.56) is equivalent to $\alpha_{k+1,x}$ and gives the statement of the theorem. In the rapidly decreasing potential case we assume $\boldsymbol{q}, \boldsymbol{q}_x, ... \to 0$ as $|x| \to \infty$ which means the continuity equation (4.54) may be integrated over the infinite line to give

$$\partial_t \int_p \alpha_k \mathrm{d}x = \left(2\alpha_{k+1} + i\boldsymbol{q}^{\mathsf{T}}\boldsymbol{\gamma}_k \mp i\boldsymbol{\beta}_k^{\mathsf{T}}\overline{\boldsymbol{q}}\right)\Big|_p = 0.$$

Thus $\int_p \alpha_k \mathrm{d}x$ is constant in time t and is a conserved density of the VNLS. This procedure is equally applicable in the quasiperiodic case $\boldsymbol{q}(x+2L, t) = \exp(i\theta)\boldsymbol{q}(x, t)$ where the right-hand side is periodic in x. In this case the path of integration p is over a fundamental period between the limits $-L$ and L.

4.6 Hamiltonian structure

Faddeev and Takhtajan [FT87] detail the Hamiltonian system formed by the SNLS with appropriate boundary conditions. We now present an extended version relevant to the VNLS system.

In phase space $\mathbb{R}^{2n}$, a discrete Hamiltonian system has a defined Hamiltonian $H(\boldsymbol{q}, \boldsymbol{p}, t)$ with real variables q_k, p_k for $k = 1, ..., n$ which obey Hamilton's equations

$$\dot{q}_k = \frac{\partial H}{\partial p_k}, \qquad \dot{p}_k = -\frac{\partial H}{\partial q_k}, \tag{4.57}$$

where $\cdot$ represents the total derivative with respect to t. In conjunction with these equations, a Poisson bracket of two functions, $f(\boldsymbol{q},\boldsymbol{p})$ and $g(\boldsymbol{q},\boldsymbol{p})$, is commonly defined by

$$\{f,g\}=\sum_{k=1}^{n}\left(\frac{\partial f}{\partial q_k}\frac{\partial g}{\partial p_k}-\frac{\partial f}{\partial p_k}\frac{\partial g}{\partial q_k}\right). \tag{4.58}$$

This bracket satisfies the Poisson properties of skew-symmetry and Jacobi identity for functions f,g and h:

$$\begin{aligned}\{f,g\}+\{g,f\}&=0,\\ \{\{f,g\},h\}+\{\{h,f\},g\}+\{\{g,h\},f\}&=0,\end{aligned} \tag{4.59}$$

and may be used to rewrite Hamilton's equations as:

$$\dot{q}_k=\{q_k,H\},\qquad\qquad \dot{p}_k=\{p_k,H\}. \tag{4.60}$$

We now consider the infinite-dimensional real linear phase space with smooth complex coordinates $\boldsymbol{q}(x)=(q_1,q_2)^{\mathsf{T}}$ and $\boldsymbol{p}(x)=\overline{\boldsymbol{q}}(x)$ satisfying the quasiperiodic condition, $\boldsymbol{q}(x+2L)=\exp(i\theta)\boldsymbol{q}(x)$ where $0\leq\theta<2\pi$ is independent of t. The algebra of observables upon the phase space is made up of smooth real-analytic functionals which form a Poisson structure if we define a bracket of two functionals

$$\begin{aligned}\mathcal{J}\left(\boldsymbol{q}(x,t),\overline{\boldsymbol{q}}(x,t),t\right)&=\int_{-L}^{L}J(\boldsymbol{q},\overline{\boldsymbol{q}},t,x)\mathrm{d}x,\\ \mathcal{K}\left(\boldsymbol{q}(x,t),\overline{\boldsymbol{q}}(x,t),t\right)&=\int_{-L}^{L}K(\boldsymbol{q},\overline{\boldsymbol{q}},t,x)\mathrm{d}x\end{aligned} \tag{4.61}$$

by

$$\{J,K\}=\int_{-L}^{L}\left(\frac{\delta\mathcal{J}}{\delta\boldsymbol{q}}^{\mathsf{T}}\frac{\delta\mathcal{K}}{\delta\overline{\boldsymbol{q}}}-\frac{\delta\mathcal{K}}{\delta\boldsymbol{q}}^{\mathsf{T}}\frac{\delta\mathcal{J}}{\delta\overline{\boldsymbol{q}}}\right)\mathrm{d}x. \tag{4.62}$$

The functional derivative is defined by

$$\frac{\delta\mathcal{J}}{\delta\boldsymbol{q}}=\frac{\partial J}{\partial\boldsymbol{q}}-\partial_x\left(\frac{\partial J}{\partial\boldsymbol{q}_x}\right)+\partial_x^2\left(\frac{\partial J}{\partial\boldsymbol{q}_{xx}}\right)-... \tag{4.63}$$

with $\frac{\partial J}{\partial\boldsymbol{c}}=\left(\frac{\partial J}{\partial\boldsymbol{c_1}},\frac{\partial J}{\partial\boldsymbol{c_2}}\right)^{\mathsf{T}}$ for a 2-vector problem. We note that $\{\boldsymbol{q}(x),\boldsymbol{q}(y)\}=\{\boldsymbol{p}(x),\boldsymbol{p}(y)\}=0$ and, in order that quasiperiodicity is preserved,

$$\{\boldsymbol{q}(x),\boldsymbol{p}(y)\}=\delta_{L,\theta}(x-y)$$

where

$$\delta_{L,\theta}(x-y) = \sum_{n=-\infty}^{\infty} \exp(in\theta)\delta(x-y-2nL)$$

is the averaged Dirac δ-function.

In general, a Hamiltonian dynamical system with evolution variable t is one in which a Hamiltonian

$$\mathcal{H}\left(\boldsymbol{q}(x,t),\boldsymbol{p}(x,t),t\right) = \int H(\boldsymbol{q},\boldsymbol{p},t,x)\mathrm{d}x \tag{4.64}$$

may be identified where the range of integration is determined by the specified conditions upon $\boldsymbol{q}$ and $\boldsymbol{p}$, in this case quasiperiodicity over the fundamental domain $[-L,L]$. The conjugate variables $\boldsymbol{q}$ and $\boldsymbol{p}$ must then obey Hamilton's equations:

$$\frac{\partial \boldsymbol{q}}{\partial t} = \frac{\delta \mathcal{H}}{\delta \boldsymbol{p}}, \qquad \frac{\partial \boldsymbol{p}}{\partial t} = -\frac{\delta \mathcal{H}}{\delta \boldsymbol{q}} \tag{4.65}$$

which, as in the discrete case, may be expressed using Poisson brackets as

$$\frac{\partial \boldsymbol{q}}{\partial t} = \{\boldsymbol{q}, H\}, \qquad \frac{\partial \boldsymbol{p}}{\partial t} = \{\boldsymbol{p}, H\} \tag{4.66}$$

where $\{\boldsymbol{q}, H\}$ is the vector $(\{q_1, H\}, \{q_2, H\})^{\mathsf{T}}$.

The conserved densities $\mathcal{C}_k$ for $k \geq 1$ form suitable Hamiltonians for the attractive and repulsive VNLS hierarchies with conjugate variable $\boldsymbol{p} = \overline{\boldsymbol{q}}$. The first few evolution equations are then given by

$$\begin{aligned}
\boldsymbol{q}_{t_1} &= \frac{\delta \mathcal{C}_1}{\delta \overline{\boldsymbol{q}}} = \boldsymbol{q}_x, \\
\boldsymbol{q}_{t_2} &= \frac{\delta \mathcal{C}_2}{\delta \overline{\boldsymbol{q}}} = i\boldsymbol{q}_{xx} \pm 2i\boldsymbol{q}\boldsymbol{q}^{\dagger}\boldsymbol{q}, \\
\boldsymbol{q}_{t_3} &= \frac{\delta \mathcal{C}_3}{\delta \overline{\boldsymbol{q}}} = -\boldsymbol{q}_{xxx} \mp 3\left(\boldsymbol{q}^{\dagger}\boldsymbol{q}_x + \boldsymbol{q}_x\boldsymbol{q}^{\dagger}\right)\boldsymbol{q}.
\end{aligned} \tag{4.67}$$

Thus, with conjugate variable $\boldsymbol{p}$ set equal to $\overline{\boldsymbol{q}}$, the Manakov system has a Hamiltonian structure with an infinite set of conserved quantities, $\mathcal{C}_k$.

Two functionals are said to be in involution if $\{J,K\} = 0$ and if there are infinitely many independent integrals of motion all in involution then the Hamiltonian system is said to be completely integrable. One of the fundamental properties of equations soluble by the inverse scattering transform method is that they are completely integrable Hamiltonian systems and much work has focussed upon generating these integrals of motion through

asymptotic analysis of Jost solutions, see for example [AS81], [FT87] and [DE00]. In our case the integrals appear very neatly from elements of the Lax representations for the VNLS hierarchy. The fact that the integrals are all in involution follows from the following lemma:

Lemma 4.1 ([AS81]) *The infinite set of integrals* $\mathcal{C}_k = -\frac{1}{k+1}\int_p \alpha_{k+2}\mathrm{d}x$ *are all in involution for any motion defined by (4.16).*

Proof: We have

$$\boldsymbol{q}_{t_k} = \frac{\delta \mathcal{C}_k}{\delta \overline{\boldsymbol{q}}} \quad \text{and} \quad \overline{\boldsymbol{q}}_{t_k} = -\frac{\delta \mathcal{C}_k}{\delta \boldsymbol{q}},$$

and $\mathcal{C}_j$ is time-independent. Therefore, by computation,

$$\begin{aligned} 0 = \frac{\mathrm{d}\mathcal{C}_j}{\mathrm{d}t_k} &= \int \left(\frac{\delta \mathcal{C}_j}{\delta \boldsymbol{q}}^{\mathsf{T}} \boldsymbol{q}_{t_k} + \frac{\delta \mathcal{C}_j}{\delta \overline{\boldsymbol{q}}}^{\mathsf{T}} \overline{\boldsymbol{q}}_{t_k} \right) \mathrm{d}x \\ &= \int \left(\frac{\delta \mathcal{C}_j}{\delta \boldsymbol{q}}^{\mathsf{T}} \frac{\delta \mathcal{C}_k}{\delta \overline{\boldsymbol{q}}} - \frac{\delta \mathcal{C}_j}{\delta \overline{\boldsymbol{q}}}^{\mathsf{T}} \frac{\delta \mathcal{C}_k}{\delta \boldsymbol{q}} \right) \mathrm{d}x \\ &= \frac{1}{(j+1)(k+1)} \{\alpha_{j+2}, \alpha_{k+2}\}. \end{aligned}$$

4.7 Homology basis of the spectral curve

From the form of the spectral curve (4.40), we know that the coefficients of the polynomials $a_2(z)$ and $a_0(z)$ are pure imaginary and the coefficients of $a_1(z)$ are real. Consider the anti-holomorphic mapping $z \to \overline{z}$ then we may construct an anti-holomorphic involution, referred to as an anti-involution by Elgin et al. [EEI07],

$$\begin{aligned} \sigma &: X \to X \\ \sigma &: P = (z, \mu) \to (\overline{z}, -\overline{\mu}). \end{aligned} \tag{4.68}$$

applicable in both attractive and repulsive cases. Along with $\sigma \circ f(z, \mu) = 0$ we may also show

$$\sigma \circ \frac{\partial f}{\partial z}(z, \mu) = -\overline{\frac{\partial f}{\partial z}(z, \mu)}. \tag{4.69}$$

This means that the sets of branch points $\{z_1^+, ..., z_{4n-2}^+\}$ and $\{z_1^-, ..., z_{4n-2}^-\}$ which satisfy

$$f(z_k^\pm, \mu_k^\pm) = \frac{\partial f}{\partial z}(z_k^\pm, \mu_k^\pm) = 0 \tag{4.70}$$

must also satisfy

$$f(\overline{z_k^{\pm}}, -\overline{\mu_k^{\pm}}) = \frac{\partial f}{\partial z}(\overline{z_k^{\pm}}, -\overline{\mu_k^{\pm}}) = 0 \tag{4.71}$$

and so are fixed under this involution.

We shall make the assumption in the attractive case that all branch points have non-zero imaginary part meaning the branch points z_k^+ must occur as a finite number of conjugate pairs which shall be labelled

$$\overline{z_{2k-1}^+} = z_{2k}^+ \quad \text{for } k = 1, ..., 2n-1 \tag{4.72}$$

with $\mathbb{I}\mathrm{m}(z_{2k}^+) > 0$ and $\mathbb{R}\mathrm{e}(z_{2k}^+) < \mathbb{R}\mathrm{e}(z_{2k+2}^+)$.

A suitable, but not unique, canonical basis, $\{a_j, b_j | j = 1, ..., g\}$, of the first homology group is given in [EEI07] and is presented in the genus one and genus three cases in Figures 4.1 and 4.2.

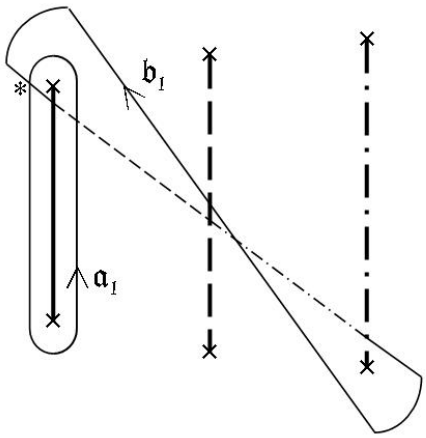

Figure 4.1: Three-sheeted Riemann surface of genus one - *branch points described by equation (4.72) are denoted by crosses. These are connected by branch cuts with a solid line denoting a cut connecting sheets 1 and 2, a dashed line connecting sheets 2 and 3, and a dashed/dotted line connecting sheets 3 and 1. a and b cycles are on sheet 1 if solid, sheet 2 if dashed and sheet 3 if dashed/dotted. Asterisks denote cycle intersections.*

This satisfies the involution properties

$$\begin{aligned} \sigma(a_j) &= -a_j \\ \sigma(b_j) &= b_j - a_j - \sum_{k=1}^{g} a_k. \end{aligned} \tag{4.73}$$

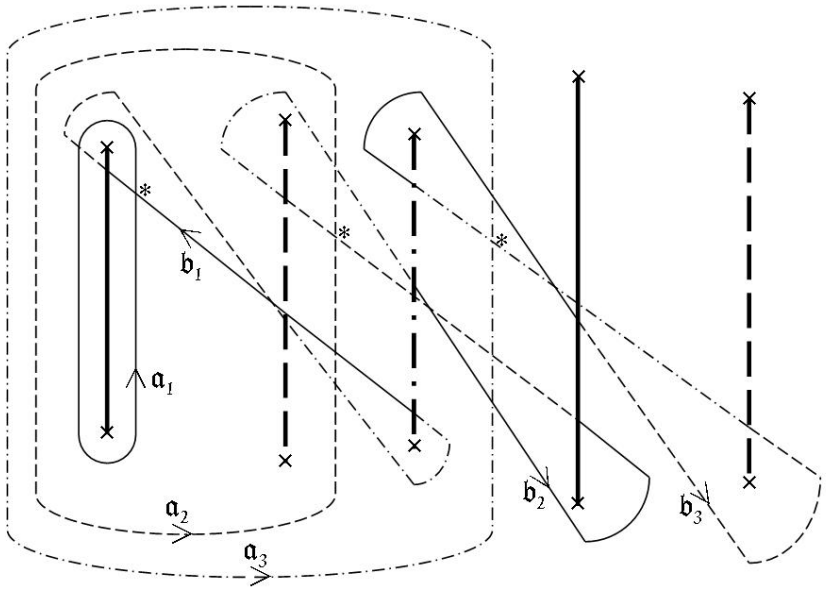

Figure 4.2: Three-sheeted Riemann surface of genus three

For the repulsive case all branch points must be real as the eigenvalue operator is self-adjoint. An example homology basis and branch cut configuration is given by Figure 4.3. However henceforth we shall confine ourselves to studying the attractive case.

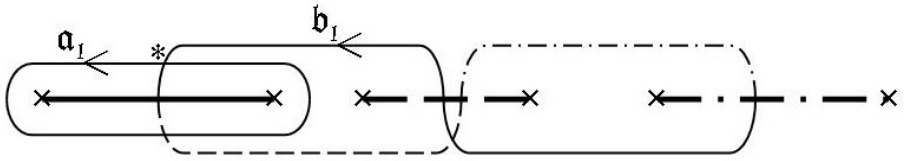

Figure 4.3: Three-sheeted Riemann surface of genus one for the repulsive case scattering problem

4.8 Holomorphic differentials

Suitable local parameters at a point $P_0 = (z_0, \mu(z_0)) \in X$ are given by

$$\xi = \begin{cases} z - z_0 & \text{if } P_0 \text{ is a regular point,} \\ \sqrt{z - z_0} & \text{if } P_0 \text{ is a branch point,} \\ z^{-1} & \text{as } z_0 \to \infty. \end{cases} \tag{4.74}$$

The behaviour of μ at ∞_1, ∞_2 and ∞_3 may be determined by expanding μ as a Laurent series in $\xi = z^{-1}$ and substituting into $f(z,\mu)$. It is convenient to rewrite $f(z,\mu)$ as

$$(\mu - \alpha_0 z^n)\left\{\mu - (i+\alpha_0)z^n\right\}^2 - \frac{P_{n-1}(z)}{2}\left\{\mu - (i+\alpha_0)z^n\right\} - \frac{T_{n-2}(z)}{3} = 0 \qquad (4.75)$$

from which it follows, on sheets 1,2 and 3 respectively,

$$\mu = \begin{cases} \alpha_0\,\xi^{-n} + \frac{i}{2}\lambda_{n+1}\xi + \frac{i}{2}\lambda_{n+2}\xi^2 + O(\xi^3) \\ (i+\alpha_0)\xi^{-n} + A^{(2)}\xi + B^{(2)}\xi^2 + O(\xi^3) \\ (i+\alpha_0)\xi^{-n} + A^{(3)}\xi + B^{(3)}\xi^2 + O(\xi^3) \end{cases} \qquad (4.76)$$

where

$$A^{(2)} = -\frac{i}{4}\left(\lambda_{n+1} + \sqrt{\Delta}\right), \qquad A^{(3)} = -\frac{i}{4}\left(\lambda_{n+1} - \sqrt{\Delta}\right),$$
$$B^{(2)} = \left(\lambda_{n+2}A^{(2)} + \frac{2}{3}\mu_{2n+3}\right)\Big/\sqrt{\Delta}, \qquad B^{(3)} = \left(-\lambda_{n+2}A^{(3)} - \frac{2}{3}\mu_{2n+3}\right)\Big/\sqrt{\Delta}.$$

As for the hyperelliptic curve, a basis of holomorphic differentials may be defined:

$$\mathrm{d}\widetilde{\omega}_k = \begin{cases} \frac{iz^{k-1}}{\frac{\partial f}{\partial \mu}(z,\mu)}\mathrm{d}z & k = 1,\ldots,n-2 \\ \\ \frac{z^{2n-3-k}\{\mu-(i+\alpha_0^{\pm})z^n\}}{\frac{\partial f}{\partial \mu}(z,\mu)}\mathrm{d}z & k = n-1,\ldots,2n-3. \end{cases} \qquad (4.77)$$

These are constructed using a method described by Deconinck and van Hoeij [DH01]. That they are holomorphic may readily be checked using the local parameters described previously. The multiplying factor, i, in the first set of differentials simplifies the next calculations.

The anti-involution $\sigma : (z,\mu) \to (\overline{z}, -\overline{\mu})$ has action σ^*, which when applied to $\mathrm{d}\widetilde{\omega}_k$ gives

$$\sigma^*\mathrm{d}\widetilde{\omega}_k = -\overline{\mathrm{d}\widetilde{\omega}_k}. \qquad (4.78)$$

A matrix of a-cycle integrals, $A = (A_{kj})$, may be defined by

$$A_{kj} = \int_{a_j} \mathrm{d}\widetilde{\omega}_k, \qquad (4.79)$$

with conjugate

$$\overline{A_{kj}} = \int_{a_j} \overline{\mathrm{d}\widetilde{\omega}_k} = -\int_{a_j} \sigma^*\mathrm{d}\widetilde{\omega}_k = -\int_{\sigma(a_j)} \mathrm{d}\widetilde{\omega}_k = \int_{a_j} \mathrm{d}\widetilde{\omega}_k = A_{kj}.$$

Thus all elements A_{kj} are real and the set of normalised differentials, defined by

$$\mathrm{d}\boldsymbol{\omega} = 2\pi i A^{-1}\mathrm{d}\widetilde{\boldsymbol{\omega}}, \tag{4.80}$$

obey $\int_{a_j}\mathrm{d}\omega_k = 2\pi i\delta_{kj}$ and have the anti-involution property

$$\sigma^*\mathrm{d}\omega_k = \overline{\mathrm{d}\omega_k}. \tag{4.81}$$

The period matrix $B = (\int_{b_j}\mathrm{d}\omega_k)$ then has the property

$$\begin{aligned}\overline{B_{kj}} &= \int_{b_j}\overline{\mathrm{d}\omega_k} = \int_{b_j}\sigma^*\mathrm{d}\omega_k = \int_{\sigma(b_j)}\mathrm{d}\omega_k\\ &= \int_{b_j}\mathrm{d}\omega_k - \int_{a_j}\mathrm{d}\omega_k - \sum_{l=1}^{g}\int_{a_l}\mathrm{d}\omega_k\\ &= B_{kj} - 2\pi i\delta_{jk} - 2\pi i\end{aligned}$$

As $P^{(i)}\to\infty_i$, the integral of the vector of normalised holomorphic differentials has the asymptotic expansion, in local parameter ξ,

$$\int_{P_0}^{P^{(i)}}\mathrm{d}\boldsymbol{\omega} = \boldsymbol{U}^{(i)} + \boldsymbol{V}^{(i)}\xi + \boldsymbol{W}^{(i)}\xi^2 + ... \tag{4.82}$$

where $\boldsymbol{U}^{(i)} = \int_{P_0}^{\infty_i}\mathrm{d}\boldsymbol{\omega}$. The first few terms are calculated as

$$\begin{aligned}\boldsymbol{V}^{(1)} &= -i\boldsymbol{c}_{n-1}\\ \boldsymbol{V}^{(2)} &= -\frac{2i}{\sqrt{\Delta}}\boldsymbol{c}_{n-2} - \frac{2}{\sqrt{\Delta}}A^{(2)}\boldsymbol{c}_{n-1}\\ \boldsymbol{V}^{(3)} &= +\frac{2i}{\sqrt{\Delta}}\boldsymbol{c}_{n-2} + \frac{2}{\sqrt{\Delta}}A^{(3)}\boldsymbol{c}_{n-1}\\ \boldsymbol{W}^{(1)} &= -\frac{i}{2}\boldsymbol{c}_n\\ \boldsymbol{W}^{(2)} &= -\frac{i}{\sqrt{\Delta}}\boldsymbol{c}_{n-3} + \frac{2i}{\sqrt{\Delta}}\left(2iB^{(2)} - \frac{\lambda_{n+2}}{2}\right)\boldsymbol{c}_{n-2}\\ &\quad -\frac{1}{\sqrt{\Delta}}\left(B^{(2)} - \frac{2A^{(2)}}{\sqrt{\Delta}}\left(2iB^{(2)} - \frac{\lambda_{n+2}}{2}\right)\right)\boldsymbol{c}_{n-1} - \frac{A^{(2)}}{\sqrt{\Delta}}\boldsymbol{c}_n\\ \boldsymbol{W}^{(3)} &= +\frac{i}{\sqrt{\Delta}}\boldsymbol{c}_{n-3} + \frac{2i}{\sqrt{\Delta}}\left(2iB^{(3)} - \frac{\lambda_{n+2}}{2}\right)\boldsymbol{c}_{n-2}\\ &\quad +\frac{1}{\sqrt{\Delta}}\left(B^{(3)} + \frac{2A^{(3)}}{\sqrt{\Delta}}\left(2iB^{(3)} - \frac{\lambda_{n+2}}{2}\right)\right)\boldsymbol{c}_{n-1} + \frac{A^{(3)}}{\sqrt{\Delta}}\boldsymbol{c}_n\end{aligned}$$

where $\boldsymbol{c}_k = (c_{1k},...,c_{gk})^{\mathsf{T}}$ and c_{jk} is the $(j,k)^{\text{th}}$ element of the normalising matrix $2\pi i A^{-1}$. $\boldsymbol{c}_k = \boldsymbol{0}$ if $k > g$ or $k < 1$.

4.9 Finite gap solutions to the VNLS

The scattering problem for the VNLS is 3×3 and thus we require a Baker-Akhiezer function with 3 components. We begin by stating two theorems which will allow us to identify the finite gap potential $\boldsymbol{q}(x,t)$ once the Baker-Akhiezer function solutions to the Manakov system have been found.

Theorem 4.8 *Consider a 3×3 matrix function, $\Psi(x,t,z)$, which is holomorphic in a neighbourhood of infinity on the Riemann sphere, $\mathbb{C} \cup \{\infty\}$, and smoothly dependent on real variables x and t. Suppose Ψ has the following asymptotic expansion as $z \to \infty$:*

$$\Psi(x,t,z) = \left(\mathbb{I}_3 + \sum_{k=1}^{\infty} \Psi_k(x,t) z^{-k} \right) \exp\left(L_0^{\pm}(zx + z^2 t) \right) C(z); \tag{4.83}$$

where $C(z)$ is a 3×3 invertible matrix, independent of x and t then, assuming (4.83) to be differentiable in x and t, as $z \to \infty$,

$$\begin{aligned} \Psi_x \Psi^{-1} &= \mathcal{K}_1^{\pm}(z) + O(z^{-1}) \\ \Psi_t \Psi^{-1} &= \mathcal{K}_2^{\pm}(z) + O(z^{-1}). \end{aligned} \tag{4.84}$$

Here,

$$\begin{aligned} \mathcal{K}_1^{\pm}(z) &= z L_0^{\pm} + \left[\Psi_1, L_0^{\pm} \right] \\ \mathcal{K}_2^{\pm}(z) &= z^2 L_0^{\pm} + z \left[\Psi_1, L_0^{\pm} \right] + \left[\Psi_2, L_0^{\pm} \right] - \left[\Psi_1, L_0^{\pm} \right] \Psi_1. \end{aligned}$$

Proof: Finding the first few terms of the asymptotic expansion

$$\Psi^{-1}(x,t,z) = C^{-1}(z) \exp\left(-L_0^{\pm}(zx + z^2 t) \right) \left(\mathbb{I}_3 + \sum_{k=1}^{\infty} \Upsilon_k(x,t) z^{-k} \right),$$

by applying $\Psi \Psi^{-1} = \mathbb{I}_3$, it may be shown equations (4.84) hold.

Theorem 4.9 *If $\Psi(x,t,z)$ satisfies the conditions and asymptotic expansions of* Theorem 4.8 *and, in addition, Ψ is an exact solution to*

$$\Psi_x = \mathcal{K}_1^{\pm}(z)\Psi, \qquad \Psi_t = \mathcal{K}_2^{\pm}(z)\Psi \tag{4.85}$$

then, if

$$\boldsymbol{q} = i \begin{pmatrix} \Psi_{1,12} \\ \Psi_{1,13} \end{pmatrix}, \qquad \overline{\boldsymbol{q}} = \pm i \begin{pmatrix} \Psi_{1,21} \\ \Psi_{1,31} \end{pmatrix} \tag{4.86}$$

it may be shown Ψ *is an exact solution to the Manakov system (4.1).*

Proof: To prove the theorem, it is only required to show that

$$\left[\Psi_2, L_0^{\pm}\right] - \left[\Psi_1, L_0^{\pm}\right]\Psi_1 \;=\; L_2^{\pm}.$$

This may be checked by splitting all matrices into the following 'diagonal' and 'off-diagonal' elements

$$A = (a_{ij}) = \begin{pmatrix} a_{11} & 0 & 0 \\ 0 & a_{22} & a_{23} \\ 0 & a_{32} & a_{33} \end{pmatrix} + \begin{pmatrix} 0 & a_{12} & a_{13} \\ a_{21} & 0 & 0 \\ a_{31} & 0 & 0 \end{pmatrix} = A^{(D)} + A^{(O)} \tag{4.87}$$

so that

$$\begin{aligned} \left(\left[\Psi_2, L_0^{\pm}\right] - \left[\Psi_1, L_0^{\pm}\right]\Psi_1\right)^{(D)} &= -\left(\left[\Psi_1, L_0^{\pm}\right]\Psi_1\right)^{(D)} \\ &= \begin{pmatrix} i\boldsymbol{q}^{\mathsf{T}}\overline{\boldsymbol{q}} & \mathbf{0}^{\mathsf{T}} \\ \mathbf{0} & \mp i\overline{\boldsymbol{q}}\boldsymbol{q}^{\mathsf{T}} \end{pmatrix} = L_2^{\pm\,(D)}. \end{aligned}$$

From equations (4.85) it follows that

$$\Psi_{1,x} \;=\; \left[L_0^{\pm}, \Psi_2\right] + \left[\Psi_1, L_0^{\pm}\right]\Psi_1$$

and thus

$$\left(\left[\Psi_2, L_0^{\pm}\right] - \left[\Psi_1, L_0^{\pm}\right]\Psi_1\right)^{(O)} = -\Psi_{1,x}^{(O)} = \begin{pmatrix} 0 & i\boldsymbol{q}_x^{\mathsf{T}} \\ \pm i\overline{\boldsymbol{q}}_x & \mathbb{O}_2 \end{pmatrix} = L_2^{\pm\,(O)}$$

which completes the proof.

So once we have found the Baker-Akhiezer functions solving the Manakov system we have formulae for determining $\boldsymbol{q}(x,t)$ and $\overline{\boldsymbol{q}}(x,t)$. We will also be interested in their moduli, found via the following corollary:

Corollary 4.4 *In attractive and repulsive cases respectively*

$$\begin{aligned} \boldsymbol{q}^{\dagger}\boldsymbol{q} &= \pm i\partial_x \Psi_{1,11} \\ |q_1(x,t)|^2 &= \mp i\partial_x \Psi_{1,22} \\ |q_2(x,t)|^2 &= \mp i\partial_x \Psi_{1,33} \end{aligned} \tag{4.88}$$

Proof: Equations (4.85) imply

$$\Psi_{1,x} \quad = \quad \left[L_0^{\pm}, \Psi_2\right] + \left[\Psi_1, L_0^{\pm}\right] \Psi_1.$$

Inspecting (1,1), (2,2) and (3,3) elements respectively and applying equations (4.86) gives the required results.

We now turn to the construction of the Baker-Akhiezer functions. Upon our trigonal Riemann surfaces given explicitly by (4.40), we define a first homology group $\{a_j, b_j | j = 1, ..., g\}$ along with a set of holomorphic differentials normalised according to (2.13). These form a period matrix B which will be used to define theta functions on the curves, $X^{\pm}$.

We also introduce normalised Abelian integrals of the second class, $\Omega_1(P)$ and $\Omega_2(P)$, with the following asymptotic expansions in z:

$$\begin{aligned}
\Omega_1(P) &= \begin{cases} \alpha_0^{\pm} z - \frac{E_1+E_2}{2} + \frac{R_1}{z} + O(z^{-2}) & P \to \infty_1 \\ (i+\alpha_0^{\pm})z + \frac{E_1-E_2}{2} + O(z^{-1}) & P \to \infty_2 \\ (i+\alpha_0^{\pm})z - \frac{E_1-E_2}{2} + O(z^{-1}) & P \to \infty_3 \end{cases} \\
\Omega_2(P) &= \begin{cases} \alpha_0^{\pm} z^2 - \frac{N_1+N_2}{2} + \frac{R_2}{z} + O(z^{-2}) \\ (i+\alpha_0^{\pm})z^2 + \frac{N_1-N_2}{2} + O(z^{-1}) \\ (i+\alpha_0^{\pm})z^2 - \frac{N_1-N_2}{2} + O(z^{-1}) \end{cases}
\end{aligned} \tag{4.89}$$

and normalised Abelian integrals of the third class, $H_2(P)$ and $H_3(P)$, with the following asymptotic expansions at the points of infinity indicted

$$\begin{aligned}
H_2(P) &= \begin{cases} \log \frac{z}{\delta_2} + O(z^{-1}) & P \to \infty_2 \\ -\log \frac{z}{\delta_2} + O(z^{-1}) & P \to \infty_1 \end{cases} \\
H_3(P) &= \begin{cases} \log \frac{z}{\delta_3} + O(z^{-1}) & P \to \infty_3 \\ -\log \frac{z}{\delta_3} + O(z^{-1}) & P \to \infty_1 \end{cases}
\end{aligned} \tag{4.90}$$

and singularities only at these points. The normalisation conditions are that integrals of the corresponding differentials around a cycles are 0.

We also define a divisor $\mathcal{D} = \sum_{k=1}^{g} P_k$ of distinct arbitrary points satisfying $\pi(P_k) \neq z_j^{\pm}$ for any $j = 1, ..., g$.

In order to calculate parameters $E_{1,2}$, $N_{1,2}$ and $\delta_{2,3}$, the following asymptotic expansions should be noted, for $P^{(i)} \to \infty_i$:

$$\begin{aligned}
\int_{P^{(1)}}^{P^{(2)}} \mathrm{d}\Omega_1 &= iz + E_1 + O(z^{-1}) \\
\int_{P^{(1)}}^{P^{(3)}} \mathrm{d}\Omega_1 &= iz + E_2 + O(z^{-1}) \\
\int_{P^{(1)}}^{P^{(2)}} \mathrm{d}\Omega_2 &= iz^2 + N_1 + O(z^{-1}) \\
\int_{P^{(1)}}^{P^{(3)}} \mathrm{d}\Omega_2 &= iz^2 + N_2 + O(z^{-1}) \\
\int_{P^{(1)}}^{P^{(2)}} \mathrm{d}H_2 &= 2\log(z) - 2\log(\delta_2) + O(z^{-1}) \\
\int_{P^{(1)}}^{P^{(3)}} \mathrm{d}H_3 &= 2\log(z) - 2\log(\delta_3) + O(z^{-1})
\end{aligned}$$

where $z = \pi(P) \to \infty$ and is assumed real and positive. The contours of integration are chosen such that no intersection with cycles in the homology basis occurs and the contours do not pass through the points at infinity.

The differentials $\mathrm{d}\Omega_1$ and $\mathrm{d}\Omega_2$ satisfy the same anti-holomorphic involution properties as the holomorphic differentials $\mathrm{d}\widetilde{\omega}_k$. That is

$$\sigma^* \mathrm{d}\Omega_k = -\mathrm{d}\Omega_k \qquad k = 1, 2. \tag{4.91}$$

This means if the appropriate anti-holomorphic involution is applied to the path of integration, we may show, in a similar manner to the conjugates of integrals of the holomorphic differentials, that

$$\overline{\int_{P^{(1)}}^{P^{(j)}} \mathrm{d}\Omega_k} = -\int_{P^{(1)}}^{P^{(j)}} \mathrm{d}\Omega_k. \tag{4.92}$$

From this we deduce that E_1, E_2 and N_1, N_2 are all pure imaginary.

Before constructing Baker-Akhiezer function solutions to the Manakov system we find relations between the Abelian integrals around b cycles and the asymptotic behaviour of the holomorphic differentials at the points at infinity.

Proposition 4.1

$$\begin{aligned}\int_{\boldsymbol{b}} \mathrm{d}\Omega_1 &= -\left(\alpha_0^{\pm}\boldsymbol{V}^{(1)} + (i+\alpha_0^{\pm})\boldsymbol{V}^{(2)} + (i+\alpha_0^{\pm})\boldsymbol{V}^{(3)}\right) = \boldsymbol{c}_{n-1},\\ \int_{\boldsymbol{b}} \mathrm{d}\Omega_2 &= -2\left(\alpha_0^{\pm}\boldsymbol{W}^{(1)} + (i+\alpha_0^{\pm})\boldsymbol{W}^{(2)} + (i+\alpha_0^{\pm})\boldsymbol{W}^{(3)}\right) = \boldsymbol{c}_n\end{aligned} \tag{4.93}$$

where $\boldsymbol{V}^{(i)}$ *and* $\boldsymbol{W}^{(i)}$ *are coefficients in the expansion of* $\boldsymbol{\omega}$ *given by* (4.82) *and* $\int_{\boldsymbol{b}} = \left(\int_{b_1}, ..., \int_{b_g}\right)^{\mathsf{T}}$.

Proof: Application of Theorem 2.6 implies

$$\begin{aligned}\int_{\partial\widetilde{X}} \omega_k \mathrm{d}\Omega_j &= 2\pi i \int_{b_k} \mathrm{d}\Omega_j\\ \sum_{i=1}^{3} \mathrm{Res}(\omega_k \mathrm{d}\Omega_j, \infty_i) &= \int_{b_k} \mathrm{d}\Omega_j\end{aligned}$$

which gives the first set of equalities for $\int_{\boldsymbol{b}} \mathrm{d}\Omega_1$ and $\int_{\boldsymbol{b}} \mathrm{d}\Omega_2$. The second set are found by substituting for $\boldsymbol{V}^{(i)}$ and $\boldsymbol{W}^{(i)}$ using the expressions found in the previous chapter. As the constants c_{jk} are pure imaginary it follows that so too are the integrals $\int_{\boldsymbol{b}} \mathrm{d}\Omega_k$ for $k = 1, 2$.

Similarly, if vectors $\boldsymbol{r}^{(2)}$ and $\boldsymbol{r}^{(3)}$ are defined by

$$\boldsymbol{r}^{(2)} = \int_{\infty_1}^{\infty_2} \mathrm{d}\boldsymbol{\omega} = \boldsymbol{U}^{(2)} - \boldsymbol{U}^{(1)}, \qquad \boldsymbol{r}^{(3)} = \int_{\infty_1}^{\infty_3} \mathrm{d}\boldsymbol{\omega} = \boldsymbol{U}^{(3)} - \boldsymbol{U}^{(1)} \tag{4.94}$$

then

$$r_k^{(2)} = -\int_{b_k} \mathrm{d}H_2(P), \qquad r_k^{(3)} = -\int_{b_k} \mathrm{d}H_3(P). \tag{4.95}$$

The vector-valued Baker-Akhiezer function $\boldsymbol{\psi}(x,t,P) = (\psi_1, \psi_2, \psi_3)^{\mathsf{T}}$ used to construct the finite gap potential is uniquely defined by the following conditions:

1. $\boldsymbol{\psi}(x,t,P)$ is meromorphic on $X\backslash\{\infty_{1,2,3}\}$ with each component having divisor of poles $\mathcal{D}$.

2. $\boldsymbol{\psi}$ has the following asymptotic expansions in z at $\infty_{1,2,3}$:

$$\begin{aligned}
\boldsymbol{\psi}(P) &= \left[\begin{pmatrix}1\\0\\0\end{pmatrix} + O(z^{-1})\right] \exp\{\alpha_0^{\pm}(zx+z^2t)\} && P\to\infty_1,\\
\boldsymbol{\psi}(P) &= \left[\begin{pmatrix}0\\1\\0\end{pmatrix} + O(z^{-1})\right] \alpha_2 z\exp\{(i+\alpha_0^{\pm})(zx+z^2t)\} && P\to\infty_2,\\
\boldsymbol{\psi}(P) &= \left[\begin{pmatrix}0\\0\\1\end{pmatrix} + O(z^{-1})\right] \alpha_3 z\exp\{(i+\alpha_0^{\pm})(zx+z^2t)\} && P\to\infty_3.
\end{aligned}$$

The Baker-Akhiezer functions corresponding uniquely to these two conditions are found applying Theorem 2.11 in Section 2.8,

$$\begin{aligned}
\psi_1(P) &= A_1(x,t)\frac{\theta(\boldsymbol{\omega}(P)+\boldsymbol{g}(x,t)-\boldsymbol{e})}{\theta(\boldsymbol{\omega}(P)-\boldsymbol{e})}\exp\{\Phi_1(x,t,P)\},\\
\psi_i(P) &= A_i(x,t)\frac{\theta(\boldsymbol{\omega}(P)+\boldsymbol{g}^{(i)}(x,t)-\boldsymbol{e})}{\theta(\boldsymbol{\omega}(P)-\boldsymbol{e})}\exp\{\Phi_i(x,t,P)+H_i(P)\}
\end{aligned} \tag{4.96}$$

for $i=2,3$, where

$$\begin{aligned}
g_k(x,t) &= x\int_{b_k}\mathrm{d}\Omega_1 + t\int_{b_k}\mathrm{d}\Omega_2,\\
g_k^{(i)}(x,t) &= g_k(x,t) + \int_{b_k}\mathrm{d}H_i(P) \quad \text{for } i=2,3,\\
\Phi_1(x,t,P) &= x\left(\Omega_1(P)+\frac{E_1+E_2}{2}\right) + t\left(\Omega_2(P)+\frac{N_1+N_2}{2}\right),\\
\Phi_2(x,t,P) &= x\left(\Omega_1(P)-\frac{E_1-E_2}{2}\right) + t\left(\Omega_2(P)-\frac{N_1-N_2}{2}\right),\\
\Phi_3(x,t,P) &= x\left(\Omega_1(P)+\frac{E_1-E_2}{2}\right) + t\left(\Omega_2(P)+\frac{N_1-N_2}{2}\right).
\end{aligned}$$

$\boldsymbol{\omega}(P)=\int_{P_0}^{P}\mathrm{d}\boldsymbol{\omega}$ takes the same path of integration as $\Omega_k(P)=\int_{P_0}^{P}\mathrm{d}\Omega_k$ for $k=1,2$ and $H_i(P)=\int_{P_0}^{P}\mathrm{d}H_i$ for $i=2,3$. Vector $\boldsymbol{e}$ is defined in Theorem 2.9. The functions $A_1(x,t)$, $A_2(x,t)$ and $A_3(x,t)$ are specified by the behaviour of $\boldsymbol{\psi}$ at $\infty_{1,2,3}$ and are found to be

$$\begin{aligned}
A_1(x,t) &= \frac{\theta(\boldsymbol{\omega}(\infty_1)-\boldsymbol{e})}{\theta(\boldsymbol{\omega}(\infty_1)+\boldsymbol{g}(x,t)-\boldsymbol{e})}\\
A_i(x,t) &= \frac{\theta(\boldsymbol{\omega}(\infty_i)-\boldsymbol{e})}{\theta(\boldsymbol{\omega}(\infty_i)+\boldsymbol{g}^{(i)}(x,t)-\boldsymbol{e})}\alpha_i\delta_i \qquad i=2,3.
\end{aligned}$$

Consider the matrix function $\Psi(x,t,z)$ with the following asymptotic expansion as $z \to \infty$:

$$\Psi(x,t,z) = \left(\boldsymbol{\psi}(P^{(1)})\,,\ \boldsymbol{\psi}(P^{(2)})\,,\ \boldsymbol{\psi}(P^{(3)})\right) \qquad P^{(j)} \to \infty_j. \tag{4.97}$$

This satisfies all the conditions of Theorem 4.8 when

$$C(z) = \begin{pmatrix} 1 & 0 & 0 \\ 0 & \alpha_2 z & 0 \\ 0 & 0 & \alpha_3 z \end{pmatrix}.$$

It remains to show that Ψ also satisfies Theorem 4.9. This may be proved by considering

$$\begin{aligned} f(P^{(j)}) &= \Psi_x(P^{(j)}) - \mathcal{L}_1^{\pm}(z)\Psi(P^{(j)}) \\ &= \left\{\Psi_x(P^{(j)})\Psi^{-1}(P^{(j)}) - \mathcal{L}_1^{\pm}(z)\right\}\Psi(P^{(j)}) \end{aligned}$$

which for $j = 1$ reads

$$f(P^{(1)}) = o(1)\exp\{\alpha_0^{\pm}(zx + z^2 t)\}$$

thus satisfying Corollary 2.5 and proving

$$\Psi_x(z) = \mathcal{L}_1(z)\Psi(z).$$

Similarly it can be shown $\Psi_t(z) = \mathcal{L}_2(z)\Psi(z)$ and Theorem 4.9 is satisfied. The solution $\boldsymbol{q}(x,t) = (q_1, q_2)^{\mathsf{T}}$ is then given by 4.86:

$$\begin{aligned} q_1(x,t) &= \frac{i}{\alpha_2}\psi_1(\infty_2)\exp\{-(i + \alpha_0^{\pm})(zx + z^2 t)\}, \\ q_2(x,t) &= \frac{i}{\alpha_3}\psi_1(\infty_3)\exp\{-(i + \alpha_0^{\pm})(zx + z^2 t)\}, \end{aligned}$$

$$\begin{aligned} q_1(x,t) &= Q_1 \frac{\theta(\boldsymbol{\omega}(\infty_2) + \boldsymbol{g}(x,t) - \boldsymbol{e})}{\theta(\boldsymbol{\omega}(\infty_1) + \boldsymbol{g}(x,t) - \boldsymbol{e})}\exp(E_1 x + N_1 t), \\ q_2(x,t) &= Q_2 \frac{\theta(\boldsymbol{\omega}(\infty_3) + \boldsymbol{g}(x,t) - \boldsymbol{e})}{\theta(\boldsymbol{\omega}(\infty_1) + \boldsymbol{g}(x,t) - \boldsymbol{e})}\exp(E_2 x + N_2 t) \end{aligned} \tag{4.98}$$

where

$$Q_k = \frac{i}{\alpha_{k+1}}\frac{\theta(\boldsymbol{\omega}(\infty_1) - \boldsymbol{e})}{\theta(\boldsymbol{\omega}(\infty_{k+1}) - \boldsymbol{e})} \qquad k = 1, 2.$$

Proposition 4.2

$$\boldsymbol{q}^{\dagger}\boldsymbol{q} = \pm\partial_x^2 \log\theta(\boldsymbol{\omega}(\infty_1) + \boldsymbol{g}(x,t) - \boldsymbol{e}) \pm iR_1 \tag{4.99}$$

Proof: Inspecting (1,1) elements of expansion (4.83) with $C_{11}(z) = 1$ gives

$$\begin{aligned}\Psi_{11}(x,t,z) &= \left(1 + \frac{\Psi_{1,11}}{z} + O(z^{-2})\right)\exp\{\alpha_0(zx + z^2 t)\}\\ \Rightarrow\ \log\Psi_{11}(x,t,z) &= \alpha_0(zx+z^2t) + \log\left(1 + \frac{\Psi_{1,11}}{z} + O(z^{-2})\right)\\ &= \alpha_0(zx+z^2t) + \frac{\Psi_{1,11}}{z} + O(z^{-2})\end{aligned}$$

as $z \to \infty$. Also, as $P^{(1)} \to \infty_1$,

$$\begin{aligned}\Psi_{11}(x,t,z) &= \psi_1(P^{(1)})\\ &= A_1(x,t)\frac{\theta(\boldsymbol{\omega}(P^{(1)}) + \boldsymbol{g}(x,t) - \boldsymbol{e})}{\theta(\boldsymbol{\omega}(P^{(1)}) - \boldsymbol{e})}\exp\{\Phi_1(x,t,P^{(1)})\}\\ \Rightarrow \log\Psi_{11}(x,t,z) &= \log\left\{A_1(x,t)\frac{\theta(\boldsymbol{\omega}(P^{(1)}) + \boldsymbol{g}(x,t) - \boldsymbol{e})}{\theta(\boldsymbol{\omega}(P^{(1)}) - \boldsymbol{e})}\right\}\\ &\quad + \alpha_0(zx+z^2t) + \frac{R_1}{z}x + \frac{R_2}{z}t + O(z^{-2})\end{aligned}$$

From these two expressions for $\log\Psi_{11}(x,t,z)$, in terms of local parameter, $\xi = z^{-1}$, we have

$$\begin{aligned}\Psi_{1,11}\,\xi =& \log\left\{A_1(x,t)\frac{\theta(\boldsymbol{\omega}(P^{(1)}) + \boldsymbol{g}(x,t) - \boldsymbol{e})}{\theta(\boldsymbol{\omega}(P^{(1)}) - \boldsymbol{e})}\right\}\\ &+ \xi R_1 x + \xi R_2 t + O(\xi^2).\end{aligned}$$

Differentiating with respect to x and ξ and evaluating at $\xi = 0$ implies

$$\partial_x\Psi_{1,11}(x,t) = \partial_x\partial_\xi \log\theta(\boldsymbol{\omega}(P^{(1)}) + \boldsymbol{g}(x,t) - \boldsymbol{e})\Big|_{\xi=0} + R_1$$

to which Corollary 4.4 may be applied to give

$$\boldsymbol{q}^\dagger\boldsymbol{q} = \pm i\partial_x\partial_\xi \log\theta(\boldsymbol{\omega}(P^{(1)}) + \boldsymbol{g}(x,t) - \boldsymbol{e})\Big|_{\xi=0} \pm iR_1.$$

We also note that, upon inspection of the asymptotic expansions of $\boldsymbol{\omega}(P^{(1)})$ and $\int_{\boldsymbol{b}} \mathrm{d}\Omega_1$, ∂_ξ acts like $-i\partial_x$ on $\log\theta(\boldsymbol{\omega}(P^{(1)}) + \boldsymbol{g}(x,t) - \boldsymbol{e})$ near ∞_1 and hence the formula (4.99) holds.

Chapter 5

Genus two finite gap solutions to the VNLS

By seeking a separable solution to the attractive VNLS, Christiansen et al. [CEE00] are able to set the resulting system into Lax pair form before solving using Kleinian sigma functions. We are interested in seeing if this finite gap solution is part of the family of solutions generated by the algebrogeometric method described in Chapter 4.

Results from this chapter form part of an article [WWE07] which has been published in Journal of Physics A: Mathematics and Theoretical.

5.1 Separable solutions of genus two

We now describe the method published by Christiansen et al. [CEE00] for constructing separable solutions of genus two.

Consider the following separable ansatz for a potential $\boldsymbol{q} = (q_1, q_2)^{\mathsf{T}}$ solving the VNLS (1.1):

$$\begin{aligned} q_1(x,t) &= Q_1(x)\exp\left(ia_1 t + i\phi_1(x)\right), \\ q_2(x,t) &= Q_2(x)\exp\left(ia_2 t + i\phi_2(x)\right), \end{aligned} \tag{5.1}$$

where $Q_i(x)$ and $\phi_i(x)$ are real functions of x and a_i are real constants. Substituting this ansatz into (1.1) and comparing imaginary parts gives

$$\phi_i(x) = C_i \int^x \frac{\mathrm{d}x'}{Q_i^2(x')} \qquad i = 1, 2 \tag{5.2}$$

where C_i are constants of integration. Comparing real parts and applying (5.2) means the functions $Q_i(x)$ must satisfy the ODEs

$$\begin{aligned} Q_{1,xx} + 2Q_1(Q_1^2 + Q_2^2) - a_1 Q_1 - C_1^2 Q_1^{-3} = 0, \\ Q_{2,xx} + 2Q_2(Q_1^2 + Q_2^2) - a_2 Q_2 - C_2^2 Q_2^{-3} = 0. \end{aligned} \tag{5.3}$$

Multiplying these by $Q_{1,x}$ and $Q_{2,x}$ respectively and summing gives an exactly integrable equation and the following Hamiltonian:

$$H(Q_i, P_i) = \sum_{k=1}^{2} \left(P_k^2 - a_k Q_k^2 + C_k^2 Q_k^{-2} \right) + \left(Q_1^2 + Q_2^2 \right)^2 \tag{5.4}$$

with canonical momenta $P_i = Q_{i,x}$ satisfying Hamilton's equations. A simple scaling: $Q_i \to \sqrt{2} Q_i$ and $C_i \to 2C_i$ for $i = 1, 2$; gives the results published in [CEE00].

Based upon a method developed by Kostov in an earlier paper, Christiansen et al. present a Lax representation for the system (5.3):

$$\frac{\mathrm{d}L(\lambda)}{\mathrm{d}x} = [M(\lambda), L(\lambda)]. \tag{5.5}$$

$L(\lambda) = \begin{pmatrix} V(\lambda) & U(\lambda) \\ W(\lambda) & -V(\lambda) \end{pmatrix}$, $M(\lambda) = \begin{pmatrix} 0 & 1 \\ Q(\lambda) & 0 \end{pmatrix}$ with components:

$$\begin{aligned} V(\lambda) &= -\frac{1}{2} U_x(\lambda), \\ U(\lambda) &= a(\lambda) \left(1 + \sum_{k=1}^{2} \frac{Q_k^2}{(\lambda - a_k)} \right), \\ W(\lambda) &= a(\lambda) \left\{ \lambda - \sum_{k=1}^{2} Q_k^2 - \sum_{k=1}^{2} \frac{1}{\lambda - a_k} \left(P_k^2 + \frac{C_k^2}{Q_k^2} \right) \right\}, \\ Q(\lambda) &= \lambda - 2 \sum_{k=1}^{2} Q_k^2 \end{aligned}$$

where $a(\lambda) = (\lambda - a_1)(\lambda - a_2)$. The accompanying spectral curve, $\det(L(\lambda) - \frac{\nu}{2} \mathbb{I}_2) = 0$, is a genus 2 hyperelliptic curve,

$$\begin{aligned} \nu^2 &= 4\{V^2(\lambda) + U(\lambda) W(\lambda)\} \\ &= 4\lambda^5 + \alpha_4 \lambda^4 + \alpha_3 \lambda^3 + \alpha_2 \lambda^2 + \alpha_1 \lambda + \alpha_0 \\ &= 4 \prod_{i=0}^{4} (\lambda - \lambda_i), \end{aligned} \tag{5.6}$$

whose coefficients, α_i, may be expressed in terms of the Hamiltonian and a second inde-

pendent conserved quantity,

$$\begin{aligned} G = \ & (P_1Q_2 - P_2Q_1)^2 + \left(a_1a_2 - a_2Q_1^2 - a_1Q_2^2\right)\sum_{k=1}^{2} Q_k^2 \\ & - a_2P_1^2 - a_1P_2^2 - (a_2 - Q_2^2)\frac{C_1^2}{Q_1^2} - (a_1 - Q_1^2)\frac{C_2^2}{Q_2^2}, \end{aligned} \tag{5.7}$$

which is a consequence of rotational symmetry in the system and may be found by multiplying the first and second of equations (5.3) by Q_2 and Q_1 respectively and subtracting.

The hyperelliptic curve (5.6) has branch points λ_i for $i = 0, ..., 4$ and ∞ with branch cuts chosen along the closed intervals $[\lambda_0, \lambda_1]$, $[\lambda_2, \lambda_3]$ and $[\lambda_4, \infty]$ on the real axis and is regular elsewhere. By defining the zeros of $U(\lambda)$ to be μ_1 and μ_2, Christiansen et al. are able to define solutions:

$$\begin{aligned} Q_1^2 &= \frac{(a_1 - \mu_1)(a_1 - \mu_2)}{a_1 - a_2}, \\ Q_2^2 &= \frac{(a_2 - \mu_1)(a_2 - \mu_2)}{a_2 - a_1}, \end{aligned} \tag{5.8}$$

which, in conjunction with the spectral curve (5.6), give the relations:

$$\nu(\mu_i) = 2V(\mu_i) = -U_x(\mu_i) \tag{5.9}$$

for $i = 1, 2$. Note that this is similar to the procedure performed in Subsection 1.4.4 to find finite gap solutions to the SNLS. The μ_i represent the auxiliary spectrum.

As μ_i are the roots of $U(\lambda)$,

$$U(\lambda) = (\lambda - \mu_1)(\lambda - \mu_2)$$

and hence

$$\begin{aligned} \mu_{1,x} &= \frac{U_x(\mu_1)}{\mu_2 - \mu_1} = \frac{\nu(\mu_1)}{\mu_1 - \mu_2}, \\ \mu_{2,x} &= \frac{U_x(\mu_2)}{\mu_1 - \mu_2} = \frac{\nu(\mu_2)}{\mu_2 - \mu_1}. \end{aligned} \tag{5.10}$$

With respect to the hyperelliptic curve (5.6), the two standard independent canonical holomorphic differentials are defined to be:

$$\mathrm{d}u_1 = \frac{\mathrm{d}\lambda}{\nu}, \qquad \mathrm{d}u_2 = \frac{\lambda \mathrm{d}\lambda}{\nu}. \tag{5.11}$$

The Abelian mapping of the divisor $\mathcal{D} = \sum_{i=1}^{2}(\mu_i - a_i)$ is then given by

$$\boldsymbol{u}(\mathcal{D}) = \int_{a_1}^{\mu_1} \mathrm{d}\boldsymbol{u} + \int_{a_2}^{\mu_2} \mathrm{d}\boldsymbol{u} \tag{5.12}$$

for $\mathrm{d}\boldsymbol{u} = (\mathrm{d}u_1, \mathrm{d}u_2)^{\mathsf{T}}$. Considering $\boldsymbol{u}(\mathcal{D})$ as a function of μ_1 and μ_2 we may differentiate with respect to x and apply (5.10) to give $\boldsymbol{u}_x(\mathcal{D}) = (0,1)^{\mathsf{T}}$ which in turn implies

$$\boldsymbol{u}(\mathcal{D}) = \begin{pmatrix} u_1^{(0)} \\ x + u_2^{(0)} \end{pmatrix}. \tag{5.13}$$

where $u_1^{(0)}$ and $u_2^{(0)}$ are constants of integration.

A homology basis of cycles $\{a_1, b_1, a_2, b_2\}$ upon the curve (5.6) is also defined along with two independent meromorphic differentials of the second kind:

$$\mathrm{d}r_1 = \frac{\alpha_3\lambda + 2\alpha_4\lambda^2 + 12\lambda^3}{\nu}\mathrm{d}\lambda, \qquad \mathrm{d}r_2 = \frac{\lambda^2}{\nu}\mathrm{d}\lambda. \tag{5.14}$$

These canonical differentials of the first and second kind may be generalised to higher genus hyperelliptic curves by the formulae:

$$\mathrm{d}u_j = \frac{\lambda^{j-1}}{\nu}\mathrm{d}\lambda \tag{5.15}$$

$$\mathrm{d}r_j = \sum_{k=j}^{2g+1-j}(k+1-j)\lambda_{k+1+j}\frac{\lambda^k}{4\nu}\mathrm{d}\lambda, \tag{5.16}$$

for $j = 1, ..., g$. These are presented in [BEL96] and are defined such that the period matrices ω, ω', η and η' with components

$$\begin{aligned} 2\omega_{ij} &= \textstyle\int_{a_j} \mathrm{d}u_i, \qquad & 2\omega'_{ij} &= \textstyle\int_{b_j} \mathrm{d}u_i \\ 2\eta_{ij} &= \textstyle\int_{a_j} \mathrm{d}r_i, \qquad & 2\eta'_{ij} &= \textstyle\int_{b_j} \mathrm{d}r_i \end{aligned} \tag{5.17}$$

for $i, j = 1, ..., g$, satisfy the following generalisations of Legendre's relations in the genus one case:

$$\begin{aligned} \omega'\omega^{\mathsf{T}} - \omega\omega'^{\mathsf{T}} &= 0, \\ \eta'\omega^{\mathsf{T}} - \eta\omega'^{\mathsf{T}} &= -\frac{i\pi}{2}\mathbb{I}_g, \\ \eta'\eta^{\mathsf{T}} - \eta\eta'^{\mathsf{T}} &= 0. \end{aligned} \tag{5.18}$$

With these in mind a sensible, generalised Weierstrass elliptic function is the Kleinian σ

function, defined by

$$\sigma(\boldsymbol{u}) = \frac{\pi}{\sqrt{\det(2\omega)}} \frac{\epsilon}{\sqrt[4]{\prod_{i<j}(\lambda_i - \lambda_j)}} \exp\left\{\boldsymbol{u}^{\mathsf{T}}\eta(2\omega)^{-1}\boldsymbol{u}\right\} \theta[\varepsilon]((2\omega)^{-1}\boldsymbol{u}, \omega'\omega^{-1}). \quad (5.19)$$

Here ϵ is an eighth root of unity and ε is an odd 2-characteristic in the genus two case, chosen so that no Riemann vector is required in the theta function argument - see Lemma 2.1.

$\sigma(\boldsymbol{u})$ is a quasiperiodic function with respect to periods 2ω and $2\omega'$. Christiansen et al. also use Kleinian hyperelliptic functions:

$$\zeta_i(\boldsymbol{u}) = \frac{\partial}{\partial u_i}\log\sigma(\boldsymbol{u}), \qquad \wp_{ij}(\boldsymbol{u}) = -\frac{\partial}{\partial u_j}\zeta_i(\boldsymbol{u}) \quad (5.20)$$

the hyperelliptic generalisations of the Weierstrass ζ and $\wp$ functions.

In order to solve the Jacobi inversion problem (5.13) a theorem presented in [BEL96] is used:

Theorem 5.1 [BEL96] *Consider the Jacobi inversion problem*

$$\boldsymbol{u} = \sum_{k=1}^{g}\int_{a_k}^{\mu_k} \mathrm{d}\boldsymbol{u} \quad (5.21)$$

where the points $(\mu_k, \nu(\mu_k)$ are distinct on the genus g Riemann surface,

$$X = \{(\lambda, \nu(\lambda))\big|\nu^2 = \sum_{i=0}^{2g+2}\alpha_i\lambda^i\},$$

and, for all $j, k = 1, ..., g$, $\phi(\mu_k, \nu(\mu_k)) \neq (\mu_j, \nu(\mu_j))$, where ϕ is the hyperelliptic involution $\phi : (\lambda, \nu(\lambda)) \to (\lambda, -\nu(\lambda))$.

If the pre-image of the point $\boldsymbol{u} \in \mathrm{Jac}(X)$ is a non-special divisor, then the set $\{\mu_1, ..., \mu_g\}$ forms the zeros of the polynomial

$$\mathcal{P}(\lambda, \boldsymbol{u}) = \lambda^g - \sum_{k=1}^{g}\lambda^{k-1}\wp_{gk}(\boldsymbol{u}). \quad (5.22)$$

This means that the points μ_1 and μ_2 are the solutions to the quadratic polynomial

$$\lambda^2 - \lambda\wp_{22}(\boldsymbol{u}) - \wp_{21}(\boldsymbol{u}) \quad (5.23)$$

and thus must satisfy

$$\mu_1 + \mu_2 = \wp_{22}(\boldsymbol{u}), \qquad \mu_1\mu_2 = -\wp_{21}(\boldsymbol{u}). \tag{5.24}$$

Substituting these results into (5.8) gives the solutions

$$\begin{aligned} Q_1^2 &= \frac{a_1^2 - a_1\wp_{22}(\boldsymbol{u}) - \wp_{12}(\boldsymbol{u})}{a_1 - a_2}, \\ Q_2^2 &= \frac{a_2^2 - a_2\wp_{22}(\boldsymbol{u}) - \wp_{12}(\boldsymbol{u})}{a_2 - a_1}. \end{aligned} \tag{5.25}$$

with $\boldsymbol{u} = (u_1^{(0)}, x + u_2^{(0)})^{\mathsf{T}}$. Adding these solutions together gives the square modulus of $\boldsymbol{q}(x,t)$,

$$\boldsymbol{q}^\dagger\boldsymbol{q} = a_1 + a_2 - \wp_{22}(\boldsymbol{u}). \tag{5.26}$$

The individual components of $\boldsymbol{q}(x,t)$ may also be written explicitly as

$$\begin{aligned} q_1(x,t) &= \sqrt{\frac{\mathcal{P}(a_2,\boldsymbol{u})}{a_1 - a_2}}\exp\left\{ia_1t - \nu(a_1)\int_{u_1^{(0)}}^{x}\frac{\mathrm{d}x}{\mathcal{P}(a_1,\boldsymbol{u})}\right\}, \\ q_2(x,t) &= \sqrt{\frac{\mathcal{P}(a_2,\boldsymbol{u})}{a_2 - a_1}}\exp\left\{ia_2t - \nu(a_2)\int_{u_1^{(0)}}^{x}\frac{\mathrm{d}x}{\mathcal{P}(a_2,\boldsymbol{u})}\right\}, \end{aligned} \tag{5.27}$$

To see this solution in the framework of Baker-Akhiezer functions, Christiansen et al. consider a particular Baker-Akhiezer function, $\Psi(\lambda,\boldsymbol{u})$, expressed in terms of Kleinian σ functions by

$$\Psi(\lambda,\boldsymbol{u}) = \frac{\sigma\left(\int_a^\lambda \mathrm{d}\boldsymbol{u} - \boldsymbol{u}\right)}{\sigma(\boldsymbol{u})}\exp\left\{\int_a^\lambda \mathrm{d}\boldsymbol{r}^{\mathsf{T}}\boldsymbol{u}\right\}. \tag{5.28}$$

We now present two results derived in [BEL96]. We will not elaborate on their proofs as this requires some detailed algebra and draws on several other results.

$$\frac{\partial}{\partial u_2}\Psi(\lambda,\boldsymbol{u}) = \frac{1}{2\mathcal{P}(\lambda,\boldsymbol{u})}\left(\nu(\lambda) + \frac{\partial}{\partial u_2}\mathcal{P}(\lambda,\boldsymbol{u})\right)\Psi(\lambda,\boldsymbol{u}), \tag{5.29}$$

$$\frac{\partial^2}{\partial u_2^2}\Psi(\lambda,\boldsymbol{u}) - 2\wp_{22}(\boldsymbol{u})\Psi(\lambda,\boldsymbol{u}) = \left(\lambda + \frac{\alpha_4}{4}\right)\Psi(\lambda,\boldsymbol{u}). \tag{5.30}$$

Thus $\Psi(\lambda,\boldsymbol{u})$ satisfies the Schrödinger equation (5.30) and, as u_1 is constant, we may integrate (5.29) to give

$$\Psi(\lambda,\boldsymbol{u}) = C\sqrt{\mathcal{P}(\lambda,\boldsymbol{u})}\exp\left\{\frac{\nu(\lambda)}{2}\int_a^{u_2}\frac{\mathrm{d}u_2}{\mathcal{P}(\lambda,\boldsymbol{u})}\right\}, \tag{5.31}$$

where C is constant with respect to u_2. Substituting this form for Ψ into (5.30) and comparing with the VNLS equations Christiansen et al. conclude that $\Psi(a_1, x) = q_1(x, t = 0)$ and $\Psi(a_2, x) = q_2(x, t = 0)$.

In a later paper [EEK00], Eilbeck et al. extend the method to a system of nonlinear Schrödinger equations with n components:

$$iq_{j,t} + q_{j,xx} + 2q_j \sum_{k=1}^{n} q_k \overline{q}_k = 0 \qquad j = 1, ..., n. \tag{5.32}$$

The relevant Lax form in this case has a hyperelliptic spectral curve of genus n, although a link to the solutions to the two component problem which we presented in the last chapter would not seem apparent given the extra components. Our main interest is to investigate whether the separable solutions found by Christiansen et al. can be linked to the quasiperiodic solutions found in [EEI07].

5.2 Spectral curve of genus two

Let us introduce constants of integration attached to L_2 in the attractive scattering problem (4.1). Throughout this section we will be referring to the attractive problem so we drop the + sign. Let $\alpha_0 = -i$ so that

$$L_0 = \begin{pmatrix} -i & \mathbf{0}^{\mathsf{T}} \\ \mathbf{0} & \mathbb{O}_2 \end{pmatrix} \tag{5.33}$$

and set

$$L_2 = \begin{pmatrix} i\boldsymbol{q}^{\dagger}\boldsymbol{q} & i\boldsymbol{q}_x^{\mathsf{T}} \\ i\overline{\boldsymbol{q}}_x & -i\overline{\boldsymbol{q}}\boldsymbol{q}^{\mathsf{T}} \end{pmatrix} + i \begin{pmatrix} C_{11} & 0 & 0 \\ 0 & C_{22} & 0 \\ 0 & 0 & C_{33} \end{pmatrix} \tag{5.34}$$

with L_1 remaining unchanged. The constants C_{ii} are all real and chosen such that $C_{11} = -(C_{22} + C_{33})$ so that L_2 remains traceless. Since the second of equations (4.1) is altered by the addition of these constants, we replace t by τ in the modified scattering problem. Applying the consistency condition $\boldsymbol{v}_{x\tau} = \boldsymbol{v}_{\tau x}$ gives

$$i\boldsymbol{q}_{\tau} + \boldsymbol{q}_{xx} + 2\boldsymbol{q}\boldsymbol{q}^{\dagger}\boldsymbol{q} - \begin{pmatrix} a_1 q_1 \\ a_2 q_2 \end{pmatrix} = 0 \tag{5.35}$$

with $a_1 = C_{22} - C_{11}$ and $a_2 = C_{33} - C_{11}$. The stationary spectral curve of the new system takes the form

$$f(z,\mu) = -\det(\mathcal{L}_2(z) - \mu\mathbb{I}_3) = \mu^2(\mu + iz^2) + \mu P(z) + Q(z) = 0. \tag{5.36}$$

$P(z) = \rho_2 z^2 + \rho_1 z + \rho_0$ and $Q(z) = \eta_2 z^2 + \eta_1 z + \eta_0$ are second-order polynomials in z with constant coefficients. Using the technique of Section 4.3 the genus of (5.36) is determined to be two, provided

$$\Delta = \rho_2^2 - 4i\eta_2 \neq 0. \tag{5.37}$$

An example of a possible configuration of branch points and first homology basis for this three-sheeted Riemann surface is presented in Figure 5.1 with an explanation attached to Figure 4.1. Choosing local parameter $\xi = z^{-1}$ at the points at infinity, the behaviour of μ

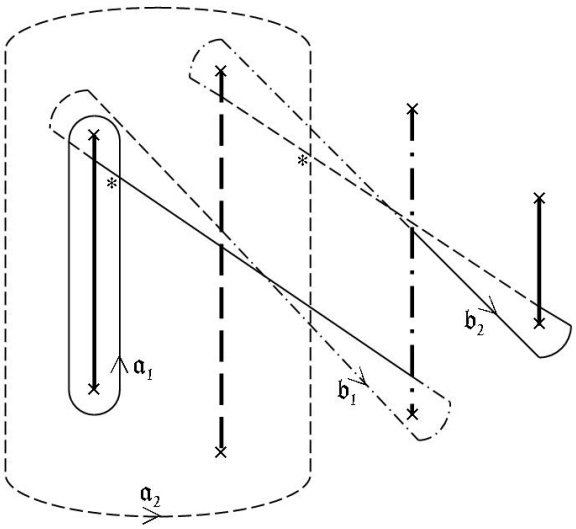

Figure 5.1: Three-sheeted Riemann Surface of Genus 2

is given by

$$\mu = \begin{cases} -i\xi^{-2} - i\rho_2 - i\rho_1\xi + O(\xi^2) & \text{at } \infty_1 \\ \\ a_0^{(2,3)} + a_1^{(2,3)}\xi + O(\xi^2) & \text{at } \infty_{2,3} \end{cases} \tag{5.38}$$

with

$$\begin{aligned} a_0^{(2,3)} &= i\big(\rho_2 \pm \sqrt{\Delta}\big)/2, \\ a_1^{(2,3)} &= \pm\big(\rho_1 a_0^{(2,3)} + \eta_1\big)/\sqrt{\Delta}. \end{aligned}$$

A set of holomorphic differentials for this curve can be found using the technique of Deconinck and Van Hoeij [DH01]:

$$\mathrm{d}\widetilde{\omega}_1 = \frac{i}{f_\mu(z,\mu)}\mathrm{d}z, \qquad \mathrm{d}\widetilde{\omega}_2 = \frac{\mu}{f_\mu(z,\mu)}\mathrm{d}z, \tag{5.39}$$

in terms of which a normalised set, satisfying $\int_{a_k} \mathrm{d}\omega_j = 2\pi i\delta_{jk}$, is given by

$$\mathrm{d}\omega_j = 2\pi i \sum_{k=1}^{2} (A^{-1})_{jk}\mathrm{d}\widetilde{\omega}_k = \sum_{k=1}^{2} c_{jk}\mathrm{d}\widetilde{\omega}_k \tag{5.40}$$

with A the 2×2 matrix with components $A_{jk} = \int_{a_k} \mathrm{d}\widetilde{\omega}_j$. The expansion of the Abelian integral of the vector differential $\mathrm{d}\boldsymbol{\omega}$ at the points at infinity is given by

$$\int_{\infty_1}^{P^{(k)}} \mathrm{d}\boldsymbol{\omega} = \boldsymbol{U}^{(k)} + \boldsymbol{V}^{(k)}\xi + \boldsymbol{W}^{(k)}\xi^2 + \ldots \tag{5.41}$$

where $P^{(k)} \to \infty_k$ and $\boldsymbol{U}^{(k)} = \int_{\infty_1}^{\infty_k} \mathrm{d}\boldsymbol{\omega}$. That is we have selected the base point, $\infty^{(1)}$. Straightforward calculations determine

$$\begin{aligned}
\boldsymbol{V}^{(1)} &= -i\boldsymbol{c}_2,\\
\boldsymbol{W}^{(1)} &= \boldsymbol{0},\\
\boldsymbol{V}^{(2,3)} &= \pm\Delta^{-\frac{1}{2}}(i\boldsymbol{c}_1 + a_0^{(2,3)}\boldsymbol{c}_2),\\
\boldsymbol{W}^{(2,3)} &= \frac{i}{2\Delta}(2ia_1^{(2,3)} + \rho_1)\boldsymbol{c}_1 + \left(\frac{a_0^{(2,3)}}{2\Delta}(2ia_1^{(2,3)} + \rho_1) \pm \frac{a_1^{(2,3)}}{2\Delta^{\frac{1}{2}}}\right)\boldsymbol{c}_2,
\end{aligned} \tag{5.42}$$

where $\boldsymbol{c}_k = (c_{1k}, c_{2k})^{\mathsf{T}}$.

Using the method of Elgin et al. [EEI07], as demonstrated in Chapter 4, finite gap solutions to the VNLS (1.1) may be derived:

$$\begin{aligned}
q_1(x,t) &= \chi_1 \frac{\theta(\boldsymbol{\omega}(\infty_2) + \boldsymbol{g}(x,t) - \boldsymbol{e})}{\theta(\boldsymbol{g}(x,t) - \boldsymbol{e})}\exp(E_1x + N_1t)\\
q_2(x,t) &= \chi_2 \frac{\theta(\boldsymbol{\omega}(\infty_3) + \boldsymbol{g}(x,t) - \boldsymbol{e})}{\theta(\boldsymbol{g}(x,t) - \boldsymbol{e})}\exp(E_2x + N_2t)
\end{aligned} \tag{5.43}$$

where

$$\begin{aligned} \chi_k &= i\delta_k \frac{\theta(\boldsymbol{e})}{\theta(\boldsymbol{r}^{(k+1)} - \boldsymbol{e})}, \\ \boldsymbol{\omega}(\infty_k) &= \int_{\infty_1}^{\infty_k} \mathrm{d}\boldsymbol{\omega}, \\ \boldsymbol{e} &= \sum_{j=1}^{2} \int_{\infty_1}^{P_j} \mathrm{d}\boldsymbol{\omega} - \boldsymbol{K} \end{aligned}$$

with $\boldsymbol{K}$ the vector of Riemann constants with base point ∞_1 and $\mathcal{D} = P_1 + P_2$ a divisor of general position. $\boldsymbol{g}(x,t) = \boldsymbol{V}x + \boldsymbol{W}t$ with $\boldsymbol{V}$ and $\boldsymbol{W}$ calculated using the Riemann bilinear relations:

$$\boldsymbol{V} = i\boldsymbol{V}^{(1)} = \boldsymbol{c}_2, \tag{5.44}$$

$$\boldsymbol{W} = i\boldsymbol{W}^{(1)} = \boldsymbol{0}. \tag{5.45}$$

Importantly, the constants N_k may also be calculated using these relations:

Proposition 5.1

$$N_k = ia_k \qquad k = 1, 2. \tag{5.46}$$

Proof: Setting $\hat{\Omega} = \Omega_2$ and $\mathrm{d}\widetilde{\Omega} = z\mathrm{d}\widetilde{\omega}_k$ for $k = 1, 2$ in the Riemann bilinear relations (2.6), we obtain the two relations:

$$N_1 - N_2 = i(a_1 - a_2) \qquad \text{and} \qquad N_1 + N_2 = i(a_1 + a_2)$$

from which the proposition is deduced.

Since $\boldsymbol{W} = \boldsymbol{0}$ and $N_k = ia_k$ it follows that the solutions (5.43) must necessarily take the form (5.1). We may also derive the square intensity formula

$$\boldsymbol{q}^\dagger \boldsymbol{q} = \partial_x^2 \ln \theta(\boldsymbol{V}x - \boldsymbol{e}) + iR_1 \tag{5.47}$$

which appears to take an identical form to the solution (5.26).

5.3 Birational transformation to a hyperelliptic curve

It is an elementary corollary of Theorem 2.4 that every Riemann surface of genus two is hyperelliptic in form [RF74]. It follows that the curve (5.36) must be birationally equivalent to a hyperelliptic curve. The explicit form of the birational transformation is

as follows:

$$z = \frac{i\mu\rho_1 + i(\eta_1 - \nu)}{2\left(\mu^2 - i\rho_2\mu - i\eta_2\right)}, \qquad \mu = i\Big(\lambda - \frac{1}{3}(a_1 + a_2)\Big). \tag{5.48}$$

Under this transformation, the curve $f(z,\mu)$ maps to

$$\widetilde{f}(\lambda,\nu) = \nu^2 - \sum_{k=0}^{5} \alpha_k \lambda^k = 0 \tag{5.49}$$

where $\alpha_5 = 4$ and

$$\begin{aligned}
\alpha_4 &= -8(a_1 + a_2),\\
\alpha_3 &= -4H + 4(a_1 + a_2)^2 + 8a_1a_2,\\
\alpha_2 &= 4H(a_1 + a_2) - 4G - 4C_1^2 - 4C_2^2 - 8a_1a_2(a_1 + a_2),\\
\alpha_1 &= 4G(a_1 + a_2) - 4a_1a_2H + 8C_1^2a_2 + 8C_2^2a_1 + 4a_1^2a_2^2,\\
\alpha_0 &= -4a_1a_2G - 4C_1^2a_2^2 - 4C_2^2a_1^2.
\end{aligned}$$

Considering (5.36) as a quadratic in z, it is clear that $(z,\mu) \mapsto w$ is a two-sheeted covering of $\mathbb{C}$. This is why μ depends so simply on λ above. Not only does (5.48) map the spectral curve into the form (5.6) of the spectral curve in [CEE00], it precisely recovers the functional dependence of the coefficients α_k on $q\,(x,t)$ and its derivatives, up to the aforementioned re-scaling of the constants C_k. In doing this calculation, the coefficients in the curve $f(z,\mu)$ have also been expressed in terms of a_1, a_2, H and G as follows:

$$\begin{aligned}
\rho_2 &= (a_1 + a_2)/3,\\
\rho_1 &= -2(C_1 + C_2),\\
\rho_0 &= (a_1 + a_2)^2/9 - (2a_1 - a_2)(2a_2 - a_1)/9 + H,\\
\eta_2 &= -i(2a_1 - a_2)(2a_2 - a_1)/9,\\
\eta_1 &= 2iC_1(2a_2 - a_1)/3 + 2iC_2(2a_1 - a_2)/3,\\
\eta_0 &= -i(a_1 + a_2)(2a_1 - a_2)(2a_2 - a_1)/27\\
&\quad -2iC_1C_2 + iG + 2i(a_1 + a_2)H/3.
\end{aligned}$$

The birational equivalence of the spectral curves is important because it means that the fields of meromorphic functions on the two curves are isomorphic.

Applying the relations $\nu = f_z(z,\mu)$ and $\mathrm{d}f = f_z\mathrm{d}z + f_\mu\mathrm{d}\mu = 0$, the differentials (5.39) are

given in terms of λ and ν by

$$\mathrm{d}\widetilde{\omega}_1 = \mathrm{d}u_1, \qquad \mathrm{d}\widetilde{\omega}_2 = \mathrm{d}u_2 - \left(\frac{1}{3}(a_1 + a_2)\right)\mathrm{d}u_1, \tag{5.50}$$

where $\mathrm{d}u_1 = \frac{1}{\nu}\mathrm{d}\lambda$ and $\mathrm{d}u_2 = \frac{\lambda}{\nu}\mathrm{d}\lambda$ are the differentials used by Christiansen et al. [CEE00]. Given that our choice of first homology basis on the three-sheeted surface has been free up until now, we choose it such that a and b cycles are directly transferred between two and three-sheeted coverings. This means we have

$$(2\omega)^{-1} = \frac{1}{2\pi i}\begin{pmatrix} c_{11} - \frac{a_1+a_2}{3} & c_{12} \\ c_{21} - \frac{a_1+a_2}{3} & c_{22} \end{pmatrix} \tag{5.51}$$

where $(2\omega)_{jk} = \int_{a_k} \mathrm{d}u_j$ using the notation of [CEE00]. The expression (5.26) for the modulus of $\boldsymbol{q}$ is effectively formed of a constant minus two x derivatives of $\ln\theta[\varepsilon](\boldsymbol{u})$. This is precisely the form of the solution derived via the algebrogeometric approach, (5.47). The exact correspondence of the two solutions should be verifiable although this may require an appropriate choice of Riemann vector and other parameters. This may also mean that a transformation exists between the two Lax pair systems, (5.5) and (4.1) although this is by no means obvious.

It is natural to ask at this stage whether any of the higher genus spectral curves of the VNLS hierarchy are hyperelliptic. According to a theorem in [FK80], a hyperelliptic Riemann surface of genus g does not support functions whose degree is odd and less than or equal to g. Therefore, as the function $p : (z, \mu) \to z$ is a function of degree three, any curve of the form (5.36) and of genus greater than two cannot be hyperelliptic. There may however be some special cases where a reduction is possible.

Chapter 6

Polarisation state evolution

6.1 The Heisenberg ferromagnet hierarchy

The continuous isotropic Heisenberg ferromagnet (HF) equation, given by

$$\mathbf{T}_t(x,t) = \mathbf{T}(x,t) \times \mathbf{T}_{xx}(x,t), \tag{6.1}$$

is a completely integrable equation which has previously been solved using the inverse scattering transform method. Here $\mathbf{T}(x,t) = (T_1, T_2, T_3)^{\mathsf{T}}$ is a unit vector denoting the polarisation state of a spin system in the continuum limit in one dimension. Importantly in the context of this thesis, Lakshmanan [Lak77] found a connection between (6.1) and the attractive case SNLS:

$$iq_t + q_{xx} + 2q^2\overline{q} = 0. \tag{6.2}$$

By letting $\mathbf{T}(x,t)$ represent a unit tangent vector to a curve parametrised by x and choosing orthonormal vectors

$$\begin{aligned} \mathbf{N} &= \kappa^{-1}\mathbf{T}_x, \\ \mathbf{B} &= \mathbf{T} \times \mathbf{N} \end{aligned} \tag{6.3}$$

where $\kappa = |\mathbf{T}_x|$, we form a basis of orthonormal vectors which must satisfy the well-known Serret-Frenet equations

$$\big(\mathbf{T}, \mathbf{N}, \mathbf{B}\big)_x = \big(\mathbf{T}, \mathbf{N}, \mathbf{B}\big) \begin{pmatrix} 0 & -\kappa & 0 \\ \kappa & 0 & -\tau \\ 0 & \tau & 0 \end{pmatrix}. \tag{6.4}$$

Here κ is the curvature and τ, the torsion, may be calculated as

$$\tau = \kappa^{-2}\mathbf{T}\cdot(\mathbf{T}_x \times \mathbf{T}_{xx}). \tag{6.5}$$

Consider now the evolution with respect to t of the orthonormal basis. From equation (6.1) and the Serret-Frenet equations, we derive

$$\mathbf{T}_t = -\kappa\tau\mathbf{N} + \kappa_x\mathbf{B} \tag{6.6}$$

which may be usefully rewritten as

$$\begin{aligned}(\mathbf{N}\times\mathbf{B})_t &= -\kappa\tau\mathbf{N} + \kappa_x\mathbf{B},\\ \mathbf{N}_t\times\mathbf{B} + \mathbf{N}\times\mathbf{B}_t &= -\kappa\tau\mathbf{N} + \kappa_x\mathbf{B}.\end{aligned} \tag{6.7}$$

Then, since $\mathbf{N}$ and $\mathbf{B}$ are orthonormal vectors, $\mathbf{N}_t\cdot\mathbf{N} = \mathbf{B}_t\cdot\mathbf{B} = (\mathbf{N}\cdot\mathbf{B})_t = 0$ and the t-derivatives must take the form

$$\begin{aligned}\mathbf{N}_t &= \alpha\mathbf{T} + \beta\mathbf{B}\\ \mathbf{B}_t &= \gamma\mathbf{T} - \beta\mathbf{N}.\end{aligned} \tag{6.8}$$

Substitution into (6.7) implies $\alpha = \kappa\tau$ and $\gamma = -\kappa_x$. Finally, with the aid of the Serret-Frenet equations we compute

$$\begin{aligned}\mathbf{T}_{xt} &= \mathbf{T}_{tx}\\ \kappa_t\mathbf{N} + \kappa\mathbf{N}_t &= -(\kappa\tau)_x\mathbf{N} - \kappa\tau\mathbf{N}_x + \kappa_{xx}\mathbf{B} + \kappa_x\mathbf{B}_x\\ \kappa_t\mathbf{N} + \kappa\beta\mathbf{B} &= -(2\kappa_x\tau + \kappa\tau_x)\mathbf{N} + (\kappa_{xx} - \kappa\tau^2)\mathbf{B}\end{aligned}$$

and deduce $\beta = \kappa^{-1}\kappa_{xx} - \tau^2$ and

$$\kappa_t = -2\kappa_x\tau - \kappa\tau_x. \tag{6.9}$$

Similarly applying $\mathbf{N}_{xt} = \mathbf{N}_{tx}$ the evolution of τ is found to be

$$\tau_t = \left(\frac{\kappa_{xx}}{\kappa} - \tau^2\right)_x + \kappa\kappa_x. \tag{6.10}$$

Lakshmanan [Lak77] noted that setting

$$q(x,t) = \frac{1}{2}\kappa(x,t)\exp\left(i\int^x \tau(x',t)\mathrm{d}x'\right), \tag{6.11}$$

equations (6.9) and (6.10) correspond to the imaginary and real parts of the attractive SNLS (6.2).

Following on from this work a gauge equivalence relation between the attractive SNLS and HF equations was found. We give a basic outline of the proof. Full details may be found in [FT87].

The scattering problem for the HF equation is given by:

$$\begin{aligned} \boldsymbol{v}_x(x,t,z) &= \mathcal{U}_1(z,x,t)\boldsymbol{v}(x,t,z), \\ \boldsymbol{v}_t(x,t,z) &= \mathcal{U}_2(z,x,t)\boldsymbol{v}(x,t,z) \end{aligned} \tag{6.12}$$

where

$$\begin{aligned} \mathcal{U}_1(z,x,t) &= \frac{iz}{2}\mathbf{T}\cdot\boldsymbol{\sigma}, \\ \mathcal{U}_2(z,x,t) &= \frac{iz^2}{2}\mathbf{T}\cdot\boldsymbol{\sigma} + \frac{iz}{2}(\mathbf{T}\times\mathbf{T}_x)\cdot\boldsymbol{\sigma} \end{aligned}$$

and they satisfy the zero-curvature representation

$$\mathcal{U}_{2,x} - \mathcal{U}_{1,t} = [\mathcal{U}_1, \mathcal{U}_2]\,. \tag{6.13}$$

Here the Stokes vector $\mathbf{T}(x,t) \in \mathbb{R}^3$ has been mapped to the special unitary group SU(2) according to

$$\mathbf{T} \to \mathbf{T}\cdot\boldsymbol{\sigma} = \sum_{k=1}^{3} T_k\sigma_k = \begin{pmatrix} T_3 & T_1 - iT_2 \\ T_1 + iT_2 & -T_3 \end{pmatrix} \tag{6.14}$$

where σ_k are the Pauli matrices, see (1.4). These satisfy the relations

$$\sigma_j\sigma_k = \delta_{jk}\mathbb{I}_2 + i\epsilon_{jkl}\sigma_l \tag{6.15}$$

so that

$$\begin{aligned} [\boldsymbol{a}\cdot\boldsymbol{\sigma}, \boldsymbol{b}\cdot\boldsymbol{\sigma}] &= 2i(\boldsymbol{a}\times\boldsymbol{b})\cdot\boldsymbol{\sigma}, \\ \{\boldsymbol{a}\cdot\boldsymbol{\sigma}, \boldsymbol{b}\cdot\boldsymbol{\sigma}\} &= 2\boldsymbol{a}\cdot\boldsymbol{b}\mathbb{I}_2 \end{aligned} \tag{6.16}$$

for 3-vectors $\boldsymbol{a}$ and $\boldsymbol{b}$. Equation (6.1) is recovered by comparing coefficients of z in (6.13). We now introduce a unitary matrix $\Omega(x,t)$ independent of z and satisfying the equations

$$\begin{aligned} \Omega_x &= L_1\Omega = \begin{pmatrix} 0 & q \\ -\overline{q} & 0 \end{pmatrix}\Omega, \\ \Omega_t &= L_2\Omega = \begin{pmatrix} iq\overline{q} & iq_x \\ i\overline{q}_x & -iq\overline{q} \end{pmatrix}\Omega. \end{aligned} \tag{6.17}$$

The gauge transformation induced by Ω^{-1} involves setting $\boldsymbol{w}(x,t,z) = \Omega(x,t)\boldsymbol{v}(x,t,z)$,

where $\boldsymbol{w}$ is a solution to the attractive SNLS scattering problem (1.13), (1.14). This means

$$\begin{aligned} \boldsymbol{v}_x &= \left(-\Omega^{-1}\Omega_x + \Omega^{-1}\mathcal{L}_1\Omega\right)\boldsymbol{v}, \\ \boldsymbol{v}_t &= \left(-\Omega^{-1}\Omega_t + \Omega^{-1}\mathcal{L}_2\Omega\right)\boldsymbol{v}. \end{aligned} \tag{6.18}$$

Setting

$$\Omega^{-1}L_0\Omega = -\frac{i}{2}\Omega^{-1}\sigma_3\Omega = \frac{i}{2}\mathbf{T}\cdot\boldsymbol{\sigma} \tag{6.19}$$

and then demonstrating

$$\Omega^{-1}L_1\Omega = \frac{i}{2}(\mathbf{T}\times\mathbf{T}_x)\cdot\boldsymbol{\sigma}$$

means

$$\begin{aligned} \left(-\Omega^{-1}\Omega_x + \Omega^{-1}\mathcal{L}_1\Omega\right) &= \frac{iz}{2}\mathbf{T}\cdot\boldsymbol{\sigma} = \mathcal{U}_1(z,x,t), \\ \left(-\Omega^{-1}\Omega_t + \Omega^{-1}\mathcal{L}_2\Omega\right) &= \frac{iz^2}{2}\mathbf{T}\cdot\boldsymbol{\sigma} + \frac{iz}{2}(\mathbf{T}\times\mathbf{T}_x)\cdot\boldsymbol{\sigma} = \mathcal{U}_2(z,x,t). \end{aligned}$$

This process represents a gauge transformation from the SNLS to the HF equation and was first shown by Zakharov and Takhtadzhyan [ZT79]. A corresponding inverse transformation exists, details of which may be found in [FT87].

Mikhailov and Shabat [MS86] investigated integrable deformations of the HF equation taking the form

$$\mathbf{T}_t = \mathbf{T}\times\mathbf{T}_{xx} + \mathbf{F}(\mathbf{T},\mathbf{T}_x)$$

with $\mathbf{F}$ some real function of $\mathbf{T}$ and $\mathbf{T}_x$ satisfying $\mathbf{F}\cdot\mathbf{T} = 0$. They demonstrated that the only integrable deformation of this form is

$$\mathbf{T}_t = \mathbf{T}\times\mathbf{T}_{xx} + \varepsilon(\mathbf{T}_x\cdot\mathbf{T}_x)\mathbf{T}_x \tag{6.20}$$

where ε is a perturbation parameter. Zhang and Yang [ZY90] extended this idea, using a prolongation structure, to develop arbitrary order deformations which agreed with [MS86] in the most simple case. We now use a more direct approach to determine a Heisenberg ferromagnet hierarchy whose members correspond to the integrable deformations given in [ZY90].

In a similar way to that followed in Chapter 3, define a general n^{th} flow

$$\boldsymbol{v}_{t_n} = \mathcal{U}_n(z,t_j)\boldsymbol{v} \tag{6.21}$$

of which equations (6.18) are the first with $t_1 = x$ and $t_2 = t$. The notation $\mathcal{U}_n(z, t_j)$ means $\mathcal{U}_n$ depends upon the spectral parameter z and variables t_j for $j = 1, ..., n$. We give the matrices $\mathcal{U}_n$ the structure

$$\mathcal{U}_n(z, t_j) = \frac{i}{2} \sum_{k=0}^{n-1} z^{n-k} \mathbf{U}_k(t_j) \cdot \boldsymbol{\sigma} \tag{6.22}$$

with

$$\mathbf{U}_0(t_j) = \mathbf{T}, \qquad \mathbf{U}_1(t_j) = \mathbf{T} \times \mathbf{T}_x.$$

Cross-differentiating $\boldsymbol{v}_x = \mathcal{U}_1 \boldsymbol{v}$ and $\boldsymbol{v}_{t_n} = \mathcal{U}_n \boldsymbol{v}$ and applying the consistency condition $\boldsymbol{v}_{xt_n} = \boldsymbol{v}_{t_n x}$, we form the zero-curvature equation

$$\mathcal{U}_{n,x} - \mathcal{U}_{1,t_n} = [\mathcal{U}_1, \mathcal{U}_n]\,. \tag{6.23}$$

Comparing z^{n-k} coefficients we see

$$\begin{aligned} \mathbf{U}_{k,x} &= \mathbf{U}_{k+1} \times \mathbf{T} \qquad k = 0, ..., n-2, \\ \mathbf{U}_{n-1,x} &= \mathbf{T}_{t_n} \end{aligned} \tag{6.24}$$

and from this deduce

$$\begin{aligned} \mathbf{U}_{k+1} &= \mathbf{T} \times \mathbf{U}_{k,x} + (\mathbf{U}_{k+1} \cdot \mathbf{T})\mathbf{T} \\ &= \mathbf{T} \times \mathbf{U}_{k,x} + \left(\int^x \mathbf{U}_{k+1} \cdot \mathbf{T}_{x'} \mathrm{d}x' \right) \mathbf{T}. \end{aligned}$$

It is then straightforward to calculate

$$\mathbf{U}_{k+1} \cdot \mathbf{T}_x = -\mathbf{U}_{k,x} \cdot (\mathbf{T} \times \mathbf{T}_x) = -\mathbf{U}_1 \cdot \mathbf{U}_{k,x}$$

which means

$$\mathbf{U}_{k+1} = \mathbf{T} \times \mathbf{U}_{k,x} - \left(\int^x \mathbf{U}_1 \cdot \mathbf{U}_{k,x'} \mathrm{d}x' \right) \mathbf{T}. \tag{6.25}$$

We now integrate by parts recursively using the first of equations (6.24) to give:

$$\begin{aligned}
\mathbf{U}_{k+1} &= \mathbf{T}\times\mathbf{U}_{k,x} - \left(\int^x \mathbf{U}_1\cdot\mathbf{U}_{k,x'}\mathrm{d}x'\right)\mathbf{T}\\
&= \mathbf{T}\times\mathbf{U}_{k,x} - (\mathbf{U}_1\cdot\mathbf{U}_k)\mathbf{T} + \left(\int^x (\mathbf{U}_2\times\mathbf{T})\cdot\mathbf{U}_k\mathrm{d}x'\right)\mathbf{T}\\
&= \mathbf{T}\times\mathbf{U}_{k,x} - (\mathbf{U}_1\cdot\mathbf{U}_k)\mathbf{T} - \left(\int^x \mathbf{U}_2\cdot(\mathbf{U}_k\times\mathbf{T})\mathrm{d}x'\right)\mathbf{T}\\
&= \mathbf{T}\times\mathbf{U}_{k,x} - (\mathbf{U}_1\cdot\mathbf{U}_k)\mathbf{T} - \left(\int^x \mathbf{U}_2\cdot\mathbf{U}_{k-1,x'}\mathrm{d}x'\right)\mathbf{T}\\
&= \mathbf{T}\times\mathbf{U}_{k,x} - (\mathbf{U}_1\cdot\mathbf{U}_k + \mathbf{U}_2\cdot\mathbf{U}_{k-1})\mathbf{T} - \left(\int^x \mathbf{U}_3\cdot\mathbf{U}_{k-2,x'}\mathrm{d}x'\right)\mathbf{T}
\end{aligned}$$

which, after repeated application, becomes

$$\mathbf{U}_{k+1} = \mathbf{T}\times\mathbf{U}_{k,x} - \frac{1}{2}\left(\sum_{j=1}^{k}\mathbf{U}_j\cdot\mathbf{U}_{k+1-j}\right)\mathbf{T}. \tag{6.26}$$

Applying in the first few cases we see

$$\begin{aligned}
\mathbf{U}_2 &= -\mathbf{T}_{xx} - \frac{3}{2}(\mathbf{T}_x\cdot\mathbf{T}_x)\mathbf{T},\\
\mathbf{U}_3 &= -\mathbf{T}\times\mathbf{T}_{3x} + \mathbf{T}_x\times\mathbf{T}_{xx} - \frac{5}{2}(\mathbf{T}_x\cdot\mathbf{T}_x)\mathbf{T}\times\mathbf{T}_x,\\
\mathbf{U}_4 &= \mathbf{T}_{4x} + \frac{5}{2}(\mathbf{T}_x\cdot\mathbf{T}_x)\mathbf{T}_{xx} + 5(\mathbf{T}_x\cdot\mathbf{T}_{xx})\mathbf{T}_x\\
&\qquad + \left(5\mathbf{T}_x\cdot\mathbf{T}_{3x} + \frac{5}{2}\mathbf{T}_{xx}\cdot\mathbf{T}_{xx} + \frac{35}{8}(\mathbf{T}_x\cdot\mathbf{T}_x)^2\right)\mathbf{T}
\end{aligned} \tag{6.27}$$

which generate the evolution equations

$$\begin{aligned}
\mathbf{T}_{t_3} &= -\mathbf{T}_{3x} - \frac{3}{2}(\mathbf{T}_x\cdot\mathbf{T}_x)\mathbf{T}_x - 3(\mathbf{T}_x\cdot\mathbf{T}_{xx})\mathbf{T},\\
\mathbf{T}_{t_4} &= -\mathbf{T}\times\mathbf{T}_{4x} - 5(\mathbf{T}_x\cdot\mathbf{T}_{xx})\mathbf{T}\times\mathbf{T}_x - \frac{5}{2}(\mathbf{T}_x\cdot\mathbf{T}_x)\mathbf{T}\times\mathbf{T}_{xx},\\
\mathbf{T}_{t_5} &= \mathbf{T}_{5x} + \frac{5}{2}(\mathbf{T}_x\cdot\mathbf{T}_x)\mathbf{T}_{3x} + 10(\mathbf{T}_x\cdot\mathbf{T}_{xx})\mathbf{T}_{xx}\\
&\qquad + \left(\frac{35}{8}(\mathbf{T}_x\cdot\mathbf{T}_x)^2 + 10\mathbf{T}_x\cdot\mathbf{T}_{3x} + \frac{15}{2}\mathbf{T}_{xx}\cdot\mathbf{T}_{xx}\right)\mathbf{T}_x\\
&\qquad + \left(\frac{35}{2}(\mathbf{T}_x\cdot\mathbf{T}_x)\mathbf{T}_x\cdot\mathbf{T}_{xx} + 5\mathbf{T}_x\cdot\mathbf{T}_{4x} + 10\mathbf{T}_{xx}\cdot\mathbf{T}_{3x}\right)\mathbf{T}
\end{aligned} \tag{6.28}$$

where $\mathbf{T}_{kx} = \frac{\partial^k\mathbf{T}}{\partial x^k}$. These equations agree with the integrable deformations found in [ZY90]. Zhang and Yang note that the flow $\mathbf{T}_{t_5}$ may be shown gauge equivalent to the fifth flow of the SNLS hierarchy, either using the method described above or applying

Lakshmanan's method which we described earlier. We now demonstrate that each member of the HF hierarchy is gauge equivalent to its corresponding member in the SNLS hierarchy using a strong induction argument.

Theorem 6.1 *The attractive SNLS and HF hierarchies are gauge equivalent.*

Proof: Let $\Omega(t_j)$ be a 2×2 unitary matrix satisfying the consistent system of equations

$$\Omega_{t_k} = L_k \Omega \qquad k = 1, 2, ... \tag{6.29}$$

where the 2×2 matrices L_k define the attractive SNLS hierarchy and are generated by equation (3.29),

$$L_{k+1} = [L_{k,x}, L_0] + [L_0, [L_1, L_k]] + \sum_{j=1}^{k} \{L_j, L_{k+1-j}\} L_0. \tag{6.30}$$

Then we may prove

$$\Omega^{-1} L_k \Omega = \frac{i}{2} \mathbf{U}_k \cdot \boldsymbol{\sigma} \qquad k = 1, 2, ... \tag{6.31}$$

using a strong induction argument:

Assume it holds up to k and and apply the action $\Omega^{-1} \circ \Omega$ to equation (6.30) to give

$$\begin{aligned}
\Omega^{-1} L_{k+1} \Omega &= \Omega^{-1} \Big([L_{k,x}, L_0] + [L_0, [L_1, L_k]] + \sum_{j=1}^{k} \{L_j, L_{k+1-j}\} L_0 \Big) \Omega \\
&= [\frac{i}{2} \mathbf{U}_{k,x} \cdot \boldsymbol{\sigma}, \frac{i}{2} \mathbf{T} \cdot \boldsymbol{\sigma}] + \sum_{j=1}^{k} \{\frac{i}{2} \mathbf{U}_j \cdot \boldsymbol{\sigma}, \frac{i}{2} \mathbf{U}_{k+1-j} \cdot \boldsymbol{\sigma}\} \frac{i}{2} \mathbf{T} \cdot \boldsymbol{\sigma} \\
&= \frac{i}{2} \left((\mathbf{T} \times \mathbf{U}_{k,x}) \cdot \boldsymbol{\sigma} - \frac{1}{2} \Big(\sum_{j=1}^{k} \mathbf{U}_j \cdot \mathbf{U}_{k+1-j} \Big) \mathbf{T} \cdot \boldsymbol{\sigma} \right) \\
&= \frac{i}{2} \mathbf{U}_{k+1} \cdot \boldsymbol{\sigma}.
\end{aligned}$$

Then applying the gauge transformation of $\Omega^{-1}(t_k)$ to $\boldsymbol{w}$, a solution of the attractive SNLS scattering problem

$$\boldsymbol{w}_{t_k} = \mathcal{L}_k \boldsymbol{w} \qquad k = 1, 2, ..., \tag{6.32}$$

we see $\boldsymbol{v} = \Omega^{-1} \boldsymbol{w}$ satisfies

$$\boldsymbol{v}_{t_k} = \mathcal{U}_k \boldsymbol{v} \qquad k = 1, 2, ... \tag{6.33}$$

the HF hierarchy scattering problem. Thus the HF and SNLS hierarchy members are gauge equivalent at every level.

We now consider the conserved densities of the HF hierarchy using this gauge equivalence. In Section 4.5 we found an infinite set of conserved densities to the VNLS. Equivalently the set of conserved densities to the attractive SNLS are given by

$$\mathcal{H}_k = \int_p \alpha_k \mathrm{d}x \qquad k = 1, 2, ..., \tag{6.34}$$

where the terms α_k are defined in Section 3.2 and the path p is over a fundamental period or over the infinite line. We also note that

$$\alpha_k \mathbb{I}_2 = i \left\{ L_0, L_k \right\}, \tag{6.35}$$

where the brackets denote the matrix anti-commutator. Applying the action $\Omega^{-1} \circ \Omega$ this becomes

$$\alpha_k \mathbb{I}_2 = -\frac{i}{4} \left\{ \mathbf{T} \cdot \boldsymbol{\sigma}, \mathbf{U}_k \cdot \boldsymbol{\sigma} \right\} = -\frac{i}{2} \mathbf{T} \cdot \mathbf{U}_k \mathbb{I}_2. \tag{6.36}$$

Therefore the conserved densities of the HF hierarchy may be written as

$$\mathcal{J}_k = \frac{1}{k-1} \int_p \mathbf{T} \cdot \mathbf{U}_k \mathrm{d}x \tag{6.37}$$

where the factor of $1/(k-1)$ neatens the forms of the corresponding flows. This gives the first two densities

$$\begin{aligned} \mathcal{J}_2 &= \int_p \mathbf{T} \cdot \mathbf{U}_2 \mathrm{d}x = -\frac{1}{2} \int_p \mathbf{T}_x \cdot \mathbf{T}_x \mathrm{d}x, \\ \mathcal{J}_3 &= \frac{1}{2} \int_p \mathbf{T} \cdot \mathbf{U}_3 \mathrm{d}x = \frac{1}{2} \int_p \mathbf{T} \cdot (\mathbf{T}_x \times \mathbf{T}_{xx}) \mathrm{d}x, \end{aligned} \tag{6.38}$$

whose integrands we note are the curvature and torsion of the HF equation. From these the flows may be found in the following Hamiltonian forms:

$$\begin{aligned} \mathbf{T}_{t_2} &= \mathbf{T} \times \frac{\delta \mathcal{J}_2}{\delta \mathbf{T}}, \\ \mathbf{T}_{t_3} &= \mathbf{T} \times \frac{\delta \mathcal{J}_3}{\delta \mathbf{T}} \end{aligned} \tag{6.39}$$

with skew-symmetric Hamiltonian operator $\mathbf{T}\times$.

An alternative approach to reducing the HF equation to a scalar PDE is pursued by Mikhailov and Shabat. In [MS86] they refer to earlier work where they considered inte-

grable equations of the form

$$u_t = a(u, \overline{u})u_{xx} + f(u, \overline{u}, u_x, \overline{u}_x).$$

As part of this work they note that if we map $\mathbf{S}$ stereographically:

$$\begin{aligned} S_1 + iS_2 &= 2u/(1 + u\overline{u}), \\ S_3 &= (1 - u\overline{u})/(1 + u\overline{u}), \end{aligned} \tag{6.40}$$

we form the equation

$$iu_t + u_{xx} - 2\frac{\overline{u}u_x^2}{1 + u\overline{u}} = 0. \tag{6.41}$$

We do not pursue this further but will briefly refer to it in the next section. The interested reader can find a full account of this area of research in Mikhailov and Shabat's two papers [MS85/6].

6.2 Stokes vector evolution

By mapping solutions to the VNLS onto a Stokes vector representing the polarisation state of the solution, it is possible to investigate the interaction and evolution of the polarisation state on the unit Poincaré sphere. Previous work has focussed on the interaction of colliding soliton pulses using Manakov's results - see for example [MGH95], [Sil99]. In this section, we will investigate the polarisation state evolution of a general solution to the VNLS.

Following Baker et al. [BEG00], define variables

$$S_i = \frac{\boldsymbol{q}^\dagger \sigma_i \boldsymbol{q}}{\boldsymbol{q}^\dagger \boldsymbol{q}} \qquad i = 1, 2, 3, \tag{6.42}$$

the components of the Stokes vector $\mathbf{S} = (S_1, S_2, S_3)^\mathsf{T}$ where $\boldsymbol{q}$ is a solution to the VNLS (1.1). Henceforth we shall adopt the notation

$$\mathbf{S} = \frac{\boldsymbol{q}^\dagger \boldsymbol{\sigma} \boldsymbol{q}}{\boldsymbol{q}^\dagger \boldsymbol{q}} \tag{6.43}$$

to encapsulate all three of equations (6.42).

As a point of passing interest, we also note that the mapping from the VNLS to the

polarisation state (6.42) is actually the following stereographic mapping:

$$S_1 + iS_2 = 2\left(\frac{q_2}{q_1}\right)\Big/\left(1+\frac{q_2}{q_1}\frac{\overline{q_2}}{\overline{q_1}}\right), \qquad S_3 = \left(1-\frac{q_2}{q_1}\frac{\overline{q_2}}{\overline{q_1}}\right)\Big/\left(1+\frac{q_2}{q_1}\frac{\overline{q_2}}{\overline{q_1}}\right); \tag{6.44}$$

that is (6.40) with $u = q_2/q_1$.

Assume the following, general form for the components of $\boldsymbol{q}$:

$$\begin{aligned} q_1(x,t) &= |\boldsymbol{q}(x,t)| \cos\left(\frac{\theta(x,t)}{2}\right) \exp\left(i\phi_1(x,t)\right), \\ q_2(x,t) &= |\boldsymbol{q}(x,t)| \sin\left(\frac{\theta(x,t)}{2}\right) \exp\left(i\phi_2(x,t)\right), \end{aligned} \tag{6.45}$$

where $\phi_1(x,t)$, $\phi_2(x,t)$ and $\theta(x,t)$ are real functions. The Stokes vector components are then calculated as:

$$\begin{aligned} S_1 &= \sin\theta\cos\phi, \\ S_2 &= \sin\theta\sin\phi, \\ S_3 &= \cos\theta \end{aligned} \tag{6.46}$$

where $\phi(x,t) = \phi_2(x,t) - \phi_1(x,t)$. It is clear from these forms that the Stokes vector lies on the unit sphere $\mathbf{S}\cdot\mathbf{S} = 1$. Defining the vector

$$\boldsymbol{\xi} = \begin{pmatrix} \xi_1 \\ \xi_2 \\ \xi_3 \end{pmatrix} = \begin{pmatrix} -\theta_x \sin\phi \\ \theta_x \cos\phi \\ \phi_x \end{pmatrix} \tag{6.47}$$

we find the following succinct expressions for the vectors $\boldsymbol{q}_x$ and $\boldsymbol{q}_x^\dagger$:

$$\begin{aligned} \boldsymbol{q}_x &= \left(\frac{|\boldsymbol{q}|_x}{|\boldsymbol{q}|} - \frac{i}{2}\boldsymbol{\xi}\cdot\boldsymbol{\sigma} - \frac{i}{2}\psi_x\right)\boldsymbol{q}, \\ \boldsymbol{q}_x^\dagger &= \boldsymbol{q}^\dagger\left(\frac{|\boldsymbol{q}|_x}{|\boldsymbol{q}|} + \frac{i}{2}\boldsymbol{\xi}\cdot\boldsymbol{\sigma} + \frac{i}{2}\psi_x\right) \end{aligned} \tag{6.48}$$

where $\psi(x,t) = -\big(\phi_1(x,t) + \phi_2(x,t)\big)$ and $\boldsymbol{\xi}\cdot\boldsymbol{\sigma} = \sum_{i=1}^3 \xi_i\sigma_i$. We now state the following formulae which will be used to calculate evolution equations for the Stokes vector:

$$\begin{aligned} \frac{\boldsymbol{q}_x^\dagger\boldsymbol{q} - \boldsymbol{q}^\dagger\boldsymbol{q}_x}{\boldsymbol{q}^\dagger\boldsymbol{q}} &= i\left(\boldsymbol{\xi}\cdot\mathbf{S} + \psi_x\right), \\ \frac{\boldsymbol{q}_x^\dagger\boldsymbol{\sigma}\boldsymbol{q} + \boldsymbol{q}^\dagger\boldsymbol{\sigma}\boldsymbol{q}_x}{\boldsymbol{q}^\dagger\boldsymbol{q}} &= \left(\ln|\boldsymbol{q}|^2\right)_x\mathbf{S} + \left(\boldsymbol{\xi}\times\mathbf{S}\right), \\ \frac{\boldsymbol{q}_x^\dagger\boldsymbol{\sigma}\boldsymbol{q} - \boldsymbol{q}^\dagger\boldsymbol{\sigma}\boldsymbol{q}_x}{\boldsymbol{q}^\dagger\boldsymbol{q}} &= i\left(\boldsymbol{\xi} + \psi_x\mathbf{S}\right). \end{aligned} \tag{6.49}$$

The change of $\mathbf{S}$ with x is then found to be:

$$\begin{aligned}\mathbf{S}_x &= \frac{\left(\boldsymbol{q}^\dagger\boldsymbol{\sigma}\boldsymbol{q}\right)_x}{\boldsymbol{q}^\dagger\boldsymbol{q}} - \left(\ln|\boldsymbol{q}|^2\right)_x\mathbf{S} \\ &= \left(\ln|\boldsymbol{q}|^2\right)_x\mathbf{S} + \boldsymbol{\xi}\times\mathbf{S} - \left(\ln|\boldsymbol{q}|^2\right)_x\mathbf{S} \\ &= \boldsymbol{\xi}\times\mathbf{S}. \end{aligned} \tag{6.50}$$

From equations (1.1) and (6.49) the relations

$$\begin{aligned}\left(\ln|\boldsymbol{q}|^2\right)_t &= -i\frac{\left(\boldsymbol{q}_x^\dagger\boldsymbol{q} - \boldsymbol{q}^\dagger\boldsymbol{q}_x\right)_x}{\boldsymbol{q}^\dagger\boldsymbol{q}} \\ &= \left(\boldsymbol{\xi}\cdot\mathbf{S} + \psi_x\right)_x + \left(\ln|\boldsymbol{q}|^2\right)_x\left(\boldsymbol{\xi}\cdot\mathbf{S} + \psi_x\right)\end{aligned}$$

and

$$\begin{aligned}\frac{\left(\boldsymbol{q}^\dagger\boldsymbol{\sigma}\boldsymbol{q}\right)_t}{\boldsymbol{q}^\dagger\boldsymbol{q}} &= -i\frac{\left(\boldsymbol{q}_x^\dagger\boldsymbol{\sigma}\boldsymbol{q} - \boldsymbol{q}^\dagger\boldsymbol{\sigma}\boldsymbol{q}_x\right)_x}{\boldsymbol{q}^\dagger\boldsymbol{q}} \\ &= \left(\boldsymbol{\xi} + \psi_x\mathbf{S}\right)_x + \left(\ln|\boldsymbol{q}|^2\right)_x\left(\boldsymbol{\xi} + \psi_x\mathbf{S}\right)\end{aligned}$$

may be derived which are used to calculate $\mathbf{S}_t$:

$$\begin{aligned}\mathbf{S}_t &= \frac{\left(\boldsymbol{q}^\dagger\boldsymbol{\sigma}\boldsymbol{q}\right)_t}{\boldsymbol{q}^\dagger\boldsymbol{q}} - \left(\ln|\boldsymbol{q}|^2\right)_t\mathbf{S} \\ &= \left(\boldsymbol{\xi} + \psi_x\mathbf{S}\right)_x + \left(\ln|\boldsymbol{q}|^2\right)_x\left(\boldsymbol{\xi} + \psi_x\mathbf{S}\right) - \left(\boldsymbol{\xi}\cdot\mathbf{S} + \psi_x\right)_x\mathbf{S} - \left(\ln|\boldsymbol{q}|^2\right)_x\left(\boldsymbol{\xi}\cdot\mathbf{S} + \psi_x\right)\mathbf{S} \\ &= \boldsymbol{\xi}_x + \left(\ln|\boldsymbol{q}|^2\right)_x\boldsymbol{\xi} + \psi_x\mathbf{S}_x - \left(\boldsymbol{\xi}_x\cdot\mathbf{S}\right)\mathbf{S} - \left(\boldsymbol{\xi}\cdot\mathbf{S}_x\right)\mathbf{S} - \left(\ln|\boldsymbol{q}|^2\right)_x\left(\boldsymbol{\xi}\cdot\mathbf{S}\right)\mathbf{S}.\end{aligned}$$

Applying (6.50) it is clear $\boldsymbol{\xi}\cdot\mathbf{S}_x = 0$ which also means $\mathbf{S}_t$ may be written

$$\mathbf{S}_t = \boldsymbol{\xi}_x\left(\mathbf{S}\cdot\mathbf{S}\right) - \mathbf{S}\left(\boldsymbol{\xi}_x\cdot\mathbf{S}\right) + \left(\ln|\boldsymbol{q}|^2\right)_x\left\{\left(\boldsymbol{\xi}\left(\mathbf{S}\cdot\mathbf{S}\right) - \mathbf{S}\left(\boldsymbol{\xi}\cdot\mathbf{S}\right)\right\} + \psi_x\mathbf{S}_x.$$

Applying the vector identity

$$\boldsymbol{a}\times(\boldsymbol{b}\times\boldsymbol{c}) = \boldsymbol{b}(\boldsymbol{a}\cdot\boldsymbol{c}) - \boldsymbol{c}(\boldsymbol{a}\cdot\boldsymbol{b})$$

this becomes

$$\begin{aligned}\mathbf{S}_t &= \mathbf{S}\times(\boldsymbol{\xi}_x\times\mathbf{S}) + \left(\ln|\boldsymbol{q}|^2\right)_x\left(\mathbf{S}\times(\boldsymbol{\xi}\times\mathbf{S})\right) + \psi_x\mathbf{S}_x \\ &= \mathbf{S}\times(\boldsymbol{\xi}_x\times\mathbf{S}) + \left(\ln|\boldsymbol{q}|^2\right)_x\left(\mathbf{S}\times\mathbf{S}_x\right) + \psi_x\mathbf{S}_x\end{aligned}$$

and noting

$$\begin{aligned}\mathbf{S}\times\mathbf{S}_{xx} &= \mathbf{S}\times(\boldsymbol{\xi}_x\times\mathbf{S})+\mathbf{S}\times(\boldsymbol{\xi}\times\mathbf{S}_x)\\ &= \mathbf{S}\times(\boldsymbol{\xi}_x\times\mathbf{S})+(\boldsymbol{\xi}\cdot\mathbf{S})(\mathbf{S}\times\boldsymbol{\xi})-(\boldsymbol{\xi}\cdot\boldsymbol{\xi})(\mathbf{S}\times\mathbf{S})\\ &= \mathbf{S}\times(\boldsymbol{\xi}_x\times\mathbf{S})-(\boldsymbol{\xi}\cdot\mathbf{S})\mathbf{S}_x\end{aligned}$$

we finally arrive at

$$\mathbf{S}_t = \mathbf{S}\times\mathbf{S}_{xx}+\left(\ln|\boldsymbol{q}|^2\right)_x(\mathbf{S}\times\mathbf{S}_x)+(\boldsymbol{\xi}\cdot\mathbf{S}+\psi_x)\,\mathbf{S}_x. \tag{6.51}$$

We now take a closer look at the term $\boldsymbol{\xi}\cdot\mathbf{S}+\psi_x$. Having stated all equations up to this point in terms of the standard basis, $\boldsymbol{i}=(1,0,0)^\mathsf{T}$, $\boldsymbol{j}=(0,1,0)^\mathsf{T}$ and $\boldsymbol{k}=(0,0,1)^\mathsf{T}$, we consider an alternative basis in Eulerian coordinates. This is found by performing the following operations: A rotation of angle ϕ about $\boldsymbol{k}$ to give

$$\begin{aligned}\boldsymbol{e}_1'' &= \cos\phi\boldsymbol{i}+\sin\phi\boldsymbol{j},\\ \boldsymbol{e}_2'' &= -\sin\phi\boldsymbol{i}+\cos\phi\boldsymbol{j},\\ \boldsymbol{e}_3'' &= \boldsymbol{k}\end{aligned}$$

followed by a rotation of angle θ about $\boldsymbol{e}_2''$:

$$\begin{aligned}\boldsymbol{e}_1' &= \cos\theta\boldsymbol{e}_1''-\sin\theta\boldsymbol{e}_3'',\\ \boldsymbol{e}_2' &= \boldsymbol{e}_2'',\\ \boldsymbol{e}_3' &= \sin\theta\boldsymbol{e}_1''+\cos\theta\boldsymbol{e}_3''\end{aligned}$$

and finally a rotation of angle ψ about $\boldsymbol{e}_3'$:

$$\begin{aligned}\boldsymbol{e}_1 &= \cos\psi\boldsymbol{e}_1'+\sin\psi\boldsymbol{e}_2',\\ \boldsymbol{e}_2 &= -\sin\psi\boldsymbol{e}_1'+\cos\psi\boldsymbol{e}_2',\\ \boldsymbol{e}_3 &= \boldsymbol{e}_3'.\end{aligned}$$

We then calculate $\mathbf{S}$ and $\boldsymbol{\xi}$, in the orthonormal basis $\boldsymbol{e}_i$ for $i=1,2,3$, as simply $\mathbf{S}=\boldsymbol{e}_3$ and

$$\boldsymbol{\xi} = (\theta_x\sin\psi-\phi_x\sin\theta\cos\psi)\,\boldsymbol{e}_1+(\theta_x\cos\psi+\phi_x\sin\theta\sin\psi)\,\boldsymbol{e}_2+\phi_x\cos\theta\boldsymbol{e}_3.$$

The angular momentum vector relative to the change of basis is given by

$$\begin{aligned}\boldsymbol{\omega} &= \phi_x\boldsymbol{k}+\theta_x\boldsymbol{e}_2''+\psi_x\boldsymbol{e}_3'\\ &= \boldsymbol{\xi}+\psi_x\boldsymbol{e}_3,\end{aligned} \tag{6.52}$$

see Kibble [Kib73]. Therefore

$$\begin{aligned}\boldsymbol{\xi}\times\mathbf{S}&=\boldsymbol{\omega}\times\mathbf{S}\\ \boldsymbol{\xi}\cdot\mathbf{S}+\psi_x&=(\boldsymbol{\xi}+\psi_x\mathbf{S})\cdot\mathbf{S}=\boldsymbol{\omega}\cdot\mathbf{S}\end{aligned}$$

and equations (6.50) and (6.51) become

$$\mathbf{S}_x = \boldsymbol{\omega}\times\mathbf{S}, \tag{6.53}$$

$$\mathbf{S}_t = \mathbf{S}\times\mathbf{S}_{xx}+\left(\ln|\boldsymbol{q}|^2\right)_x(\mathbf{S}\times\mathbf{S}_x)+(\boldsymbol{\omega}\cdot\mathbf{S})\,\mathbf{S}_x. \tag{6.54}$$

From these, the following continuity equation may also be derived:

$$\left(|\boldsymbol{q}|^2\mathbf{S}\right)_t-\left(|\boldsymbol{q}|^2\boldsymbol{\omega}\right)_x=0. \tag{6.55}$$

6.3 A degenerative example of the Stokes vector evolution

We now ponder under which circumstances equation (6.54) may be reduced to the Heisenberg ferromagnet equation.

As in Section 6.1, consider the Stokes vector $\mathbf{S}(x,t)$ to be a unit tangent vector to some curve. To distinguish calculations in this section from those in Section 6.1 we set $\mathbf{S}(x,t)=\widehat{\mathbf{T}}(x,t)$ and select orthonormal vectors: $\widehat{\mathbf{N}}=\widehat{\kappa}^{-1}\widehat{\mathbf{T}}_x$, $\widehat{\mathbf{B}}=\widehat{\mathbf{T}}\times\widehat{\mathbf{N}}$. These satisfy the analogous versions of the Serret-Frenet equations (6.4) and in this case the curvature $\widehat{\kappa}(x,t)$ is equal to $|\boldsymbol{\omega}\times\widehat{\mathbf{T}}|$ according to (6.53) and the torsion is, as before, given by

$$\widehat{\tau}(x,t)=\widehat{\kappa}^{-2}\widehat{\mathbf{T}}\cdot(\widehat{\mathbf{T}}_x\times\widehat{\mathbf{T}}_{xx}). \tag{6.56}$$

Applying (6.54), the t derivatives of the orthonormal vectors are found to be

$$\begin{aligned}\widehat{\mathbf{T}}_t&=\quad\alpha\widehat{\mathbf{N}}+\beta\widehat{\mathbf{B}},\\ \widehat{\mathbf{N}}_t&=-\alpha\widehat{\mathbf{T}}+\frac{1}{\kappa}(\beta_x+\tau\alpha)\widehat{\mathbf{B}},\\ \widehat{\mathbf{B}}_t&=-\beta\widehat{\mathbf{T}}-\frac{1}{\kappa}(\beta_x+\tau\alpha)\widehat{\mathbf{B}}\end{aligned} \tag{6.57}$$

where $\alpha=\widehat{\kappa}(\boldsymbol{\omega}\cdot\widehat{\mathbf{T}}-\widehat{\tau})$ and $\beta=\widehat{\kappa}_x+\widehat{\kappa}\left(\ln|\boldsymbol{q}|^2\right)_x$. From the consistency conditions $\widehat{\mathbf{T}}_{xt}=\widehat{\mathbf{T}}_{tx}$ and $\widehat{\mathbf{N}}_{xt}=\widehat{\mathbf{N}}_{tx}$ we deduce

$$\begin{aligned}\widehat{\kappa}_t&=\alpha_x-\widehat{\tau}\beta,\\ \widehat{\tau}_t&=\widehat{\kappa}\beta+\left\{\frac{1}{\widehat{\kappa}}(\beta_x+\widehat{\tau}\alpha)\right\}_x.\end{aligned} \tag{6.58}$$

Notice that if we set $|\boldsymbol{q}(x,t)| = \widehat{\kappa}(x,t)$ and $\phi_1(x,t) = \phi_2(x,t) = \int^x \widehat{\tau}(x',t)\mathrm{d}x'$ then $\boldsymbol{\omega}\cdot\widehat{\mathbf{T}} = -2\widehat{\tau}(x,t)$ and equations (6.58) become

$$\begin{aligned} \widehat{\kappa}_t &= -6\widehat{\kappa}_x\widehat{\tau} - 3\widehat{\kappa}\widehat{\tau}_x, \\ \widehat{\tau}_t &= 3\left(\frac{\widehat{\kappa}_{xx}}{\widehat{\kappa}} - \widehat{\tau}^2\right)_x + 3\widehat{\kappa}\widehat{\kappa}_x \end{aligned} \tag{6.59}$$

which, with the rescaling of the time variable $t \to 3t$, become the SNLS curvature-torsion equations (6.9) and (6.10). The same result is also obtained by setting $\theta(x,t) \equiv 0$ which reduces the VNLS to the SNLS directly, that is

$$\boldsymbol{q}(x,t) = (q_1, q_2)^{\mathsf{T}} \to (|\boldsymbol{q}(x,t)|\exp(i\phi_1(x,t)), 0)^{\mathsf{T}}$$

with $q_1(x,t)$ satisfying the SNLS.

In the special case $\boldsymbol{\omega} = |\boldsymbol{\omega}|\widehat{\mathbf{B}}$, we have

$$\widehat{\kappa} = |\boldsymbol{\omega}|, \qquad \widehat{\tau} = |\boldsymbol{\omega}|^{-2}\widehat{\mathbf{T}}\cdot(\widehat{\mathbf{T}}_x \times \widehat{\mathbf{T}}_{xx}) = -|\boldsymbol{\omega}|^{-2}\boldsymbol{\omega}_x\cdot\widehat{\mathbf{T}}_x. \tag{6.60}$$

This choice of $\boldsymbol{\omega}$ means

$$\begin{aligned} 0 &= \boldsymbol{\omega}\cdot\widehat{\mathbf{T}} \\ &= \phi_x\cos\theta + \psi_x \\ &= -2\left(\phi_{1,x}\cos^2\left(\frac{\theta}{2}\right) + \phi_{2,x}\sin^2\left(\frac{\theta}{2}\right)\right) \end{aligned}$$

and hence that

$$\phi_{1,x}\cos^2\left(\frac{\theta}{2}\right) = -\phi_{2,x}\sin^2\left(\frac{\theta}{2}\right). \tag{6.61}$$

This also means that $|\boldsymbol{q}(x,t)|$ is independent of t and if we further require that it is independent of x then equation (6.54) reduces to the HF equation. Therefore the function

$$q(x,t) = \frac{1}{2}\widehat{\kappa}(x,t)\exp\left(i\int^x \widehat{\tau}(x',t)\mathrm{d}x'\right) \tag{6.62}$$

satisfies the attractive SNLS. To get some idea of the solutions that satisfy these conditions

we look to the separable ansatz considered in [CEE00]. The particular ansatz

$$\begin{aligned} q_1(x,t) &= |\boldsymbol{q}| \cos\left(\frac{\theta(x)}{2}\right) \exp\left(ia_1 t - i\frac{C}{|\boldsymbol{q}|^2}\int^x \frac{\mathrm{d}x'}{\cos^2\left(\frac{\theta(x')}{2}\right)}\right), \\ q_2(x,t) &= |\boldsymbol{q}| \sin\left(\frac{\theta(x)}{2}\right) \exp\left(ia_2 t + i\frac{C}{|\boldsymbol{q}|^2}\int^x \frac{\mathrm{d}x'}{\sin^2\left(\frac{\theta(x')}{2}\right)}\right) \end{aligned} \tag{6.63}$$

satisfies the conditions required above.

6.4 Gauge transformation of the Heisenberg ferromagnet equation

Equation (6.54) appears to be a perturbed form of the Heisenberg ferromagnet equation. By introducing a gauge transformation of (6.1) we attempt to move to a rotating frame where (6.54) is the relevant equation and thereby link the equation governing the polarisation state of solutions of the VNLS to an equation with gauge equivalence to the SNLS.

Consider a general unitary matrix,

$$\Omega(x,t) = \exp\left(i\boldsymbol{a}(x,t)\cdot\boldsymbol{\sigma}\right), \tag{6.64}$$

independent of z with $\boldsymbol{a}(x,t) \in \mathbb{R}^3$, and apply it as a gauge transformation to the Heisenberg ferromagnet scattering problem, (6.12), to give transformed zero-curvature representations

$$\widetilde{U}(x,t,z) = \frac{iz}{2}\mathbf{S}\cdot\boldsymbol{\sigma} + i\boldsymbol{\Omega}^{(x)}\cdot\boldsymbol{\sigma}, \tag{6.65}$$

$$\begin{aligned} \widetilde{V}(x,t,z) = {} & \frac{iz^2}{2}\mathbf{S}\cdot\boldsymbol{\sigma} + \frac{z}{2}\mathbf{S}\cdot\boldsymbol{\sigma}\,\mathbf{S}_x\cdot\boldsymbol{\sigma} \\ & + i\mathbf{S}\cdot\boldsymbol{\sigma}\left[\mathbf{S}\cdot\boldsymbol{\sigma}, \boldsymbol{\Omega}^{(x)}\right] + i\boldsymbol{\Omega}^{(t)}\cdot\boldsymbol{\sigma}. \end{aligned} \tag{6.66}$$

Here, $\mathbf{S} = \Omega\mathbf{T}\Omega^{-1}$, $i\boldsymbol{\Omega}^{(x)}\cdot\boldsymbol{\sigma} = \Omega_x\Omega^{-1}$ and $i\boldsymbol{\Omega}^{(t)}\cdot\boldsymbol{\sigma} = \Omega_t\Omega^{-1}$ with

$$\boldsymbol{\Omega}^{(x)} = \boldsymbol{a}_x - h(a)\widehat{\boldsymbol{a}}_x + \frac{1}{2}\frac{\mathrm{d}h}{\mathrm{d}a}(\widehat{\boldsymbol{a}}_x\times\widehat{\boldsymbol{a}}) \tag{6.67}$$

where $a = |\boldsymbol{a}|$ and $\widehat{\boldsymbol{a}} = \boldsymbol{a}/a$, $h(a) = a - \frac{1}{2}\sin 2a$. The analogous formula with ∂_t replacing

∂_x holds for $\mathbf{\Omega}^{(t)}$. The zero-curvature equation, $\widetilde{U}_t - \widetilde{V}_x + \left[\widetilde{U}, \widetilde{V}\right] = 0$, then yields

$$\begin{aligned}\mathbf{S}_t = \mathbf{S} \times \mathbf{S}_{xx} + 2\mathbf{\Omega}_x^{(x)} - 2(\mathbf{\Omega}_x^{(x)} \cdot \mathbf{S})\mathbf{S} \\ - 4(\mathbf{\Omega}^{(x)} \cdot \mathbf{S}) \left(\mathbf{S}_x + \mathbf{\Omega}^{(x)} \times \mathbf{S}\right) - 2\mathbf{\Omega}^{(t)} \times \mathbf{S}\end{aligned} \tag{6.68}$$

at order z with order z^0, z^2 and z^3 terms all vanishing. The question of interest is now whether we can find a choice of $\boldsymbol{a}$ such that equations (6.68) and (6.54) are identical. The choices

$$\begin{aligned}\mathbf{\Omega}^{(x)} &= \mathbf{S} \times \mathbf{S}_x, \\ \mathbf{\Omega}^{(t)} &= \mathbf{S}\end{aligned} \tag{6.69}$$

reduce (6.68) to

$$\mathbf{S}_t = \mathbf{S} \times \mathbf{S}_{xx} + (\ln \widetilde{\kappa}^2)_x \mathbf{S} \times \mathbf{S}_x - 2\widetilde{\tau}\mathbf{S}_x \tag{6.70}$$

where $\widetilde{\kappa}^2 = \mathbf{S}_x \cdot \mathbf{S}_x$ and $\widetilde{\kappa}^2\widetilde{\tau} = \mathbf{S} \cdot (\mathbf{S}_x \times \mathbf{S}_{xx})$. Here $\widetilde{\kappa}$ and $\widetilde{\tau}$, as defined, are the curvature and torsion of the solution curve in the transformed frame of reference. The conditions (6.69) mean the Serret-Frenet equations are in the canonical form (6.4) but with κ and τ replaced by $\widetilde{\kappa} = \kappa/3$ and $\widetilde{\tau} = \tau$. Imposing the conditions

$$\begin{aligned}\widetilde{\kappa}(x,t) &= \frac{2}{3}\,|\boldsymbol{q}(x,t)| \\ \widetilde{\tau}(x,t) &= -\frac{1}{2}\,\boldsymbol{\omega} \cdot \mathbf{S}\end{aligned} \tag{6.71}$$

means equation (6.70) becomes the required (6.54).

The remaining step, which we do not pursue here, is the inversion of (6.67) and the analogous version for $\mathbf{\Omega}^{(t)}$ to give the required statement for $\boldsymbol{a}(x,t)$.

In the special case where $\theta(x,t) \equiv 0$, we have $q_2(x,t) \equiv 0$ and the VNLS reduces trivially to the SNLS. In this instance $\mathbf{S} = (0,0,1)^{\mathsf{T}}$ and

$$\begin{aligned}\kappa(x,t) &= 2|\boldsymbol{q}(x,t)| = 2|q_1(x,t)|, \\ \tau(x,t) &= -\frac{1}{2}\,\boldsymbol{\omega} \cdot \mathbf{S} = \phi_{1,x}(x,t)\end{aligned}$$

meaning $q_1(x,t) = \frac{1}{2}\kappa(x,t)\exp\left(i\int^x \tau(x',t)\mathrm{d}x'\right)$, the required form for $q(x,t)$ in (6.2).

Chapter 7

Conclusions

The main thrust of this thesis has been directed towards the study of finite gap solutions to the vector nonlinear Schrödinger equation. Previous work has concentrated upon soliton solutions which may be derived using inverse scattering transform methods or Hirota's method, as was discussed. Finite gap solutions have not received as much appraisal, often because the methods used in solving the scalar version of the equation were not readily adapted to the vector equation. The algebrogeometric approach, conceived in the late 70s, is a powerful exception which we have applied to the vector equation to yield quasiperiodic solutions in terms of ratios of Riemann theta functions.

The starting point for this technique is the Lax pair first introduced by Manakov [Man74]. For finite gap solutions, a salient feature is the fact that the algebraic spectral curve is, in general, a trigonal Riemann surface and not hyperelliptic as in the scalar case. An analysis of the VNLS hierarchy revealed recursive links between components of the matrix coefficients of the Lax pair and determined the form of the trigonal curve: this is discussed in Chapter 4 and results have been published in Physica D [WE07].

In Chapter 5, we reported a birational map which linked the trigonal curve in the genus two case with a hyperelliptic curve. We showed that the latter was exactly the curve reported by Christiansen et al. [CEE00] using a very different approach and that the corresponding finite gap solutions were the same. These results have been published in the Journal of Physics A: Mathematical and Theoretical [WWE07].

The link between the Heisenberg ferromagnet and attractive scalar nonlinear Schrödinger equations was first illustrated by Lakshmanan [Lak77]. Their gauge equivalence was demonstrated by Zakharov and Takhtadzhyan [ZT79] and the set of possible integrable deformations to the HF equation was considered by Zhang and Yang [ZY90], who stated its likely gauge equivalence to the attractive SNLS hierarchy. We have demonstrated that

the HF hierarchy may be generated via a recurrence relation which can also be used to express the gauge equivalence of the HF and attractive SNLS hierarchies explicitly at every level. Also, via a mapping to Stokes' vectors on the Poincaré sphere, the VNLS maps to a modified version of the HF equation. We have considered possible degenerations of this equation to the HF equation and the corresponding solutions. Results from this work are to be submitted for publication.

Future Work

Soliton solutions can in some sense be considered the infinite period limit of finite gap solutions. We have explored how finite gap solutions to the scalar problem degenerate to soliton solutions in appropriate spectral limits. This approach, we believe, could be applied to solutions to the vector equation although the process is complicated by the three-sheeted covering of the spectral curve which naturally arises from the algebra. The question of how branch cuts connecting differing Riemann surface sheets may be 'pinched' is still unanswered and remains a subject of interest.

In comparing the approaches of Elgin et al. [EEI07] and Christiansen et al. [CEE00] we have introduced an algebraic curve of genus two with corresponding solutions. Elgin et al. derive only solutions of odd genus but we believe that solutions of any even genus may be found by the addition of integration constants to higher order elements of the VNLS hierarchy, as demonstrated in the genus two case.

On a more practical level, the use of finite gap solutions in optical communication systems has yet to be demonstrated but, given that solitons were not originally used as the default transmission pulse but now account for channel capacities in the order of terabits per second, there is certainly potential for their useful application.

Appendix A

Proofs of selected results

Theorem 2.7

Part (i) is proved by writing the reduced characteristic as

$$\begin{bmatrix} \widehat{\boldsymbol{\varepsilon}'}^{\mathsf{T}} \\ \widehat{\boldsymbol{\varepsilon}''}^{\mathsf{T}} \end{bmatrix} = \begin{bmatrix} \boldsymbol{\varepsilon}'^{\mathsf{T}} + 2\boldsymbol{\nu}'^{\mathsf{T}} \\ \boldsymbol{\varepsilon}''^{\mathsf{T}} + 2\boldsymbol{\nu}''^{\mathsf{T}} \end{bmatrix}$$

where $\boldsymbol{\nu}'$ and $\boldsymbol{\nu}''$ are some integer g-vectors and then evaluating the characters on left and right-hand sides.

Part (ii) may be proved by induction on g having reduced the characteristics in light of part (i). For $g = 1$ there are 1 odd and 3 even characteristics so the formulae hold. Take a g-characteristic and add on elements to create a $(g+1)$-characteristic. Each odd g-characteristic produces 1 even and 3 odd $(g+1)$-characteristics and similarly each even g-characteristic produces 1 odd and 3 even $(g+1)$-characteristics. Thus, assuming the induction hypothesis stated in the theorem, the number of odd $(g+1)$-characteristics is $3\times 2^{g-1}(2^g-1)+2^{g-1}(2^g+1) = 2^g(2^{g+1}-1)$ and the number of even $(g+1)$-characteristics is $3 \times 2^{g-1}(2^g+1) + 2^{g-1}(2^g-1) = 2^g(2^{g+1}+1)$. These are the required forms.

Theorem 2.11

Choosing a homology basis such that no zeros of $F(P)$ lie on any cycle and the cycles all intersect in one point $P^{(I)} \in X$, a canonical dissection of the Riemann surface, X, may be performed, see Subsection 2.1.2. Integrating any differential $\mathrm{d}\phi$ around the boundary,

$\partial\widetilde{X}$, of the canonical dissection gives

$$\begin{aligned}\int_{\partial\widetilde{X}} \mathrm{d}\phi &= \sum_{i=1}^{g}\left(\int_{a_i^+}\mathrm{d}\phi + \int_{b_i^+}\mathrm{d}\phi - \int_{a_i^-}\mathrm{d}\phi - \int_{b_i^-}\mathrm{d}\phi\right)\\ &= \sum_{i=1}^{g}\left(\int_{a_i}(\mathrm{d}\phi^+ - \mathrm{d}\phi^-) + \int_{b_i}(\mathrm{d}\phi^+ - \mathrm{d}\phi^-)\right)\end{aligned}$$

where $\mathrm{d}\phi^{\pm}$ represent $\mathrm{d}\phi$ evaluated on the relevant side of the $4g$-gon, $\partial\widetilde{X}$.

By setting $\mathrm{d}\phi = \mathrm{d}\ln F$, for the integral around cycle a_i,

$$\mathrm{d}\phi^+ - \mathrm{d}\phi^- = \mathrm{d}\ln\left\{\frac{\theta[\varepsilon]\left(\int_{P_0}^{P}\mathrm{d}\boldsymbol{\omega} - \boldsymbol{e}, B\right)}{\theta[\varepsilon]\left(\int_{P_0}^{P}\mathrm{d}\boldsymbol{\omega} - \boldsymbol{e} + B\boldsymbol{e}_i, B\right)}\right\} = \mathrm{d}\omega_i(P)$$

using the $4g$-gon extension of Figure 2.4 and Property 2.1. Similarly, around cycle b_i,

$$\mathrm{d}\phi^+ - \mathrm{d}\phi^- = \mathrm{d}\ln\left\{\frac{\theta[\varepsilon]\left(\int_{P_0}^{P}\mathrm{d}\boldsymbol{\omega} - \boldsymbol{e}, B\right)}{\theta[\varepsilon]\left(\int_{P_0}^{P}\mathrm{d}\boldsymbol{\omega} - \boldsymbol{e} + 2\pi i\boldsymbol{e}_i, B\right)}\right\} = 0.$$

Thus

$$\int_{\partial\widetilde{X}}\mathrm{d}\ln F = 2\pi i g$$

but also, by Cauchy's residue theorem, it may be seen

$$\int_{\partial\widetilde{X}}\mathrm{d}\ln F = 2\pi i n,$$

where n is the number of zeros of F. Hence F has g zeros.

If the same procedure is performed but with $\mathrm{d}\phi = \omega_j\,\mathrm{d}\ln F$, where $\omega_j = \int_{P_0}^{P}\mathrm{d}\omega_j$, then on a_i,

$$\begin{aligned}\mathrm{d}\phi^+ - \mathrm{d}\phi^- &= \omega_j^+\mathrm{d}\ln F^+ - \omega_j^-\mathrm{d}\ln F^-\\ &= \omega_j^+\left\{\mathrm{d}\ln F^- + \mathrm{d}\omega_i\right\} - \omega_j^-\mathrm{d}\ln F^-\\ &= -\mathrm{d}\ln F^-\int_{b_i}\mathrm{d}\omega_j + \omega_j^+\mathrm{d}\omega_i\\ &= -B_{ji}\mathrm{d}\ln F^- + \omega_j^+\mathrm{d}\omega_i\end{aligned}$$

and on b_i,

$$\begin{aligned}\mathrm{d}\phi^+ - \mathrm{d}\phi^- &= \omega_j^+ \mathrm{d}\,\ln F^+ - \omega_j^- \mathrm{d}\,\ln F^- \\ &= \left(\omega_j^+ - \omega_j^-\right) \mathrm{d}\,\ln F^- \\ &= \mathrm{d}\,\ln F^- \int_{a_i} \mathrm{d}\omega_j \\ &= 2\pi i \delta_{ji} \mathrm{d}\,\ln F^-.\end{aligned}$$

Thus

$$\begin{aligned}\int_{\partial \widetilde{X}} \omega_j \,\mathrm{d}\,\ln F &= \sum_{i=1}^{g} \Big\{ - B_{ji} \int_{a_i} \mathrm{d}\,\ln F^- + \int_{a_i} \omega_j^+ \mathrm{d}\omega_i + \delta_{ji} \int_{b_i} \mathrm{d}\,\ln F^- \Big\} \\ &= \sum_{i=1}^{g} \Big\{ - B_{ji}(\pi i \varepsilon_i' + 2\pi i c_1) + \int_{a_i} \omega_j^+ \mathrm{d}\omega_i \\ &\qquad + 2\pi i \delta_{ji} \Big(- B_{ii}/2 - \varepsilon_i'' - \int_{P_0}^{P^{(I)}} \mathrm{d}\omega_i + e_i + 2\pi i c_2 \Big) \Big\}\end{aligned}$$

where c_1 and c_2 are integer constants to be specified. Also, by Cauchy's residue theorem,

$$\int_{\partial \widetilde{X}} \omega_j \,\mathrm{d}\,\ln F = 2\pi i \sum_{i=1}^{g} \int_{P_0}^{P_i} \mathrm{d}\omega_j,$$

implying the following equality:

$$\begin{aligned}2\pi i \sum_{i=1}^{g} \int_{P_0}^{P_i} \mathrm{d}\omega_j &= \sum_{i=1}^{g} \Big\{ - B_{ji}(\pi i \varepsilon_i' + 2\pi i c_1) + \int_{a_i} \omega_j^+ \mathrm{d}\omega_i \\ &\qquad + 2\pi i \delta_{ji} \Big(- B_{ii}/2 - \varepsilon_i'' - \int_{P_0}^{P^{(I)}} \mathrm{d}\omega_i + e_i + 2\pi i c_2 \Big) \Big\} \\ \iff \sum_{i=1}^{g} \int_{P_0}^{P_i} \mathrm{d}\omega_j &\equiv e_j - (\pi i B_{ji} \varepsilon_i'/2 + \varepsilon_j'') \\ &\qquad - \Big(B_{jj}/2 + \int_{P_0}^{P^{(I)}} \mathrm{d}\omega_j - \int_{a_i} \omega_j^+ \mathrm{d}\omega_i \Big) \ \mathrm{mod}\Lambda.\end{aligned}$$

Letting $\left(B_{jj}/2 + \int_{P_0}^{P^{(I)}} \mathrm{d}\omega_j - \int_{a_i} \omega_j^+ \mathrm{d}\omega_i\right) = K_j(P_0)$ this becomes, in vector form,

$$\sum_{k=1}^{g} \int_{P_0}^{P_k} \mathrm{d}\boldsymbol{\omega} \equiv \boldsymbol{e} - \boldsymbol{K}(P_0) - \pi i \boldsymbol{\varepsilon}' - B\boldsymbol{\varepsilon}'' \ \mathrm{mod}\,\Lambda,$$

as required. The vector $\boldsymbol{K}(P_0)$ is known as the vector of Riemann constants or the Riemann vector.

Proposition 3.3

Firstly we prove the formula for E:

$$\begin{aligned}
\sum_{k=1}^{g}\int_{a_k} z\mathrm{d}\omega_k &= \sum_{k=1}^{g}\sum_{j=1}^{g} c_{kj}\int_{a_k} z\mathrm{d}\widetilde{\omega}_j \\
&= \sum_{k=1}^{g} c_{k1}\int_{a_k} z\mathrm{d}\widetilde{\omega}_1 + \sum_{k=1}^{g}\sum_{j=2}^{g} c_{kj}\int_{a_k}\mathrm{d}\widetilde{\omega}_{j-1} \\
&= -i\sum_{k=1}^{g}\int_{b_k}\mathrm{d}\Omega_1\int_{a_k} z\mathrm{d}\widetilde{\omega}_1 + \sum_{k=1}^{g}\sum_{j=2}^{g} A_{j-1,k}c_{kj} \\
&= -i\sum_{k=1}^{g}\int_{b_k}\mathrm{d}\Omega_1\int_{a_k} z\mathrm{d}\widetilde{\omega}_1 \\
&= i\int_{\partial\widetilde{X}}\Omega_1 z\mathrm{d}\widetilde{\omega}_1 \\
&= -2\pi\mathrm{Res}\left(\Omega_1 z\mathrm{d}\widetilde{\omega}_1,\infty^+\right) - 2\pi\mathrm{Res}\left(\Omega_1 z\mathrm{d}\widetilde{\omega}_1,\infty^-\right) \\
&= 2\pi\left(E+\frac{i}{2}\phi^{\pm}\right)
\end{aligned}$$

where $\phi^{\pm}=\sum_{j=1}^{2g+2} z_j^{\pm}$ and we have used the relations $AC=2\pi i\mathbb{I}_g$, the results of Proposition 3.2 and the Riemann bilinear relations (2.6). The formula for N follows similarly:

$$\begin{aligned}
\sum_{k=1}^{g}\int_{a_k} z^2\mathrm{d}\omega_k &= \sum_{k=1}^{g}\sum_{j=1}^{g} c_{kj}\int_{a_k} z^2\mathrm{d}\widetilde{\omega}_j \\
&= \sum_{k=1}^{g} c_{k1}\int_{a_k} z^2\mathrm{d}\widetilde{\omega}_1 + \sum_{k=1}^{g} c_{k2}\int_{a_k} z^2\mathrm{d}\widetilde{\omega}_2 + \sum_{k=1}^{g}\sum_{j=3}^{g} c_{kj}\int_{a_k}\mathrm{d}\widetilde{\omega}_{j-1} \\
&= \sum_{k=1}^{g} c_{k1}\int_{a_k} z^2\mathrm{d}\widetilde{\omega}_1 + \sum_{k=1}^{g} c_{k2}\int_{a_k} z\mathrm{d}\widetilde{\omega}_1 + \sum_{k=1}^{g}\sum_{j=3}^{g} A_{j-1,k}c_{kj} \\
&= -i\sum_{k=1}^{g}\int_{b_k}\mathrm{d}\Omega_2\int_{a_k} z\mathrm{d}\widetilde{\omega}_1 - i\sum_{k=1}^{g}\int_{b_k}\mathrm{d}\Omega_1\int_{a_k} z\Big(z-\frac{1}{2}\phi^{\pm}\Big)\mathrm{d}\widetilde{\omega}_1 \\
&= i\int_{\partial\widetilde{X}}\Omega_2 z\mathrm{d}\widetilde{\omega}_1 + i\int_{\partial\widetilde{X}}\Omega_1 z\Big(z-\frac{1}{2}\phi^{\pm}\Big)\mathrm{d}\widetilde{\omega}_1 \\
&= -2\pi\mathrm{Res}\left(\Omega_2 z\mathrm{d}\widetilde{\omega}_1,\infty^+\right) - 2\pi\mathrm{Res}\left(\Omega_2 z\mathrm{d}\widetilde{\omega}_1,\infty^-\right) \\
&\quad -2\pi\mathrm{Res}\left(\Omega_1 z\Big(z-\frac{1}{2}\phi^{\pm}\Big)\mathrm{d}\widetilde{\omega}_1,\infty^+\right) - 2\pi\mathrm{Res}\left(\Omega_1 z\Big(z-\frac{1}{2}\phi^{\pm}\Big)\mathrm{d}\widetilde{\omega}_1,\infty^-\right) \\
&= 2\pi\left(N-\frac{i}{2}\sum_{j=1}^{2g+2}\left(z_j^{\pm}\right)^2 - 2R\right)
\end{aligned}$$

where $\mathrm{d}\widetilde{\omega}_1 = z\mathrm{d}\widetilde{\omega}_2 = z^g\mathrm{d}z/\mu$.

Appendix B

Hirota's method

Consider the SNLS (1.2). An ansatz,

$$q(x,t) = \frac{G(x,t)}{F(x,t)}, \tag{B.1}$$

is made where, without loss of generality, $F(x,t)$ is assumed a real function. This is substituted into (1.2) to give

$$\begin{aligned} \frac{1}{GF}\big\{i(FG_t - F_tG) + (FG_{xx} - 2F_xG_x + F_{xx}G)\big\} \\ = \frac{2}{F^2}\left\{(FF_{xx} - F_x^2) \mp G\overline{G}\right\}. \end{aligned} \tag{B.2}$$

Introducing the Hirota operator, defined by

$$D_y\left(a(y,z) \circ b(y,z)\right) = (\partial_y - \partial_{y'})a(y,z)b(y',z')\big|_{y=y',z=z'} \tag{B.3}$$

and applied repeatedly by the formula

$$D_z^m D_y^n\left(a(y,z) \circ b(y,z)\right) = (\partial_z - \partial_{z'})^m(\partial_y - \partial_{y'})^n a(y,z)b(y',z')\big|_{y=y',z=z'},$$

means equation (B.2) may be written as

$$\frac{1}{GF}\left(iD_t + D_x^2\right)(G \circ F) = \frac{1}{F^2}\left\{D_x^2(F \circ F) \mp 2G\overline{G}\right\}. \tag{B.4}$$

Adding a constant $-\tau$ to both sides gives

$$\frac{1}{GF}\left(iD_t + D_x^2 - \tau\right)(G \circ F) = \frac{1}{F^2}\left\{\left(D_x^2 - \tau\right)(F \circ F) \mp 2G\overline{G}\right\}. \tag{B.5}$$

Hirota [Hir73] makes the heuristic step of decoupling these equations by setting both left and right-hand sides of (B.5) equal to zero. Whilst solutions of the decoupled system will certainly solve the SNLS, it appears that this step produces Hirota-type soliton solutions in particular.

B.1 Soliton solutions to the attractive SNLS

For the attractive case a valid solution is found setting $\tau = 0$. The equations of interest are therefore

$$\begin{aligned} \left(iD_t + D_x^2\right)(G \circ F) &= 0 \\ D_x^2(F \circ F) &= 2G\overline{G}. \end{aligned} \tag{B.6}$$

Hirota's method relies on expanding F and G as polynomials in a dummy parameter ε which is later set to unity. This process is closely allied to the theory of Padé approximants, used to expand functions as a ratio of two power series. The particular polynomials chosen in the attractive case are

$$\begin{aligned} G(x,t) &= \varepsilon G_1(x,t) + \varepsilon^3 G_3(x,t) + \varepsilon^5 G_5(x,t) + ... \\ F(x,t) &= 1 + \varepsilon^2 F_2(x,t) + \varepsilon^4 F_4(x,t) + ... \end{aligned} \tag{B.7}$$

The simplest 1-soliton solution is found by selecting a single exponential phase solution for G_1,

$$G_1 = \exp(\eta_1),$$

where

$$\eta_1 = P_1 x + iP_1^2 t + \eta_1^{(0)}.$$

This satisfies the first of equations (B.6) at order ε and means that

$$\begin{aligned} F_2 &= \exp(\eta_1 + \overline{\eta_1} + \phi_{1\bar{1}}), \\ G_i, F_i &= 0 \quad \text{for } i \geq 3. \end{aligned}$$

Here, P_1 and $\eta_1^{(0)}$ are complex constants and $\phi_{1\bar{1}} = \ln\left(P_1 + \overline{P_1}\right)^{-2} \in \mathbb{R}$. Thus the 1-soliton solution to the attractive SNLS is given by

$$q(x,t) = \frac{\exp(\eta_1)}{1 + \exp(\eta_1 + \overline{\eta_1} + \phi_{1\bar{1}})},$$

after setting $\varepsilon = 1$. This may be rearranged to give

$$q(x,t) = \frac{1}{2}\text{sech}\left(\frac{\eta_1 + \overline{\eta_1} + \phi_{1\bar{1}}}{2}\right)\exp\left(\frac{\eta_1 - \overline{\eta_1} - \phi_{1\bar{1}}}{2}\right). \tag{B.8}$$

To obtain the 2-soliton solution, a more elaborate choice for $G_1(x,t)$ is required:

$$G_1(x,t) = \exp(\eta_1) + \exp(\eta_2) \tag{B.9}$$

where

$$\eta_j = P_j x + iP_j^2 t + \eta_j^{(0)} \tag{B.10}$$

and P_j, $\eta_j^{(0)}$ are complex constants with the P_j distinct. This is substituted into (B.6) to find F_2, G_3 and F_4, given explicitly as

$$\begin{aligned}
F_2(x,t) = {} & \exp(\eta_1 + \overline{\eta_1} + \phi_{1\bar{1}}) + \exp(\eta_1 + \overline{\eta_2} + \phi_{1\bar{2}}) \\
& + \exp(\eta_2 + \overline{\eta_1} + \phi_{2\bar{1}}) + \exp(\eta_2 + \overline{\eta_2} + \phi_{2\bar{2}}) \\
G_3(x,t) = {} & \exp(\eta_1 + \eta_2 + \overline{\eta_1} + \phi_{1\bar{1}} + \phi_{2\bar{1}} + \phi_{12}) \\
& + \exp(\eta_1 + \eta_2 + \overline{\eta_2} + \phi_{1\bar{2}} + \phi_{2\bar{2}} + \phi_{12}) \\
F_4(x,t) = {} & \exp(\eta_1 + \eta_2 + \overline{\eta_1} + \overline{\eta_2} + \phi_{1\bar{1}} + \phi_{1\bar{2}} + \phi_{2\bar{1}} + \phi_{2\bar{2}} + \phi_{12} + \phi_{\bar{1}\bar{2}})
\end{aligned}$$

where

$$\phi_{j\bar{k}} = \ln(P_j + \overline{P_k})^{-2} \tag{B.11}$$

$$\phi_{jk} = \ln(P_j - P_k)^2 \quad j \neq k \tag{B.12}$$

$$\phi_{\bar{j}\bar{k}} = \ln(\overline{P_j} - \overline{P_k})^2 \quad j \neq k. \tag{B.13}$$

The remaining terms, F_i and G_i for $i \geq 5$, are set equal to zero.

The general N-soliton solution to the attractive SNLS is presented in Section 3.5. The proof may be found in the original article [Hir73].

B.2 Soliton solutions to the repulsive SNLS

For the repulsive SNLS, τ is not set equal to zero and the decoupled system formed is

$$\begin{aligned}
\left(iD_t + D_x^2\right)(G \circ F) &= \tau GF \\
D_x^2(F \circ F) &= \tau F^2 - 2G\overline{G}.
\end{aligned} \tag{B.14}$$

The second of these equations forces the condition $\tau \in \mathbb{R}$ as $F(x,t)$ and $G(x,t)\overline{G}(x,t)$ are both real functions for all x and t. The ansatz for the expansions of $F(x,t)$ and $G(x,t)$ differs slightly to the attractive case and is:

$$\begin{aligned} G(x,t) &= G_0(x,t)\left\{1+\varepsilon G_1(x,t)+\varepsilon^2 G_2(x,t)+...\right\} \\ F(x,t) &= 1+\varepsilon F_1(x,t)+\varepsilon^2 F_2(x,t)+... \end{aligned} \tag{B.15}$$

Substituting these into (B.14) and comparing coefficients of ε^0 immediately implies $\tau > 0$ and it follows that $|G_0| = \sqrt{\frac{\tau}{2}}$. A suitable form for $G_0(x,t)$ is then

$$G_0(x,t) = \sqrt{\frac{\tau}{2}}\exp(i\theta) \tag{B.16}$$

where

$$\theta = kx - (k^2+\tau)t + \theta^{(0)}$$

and $k, \theta^{(0)}$ are real constants.

The dark 1-soliton solution is found setting

$$\begin{aligned} F_1(x,t) &= \exp(\eta_1) \\ G_1(x,t) &= a_1\exp(\eta_1) \\ F_i(x,t), G_i(x,t) &= 0 \qquad i \geq 2 \end{aligned} \tag{B.17}$$

where

$$\eta_1 = p_1 x - \omega_1 t + \eta_1^{(0)} \tag{B.18}$$

Substituting (B.17) into (B.14) and comparing real and imaginary parts at order ε gives the identities

$$\begin{aligned} \omega_1 &= p_1\left\{2k \pm \sqrt{2\tau - p_1^2}\right\}, \\ a_1 &= \left(1-\frac{p_1^2}{\tau}\right) \mp i\left(p_1\frac{\sqrt{2\tau-p_1^2}}{\alpha}\right) = -\frac{p_1 \pm i\sqrt{2\tau-p_1^2}}{p_1 \mp i\sqrt{2\tau-p_1^2}}. \end{aligned}$$

These forms solve (B.14) at all orders of ε subject to the condition $p_1^2 \leq 2\tau$. The dark 1-soliton solution is therefore given by

$$q(x,t) = \sqrt{\frac{\tau}{2}}\left\{\frac{1+a_1\exp(\eta_1)}{1+\exp(\eta_1)}\right\}\exp(i\theta). \tag{B.19}$$

It should be noticed that $|a_1| = 1$ and thus a_1 may take the form $a_1 = \exp(2i\psi_1)$ where

$\tan\psi_1 = \frac{p_1}{\mp\sqrt{2\tau-p_1^2}}$. This gives the more approachable solution

$$q(x,t) = \sqrt{\frac{\tau}{2}}\left\{\cos\psi_1 + i\sin\psi_1 \tanh\left(\frac{\eta_1}{2}\right)\right\}\exp(i\theta + i\psi_1). \tag{B.20}$$

The dark 2-soliton solution is found setting

$$\begin{aligned} F_1(x,t) &= \exp(\eta_1) + \exp(\eta_2) \\ G_1(x,t) &= a_1\exp(\eta_1) + a_2\exp(\eta_2) \end{aligned} \tag{B.21}$$

where

$$\eta_i = p_i x - \omega_i t + \eta_i^{(0)}$$

and $\eta_i \in \mathbb{R}$ for $i = 1, 2$. G_0 is unchanged from the 1-soliton case. The bilinearity of the Hirota operator means ω_i and a_i take the same forms as in the 1-soliton case:

$$\omega_i = p_i\left\{2k \pm \sqrt{2\tau - p_i^2}\right\} \tag{B.22}$$

$$a_i = \left(1 - \frac{p_i^2}{\tau}\right) \mp i\left(p_i\frac{\sqrt{2\tau-p_i^2}}{\tau}\right) = -\frac{p_i \pm i\sqrt{2\tau-p_i^2}}{p_i \mp i\sqrt{2\tau-p_i^2}} \tag{B.23}$$

with the condition

$$p_i^2 \leq 2\tau.$$

As for a_1, $|a_i| = 1$ and a_i may be expressed as

$$a_i = \exp(2i\psi_i) \tag{B.24}$$

with $\tan\psi_i = \frac{p_i}{\mp\sqrt{2\tau-p_i^2}}$. Substituting these forms for G_0, F_1 and G_1 into (B.14) at order ε^2 gives

$$\begin{aligned} F_2(x,t) &= \left[\frac{\sin\left(\frac{\psi_1-\psi_2}{2}\right)}{\sin\left(\frac{\psi_1+\psi_2}{2}\right)}\right]^2 \exp(\eta_1+\eta_2) \\ G_2(x,t) &= \left[\frac{\sin\left(\frac{\psi_1-\psi_2}{2}\right)}{\sin\left(\frac{\psi_1+\psi_2}{2}\right)}\right]^2 \exp(\eta_1+\eta_2+2i\psi_1+2i\psi_2) \end{aligned}$$

and, setting $F_i, G_i = 0$ for $i \geq 3$ and $\varepsilon = 1$, completes the consistent Hirota solution

$$q(x,t) = \sqrt{\frac{\tau}{2}} \left\{ \frac{1 + G_1 + G_2}{1 + F_1 + F_2} \right\} \exp(i\theta) \tag{B.25}$$

where

$$\begin{aligned} F_1 &= \exp(\eta_1) + \exp(\eta_2) \\ G_1 &= \exp(\eta_1 + 2i\psi_1) + \exp(\eta_2 + 2i\psi_2) \\ F_2 &= \exp(\eta_1 + \eta_2 + \Psi_{12}) \\ G_2 &= \exp(\eta_1 + \eta_2 + 2i\psi_1 + 2i\psi_2 + \Psi_{12}) \end{aligned}$$

and

$$\exp(\Psi_{12}) = \left[\frac{\sin\left(\frac{\psi_1 - \psi_2}{2}\right)}{\sin\left(\frac{\psi_1 + \psi_2}{2}\right)} \right]^2$$

Hirota infers the general dark N-soliton solution, presented in Section 3.5, from the form of the 1 and 2-solitons. The proof may be found in article [Hir76].

References

[ADK93] F Abdullaev, S Darmanyan and P Khabibullaev *Optical Solitons* Springer-Verlag, Berlin (1993)

[AC91] MJ Ablowitz and PA Clarkson *Solitons, Nonlinear Evolution Equations and Inverse Scattering* LMS Lecture Note Series **149** CUP, Cambridge (1991)

[AKN74] MJ Ablowitz, DJ Kaup, AC Newell and H Segur *The inverse scattering transform - Fourier analysis for nonlinear problems* Stud. Appl. Math. **53** 249-315 (1974)

[APT04] MJ Ablowitz, B Prinari and A Trubatch *Integrable Nonlinear Schrödinger Systems and their Soliton Dynamics* Dynamics of PDE **1** no.3 239-299 (2004)

[AS81] MJ Ablowitz and H Segur *Solitons and the Inverse Scattering Theory* SIAM, Philadelphia (1981)

[BEG00] SM Baker, JN Elgin and J Gibbons *Polarization dynamics of solitons in birefringent fibers* Phys. Rev. E **62** 4325-4332 (2000)

[BG06] S Baldwin and J Gibbons *Genus 4 trigonal reduction of the Benney equations* J. Phys. A: Math. Gen. **39** 3607-3639 (2006)

[Bel61] R Bellman *A Brief Introduction to Theta Functions* Holt, Rinehart and Winston, New York (1961)

[BBE94] ED Belokolos, AI Bobenko, VZ Enol'skii, AR Its and VB Matveev *Algebro-Geometric Approach to Nonlinear Integrable Equations* Springer-Verlag, Berlin (1994)

[BEL96] VM Buchstaber, VZ Enol'skii and DV Leykin *Hyperelliptic Kleinian Functions and Applications* Preprint ESI 380 (1996)

[CL02] Y Chen and N Lawrence *A generalization of the Chebyshev polynomials* J. Phys. A **35** 4651-4699 (2002)

[CEE00] PL Christiansen, JC Eilbeck, VZ Enol'skii and NA Kostov *Quasi-periodic and periodic solutions for systems of coupled nonlinear Schrödinger equations*, Proc. Roy. Soc. A **456** 2263-2281 (2000)

[DT76] E Date and S Tanaka *Periodic Multi-Soliton Solutions of Korteweg-de Vries Equation and Toda Lattice* Progr. Theoret. Phys. Suppl. no.59 107-125 (1976)

[DH01] B Deconinck and M van Hoeij *Computing Riemann matrices of algebraic curves* Physica D **152-153** 28-46 (2001)

[DE00] RG Docksey and JN Elgin *Closure of the Manakov System* SIAM J. Math. Anal. **32** no.1 54-79 (2000)

[DJ89] PG Drazin and RS Johnson *Solitons: an introduction* CUP, Cambridge (1989)

[EEK00] JC Eilbeck, VZ Enol'skii and NA Kostov *Quasiperiodic and periodic solutions for vector nonlinear Schrödinger equations* J. Math. Phys. **41** no.12 (2000)

[EEI07] JN Elgin, VZ Enolski and AR Its *Effective integration of the nonlinear vector Schrödinger equation* Physica D **225** 127-152 (2007)

[FT87] LD Faddeev and LA Takhtajan *Hamiltonian Methods in the Theory of Solitons* Springer-Verlag, Berlin Heidelberg (1987)

[FK80] HM Farkas and I Kra *Riemann Surfaces* Springer-Verlag, Berlin (1980)

[GGK67] CS Gardner, JM Greene, MD Kruskal and RM Miura *Method for solving the Korteweg-de Vries equation* Phys. Rev. Lett. **19** 1095-1097 (1967)

[GW86] G Gregori and S Wabnitz *New exact solutions and bifurcations in the spatial distribution of polarization in third-order nonlinear optical interactions* Phys. Rev. Lett. **56** 600-603 (1986)

[Hir73] R Hirota *Exact envelope-soliton solutions of a nonlinear wave equation* J. Math. Phys. **14** 805-809 (1973)

[Hir76] R Hirota *Direct method of finding exact solutions of nonlinear evolution equations* Springer Lecture Notes 515 (1976)

[Its82] AR Its *On Connections between Solitons and Finite-Gap Solutions of the Nonlinear Schrödinger Equation* Probl. Mat. Fiz. **10** 118-137 (1982)

[IK76] AR Its and VR Kotlyarov *Explicit formulas for the solution of the nonlinear Schrödinger equation* Dokl. Akad. Nauk. Ukrain. SSR. Ser. A **11** (1976)

[Kib73] TWB Kibble *Classical Mechanics* 2nd edition, McGraw-Hill, Maidenhead (1973)

[LRT76] M Lakshmanan, ThW Ruijgrok and CJ Thompson *On the Dynamics of a Continuum Spin System* Physica **84A** 577-590 (1976)

[Lak77] M Lakshmanan *Continuum Spin System as an Exactly Solvable Dynamical System* Physics Letters **61A** 53-54 (1977)

[Lax68] PD Lax *Integrals of nonlinear equations of evolution and solitary waves* Comm. Pure Appl. Math. **28** 141-188 (1968)

[Mag77] F Magri *A simple model of the integrable Hamiltonian equation* J. Math. Phys. **19** no.5 1156-1162 (1978)

[Man74] SV Manakov *On the theory of two-dimensional stationary self-focusing of electromagnetic waves* Sov. Phys. JETP **8** 248-253 (1974)

[MS85/6] AV Mikhailov and AB Shabat *Integrability conditions for systems of two equations of the form* $\boldsymbol{u}_t = A(\boldsymbol{u})\boldsymbol{u}_{xx} + \boldsymbol{F}(\boldsymbol{u}, \boldsymbol{u}_x)$, *I and II* Theoretical and Mathematical Physics **62** no.2 107-122, **66** no.1 31-44 (1985/6)

[MS86] AV Mikhailov and AB Shabat *Integrable Deformations of the Heisenberg Model* Phys. Lett. A **116** no.4 191-194 (1986)

[MGH95] LF Mollenauer, JP Gordon and F Heismann *Polarization scattering by soliton-soliton collisions* Optics Letters **20** no.20 2060-2062 (1995)

[Mum83] D Mumford *Tata Lectures on Theta I* Birkhäuser, Boston (1983)

[Nak00] K Nakkeeran *Exact soliton solutions for a family of N coupled nonlinear Schrödinger equations in optical fiber media* Phys. Rev. E **62** 1313-1321 (2000)

[PP99] AV Porubov and DF Parker *Some general periodic solutions to coupled nonlinear Schrödinger equations* Wave Motion **29** no.2 (1999)

[Pre85] E Previato *Hyperelliptic quasi-periodic and soliton solutions of the nonlinear Schrödinger equation* Duke Math. J. **52** no.2 329-377 (1985)

[PAB06] B Prinari, MJ Ablowitz and G Biondini *Inverse scattering transform for the vector nonlinear Schrödinger equation with nonvanishing boundary conditions* J. Math. Phys. **47** 063508 (2006)

[RL95] R Radhakrishnan and M Lakshmanan *Bright and dark soliton solutions to coupled nonlinear Schrodinger equations* J. Phys. A **28** 2683-2692 (1995)

[RF74] HE Rauch and HM Farkas *Theta Functions with Applications to Riemann Surfaces* William and Wilkins, Baltimore (1974)

[SY74] J Satsuma and N Yajima *Initial Value Problems of One-Dimensional Self-Modulation of Nonlinear Waves in Dispersive Media* Progr. Theoret. Phys. Suppl. no.55 284-306 (1974)

[SK97] AP Sheppard and YS Kivshar *Polarized dark solitons in isotropic Kerr media* Phys. Rev. E **55** no.4 4773-4782 (1997)

[Sie71] CL Siegel *Topics in Complex Function Theory Volume II, Automorphic Functions and Abelian Integrals* Wiley-Interscience, New York (1971)

[SE98] JP Silmon-Clyde and JN Elgin *Incompatibility of polarization-division multiplexing with wavelength-division multiplexing in soliton-transmission systems* Optics Letters **23** no.3 180-182 (1998)

[Sil99] JP Silmon-Clyde *Studies on the Vector Non-linear Schrödinger Equation* PhD thesis, Imperial College London (1999)

[Spr57] G Springer *Introduction to Riemann Surfaces* Addison-Wesley, Massachusetts (1957)

[TP92] RS Tasgal and MJ Potasek *Soliton solutions to coupled higher-order nonlinear Schrdinger equations* J. Math. Phys. **33** 1208-1215 (1992)

[Ton95] G Tondo *On the integrability of stationary and restricted flows of the KdV hierarchy* J. Phys. A **28** 5097-5115 (1995)

[WMC91] PKA Wai, CR Menyuk and HH Chen *Stability of solitons in randomly varying birefringent fibers* Optics Letters **16** no.16 1231-1233 (1991)

[WE07] OH Warren and JN Elgin *The vector nonlinear Schrödinger hierarchy* Physica D **228** 166-171 (2007)

[WW27] ET Whittaker and GN Watson *A Course of Modern Analysis* 4^{th} edition CUP, Cambridge (1927)

[WWE07] T Woodcock, OH Warren and JN Elgin *Genus two finite gap solutions to the vector nonlinear Schrödinger equation* J. Phys. A: Math. Theor. **40** F1-F7 (2007)

[Wri99] OC Wright *The stationary equations of a coupled nonlinear Schrödinger system* Physica D **126** 275-289 (1999)

[Zak91] VE Zakharov (Ed.) *What is Integrability?* Springer-Verlag, Berlin Heidelberg (1991)

[ZS72] VE Zakharov and AB Shabat *Exact theory of two-dimensional self-focusing and one-dimensional self-modulation of waves in nonlinear media* Zh. Eksp. Teor. Fiz. **61** 118-134 (1972)

[ZS73] VE Zakharov and AB Shabat *Interaction between solitons in a stable medium* Zh. Eksp. Teor. Fiz. **64** 1627-1639 (1973)

[ZT79] VE Zakharov and LA Takhtadzhyan *Equivalence of the nonlinear Schrödinger equation and the equation of a Heisenberg ferromagnet* Theor. Math. Phys. **38** 17-23 (1979)

[ZY90] D Zhang and G Yang *Integrable deformations of the classical Heisenberg model* J. Phys. A: Math. Gen. **23** 2133-2137 (1990)